Unterschrift BetreuerIn

BACHELORARBEIT

Software implementation of the quality assurance tool for magnetic resonance imaging distortion assessment

Betreuer:

Ao.Univ.Prof. Dipl.-Ing. Dr.techn. Martin Gröschl
Institut für Angewandte Physik
Technische Universität Wien

in Kooperation mit:

Peter Kuess, PhD
& Piotr Andrzejewski, MSc Eng
Department of Radiooncology
Medical University Vienna, AKH Vienna

von:

David Blacher
1327545

Technische Physik
E033261

October 4, 2017

Unterschrift StudentIn

Kurzzusammenfassung

deutsch?

Abstract

english

Preface

Medicine has always been a scientific area where the crossing of different fields of research accounted for breakthroughs leading to a better understanding and, consequently, improved therapeutic methods. The success of modern approaches and the development of future techniques owes to the increased interdisciplinary research and work done by both medical personnel such as doctors and nurses, but also scientists like biologists, chemists, physicists and engineers. As the knowledge about our own human body grows, the problems that we face are becoming more and more complex and need the interdisciplinary expertise. Even though some therapeutic questions appear easy to answer, because they are easily understood on a general level, the actual treatment of a real patient is something entirely different. Coming up with a treatment plan becomes exceedingly complex as we try to improve its precision and go towards targeted therapies which are tailor fit to the needs of an individual patient. Improving their quality of life and chance of survival has always come with increased costs and effort as trade-off. To make the best treatments available for everyone and, in the long run, also reduce the cost of used resources: this work shall be a small contribution to this development.

Contents

1 Introduction

1.1 Photon - matter interactions

As light (visible and invisible wavelengths) passes through matter, its intensity decreases. This phenomenon is due to photons interacting with electrons, nuclei and their electric fields. All processes either change the direction they travel in, alter their energy, or result in the disappearance of single photons. The probability of these interactions differ for each material (dependent on its density; proton number Z) and photon energy ($h\nu$).

If a photon's energy exceeds the binding energy of an orbital electron, the photoelectric interaction can occur. Also known as 'photo effect', it describes a photon being completely absorbed by a tightly bound orbital electron which then is ejected from its atom. The now free electron is called 'photo-electron'. Its kinetic energy is the difference of the photon's energy and the electron's binding energy:

$$E_{kin} = h\nu - E_{binding} \tag{1.1}$$

Instead of being absorbed, photons might also just 'bounce off' electrons or entire atoms, transferring momentum and, in some cases, part of their energy to the particle they collide with. Rayleigh (coherent) scattering happens when a photon interacts with a tightly bound orbital electron (transferring momentum to the entire atom). This event can be seen as elastic, because only a negligible part of the photon's energy is transferred.

The Compton effect (incoherent scattering) involves a essentially free electron, such as an orbital electron with a relatively small binding energy compared to the photon's energy. Due to the weak binding, momentum is transferred only to the electron. This 'recoil electron' (or 'Compton electron') leaves its atom with a significant kinetic energy, which originated from the scattered photon. Since the photon loses part of its energy, the event is considered inelastic.

When a photon with an energy above 1.022 MeV passes through the electric field of a nucleus, it might disappear to create an electron-positron pair. This effect is called pair production. The threshold of 1.022 MeV equals exactly the rest mass $E_m = 2m_ec^2$ for the two equally heavy particles (electron and positron). The new particles travel in opposite directions with the same kinetic energy:

$$E_{kin} = \frac{h\nu - 1.022\,MeV}{2} \tag{1.2}$$

A photon with energy of the order of 2 MeV or higher can also interact directly with the nucleus. Such a Photonuclear reaction is similar to the photo effect, in the sense that the photon is completely absorbed. Its energy is transferred to the nucleus resulting in the emission of either a proton or neutron.

Attenuation

The aforementioned interactions result in a gradual decrease of radiation intensity as it travels through matter. The combined effect is described by Beer's law:

$$I(x) = I_0 e^{-\mu(h\nu,Z)x} \tag{1.3}$$

where x is the thickness of a homogeneous material and μ its linear attenuation coefficient. The different probabilities for the interactions to occur is implicitly considered by the attenuation coefficient $\mu(h\nu, Z)$ (see Figure 1.1).

For a photon being transmitted through matter with varying properties, the attenuation coefficient changes, too. After travelling a distance d, the intensity can be expressed as:

(1.4)

Where $\mu(x)$ describes the attenuation at every distance x. (For whole chapter 1.1: [1], [2])

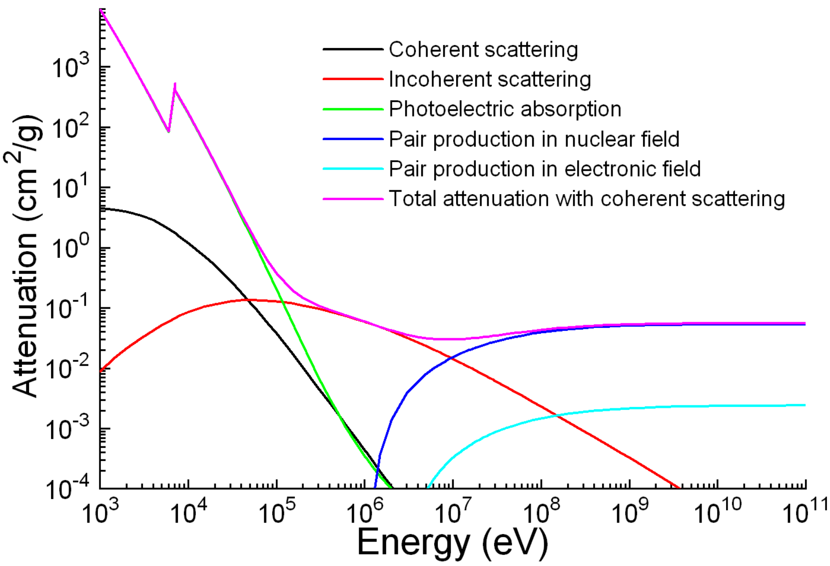

Figure 1.1: Photon attenuation for iron [1]

1.2 Basics of Radiobiology

1.2.1 The human cell

All higher organisms consist of cells working together to form what is called tissue. A collection of tissues which perform one or more functions is considered an organ.

Even though different types of cells exhibit distinctive traits which set them apart, all of them originated from the same totipotent zygote containing a original set of DNA. A zygote is a stem cell, it has the ability to replicate indefinitely, passing its DNA on to the resulting daughter cells. At the same time, it can change into any type of body cell. This feature is why it is called 'totipotent'. As soon as the zygote has divided into a sufficient number of identical cells, all of them differentiate into the various human tissues. In favour of becoming more specialised, cells lose their totipotency. During the early stages of an embryo they are still capable of developing into a number of different cell types, but already restricted to their own tissue type; either nerve, skin, or blood & muscle tissue. As those cells further specialise, they limit their potential even more. In a fully grown human body there are still stem cells present, such as bone marrow stem

[1] image source: by Materialscientist - `https://commons.wikimedia.org/wiki/File:Ironattenuation.PNG`, CC BY-SA 3.0 (`https://creativecommons.org/licenses/by-sa/3.0`) or GFDL (`http://www.gnu.org/copyleft/fdl.html`), via Wikimedia Commons

cells. Other than the zygote, bone marrow can only give rise to blood cells, but not to e.g. nerve or skin cells. A blood cell itself cannot replicate, it is considered a 'mature cell'.

The whole process follows guidelines dictated by the DNA. Every cell inherited its own personal copy of the original set. Inevitably, mistakes happen during its replication resulting in changes to the DNA called 'mutation'. Most of these alterations are repaired or do not lead to changes in the cells behaviour.

The time needed for a reparation process to be completed is not the same as the period between cell reproduction. Changes to the DNA (e.g. mutations) occurring less frequently than one reparation cycle are less probable to result in permanent alterations, than those taking place more frequently. This is the reason why cells in tissues and organs that divide more frequently (i.e. gonads) are more prone to, for example, radiation induced mutations than those reproducing more slowly (i.e. bones).

As the human body ages, the repair mechanism loses some of its efficiency and mutations accumulate. At one point, a cell may be reprogrammed to act in a unpredictable way, giving up its duties and duplicating without restraint, possibly forming tumours. Also, external factors are known to influence cell behaviour and induce such 'malign' cells (carcinogenesis). Cancer cells usually replicate more frequent than healthy cells, eventually leading to characteristic symptoms.

Different approaches have been developed to treat cancer, not all of which are suited to tackle every type of tumour. If the tumour's location is unknown or metastases have formed already in many places, chemotherapy might be considered. An easily accessible tumour could be removed in a surgery. Non invasive therapies also include radiotherapy, destroying cancer cells using ionising radiation. (see chapter 1.2.2.)

Generally, early treatments have high chances of success, but tumours are often not noticed until they reached a certain stage. Reliable ways of diagnosing tumours are made possible by imaging techniques visualising the interior of the human body. [3], [4]

1.2.2 Effects of radiation

Cell damage could either be caused by radiation interacting directly with the critical target in a cell or with other molecules and atoms within the cell. For X-rays, two thirds of the biological damage is attributed to indirect action. As described in 1.1, radiation transfers some of its energy to the medium it passes through. Most interactions, such as the photo effect, incoherent (Compton) scattering and pair production, result in free electrons. This is why it is called "ionising radiation". If the electron has a sufficiently high kinetic energy, it may free additional orbital electrons from atoms in its vicinity. The remaining ions are positively charged, with a single unpaired valence electron. This type of chemical and free electrons are both referred to as 'radicals' and considered extremely reactive. As the human body consists mainly of water, the radicals created are often H_2O^+ (water ion) and $OH\bullet$ (hydroxyl radical). They are likely to take part in chains of chemical events leading to the breakage of chemical bonds which can disrupt the structure of macromolecules. Such processes can induce changes in DNA sequences and eventually produce biological damage.

A irradiated cell can be affected in various ways ranging from no effect to immediate cell death. The cell might also survive containing a minor mutation. A more fundamental mutation might lead to carcinogenesis. Irradiated cells might also send signals to their neighbours, inducing genetic damage known as 'bystander effects'. On the other hand, surviving cells can also react to irradiation and becoming more resistant.

One classification separates cell damage into lethal, sublethal or potentially lethal. Sublethal damage can be repaired, provided it occurs only once before the repair cycle is complete. Potentially lethal damage can be manipulated by repair, provided the cell is allowed to remain in a non-dividing state.

The relative biological effectiveness (RBE), which describes the damage done by a specific type of radiation (compared to a reference test radiation) to a certain type of tissue, is dependent on various factors, including the rate at which dose is delivered. In the case of radiation causing sublethal damage, for instance, the dose rate significantly affects the RBE. If the average time between two sublethal damages in a single cell is longer than the time necessary for a full repair cycle, the cell will have a fair chance of survival. Does it sustain damage more frequently, the cell will die with a much higher probability. Increasing the radiation rate above this threshold results in a jump of the RBE.

Raising the RBE does not automatically correspond in better treatment. Only if a differential effect reduces the RBE for healthy tissue compared to the tumour, there is a therapeutic advantage. Fortunately, tissues react differently to the same type of radiation. This behaviour can be used to increase the RBE for tumours and reduce it for healthy tissue.

On a larger scale, the sum of damages done to individual cells gives rise to characteristic symptoms. Generally, these harmful effects of radiation are defined as either stochastic or deterministic. The probability of stochastic effects is directly proportional to the dose, but their severity in affected individuals is not. These effects arise in single cells (e.g. carcinogenesis), and it is assumed that the probability for such an occurrence is always greater than zero, even for small doses. If many cells show mutations, the probability of cancer development is higher, but the symptoms of growing tumours will not be worse. For deterministic effects, on the other hand, the severity scales with the dose. They are connected to tissue reaction caused by damage to a population of cells. The higher the dose, the more cells die, the graver are the biological consequences.

Changes to the DNA might not become apparent ever, others take years until they result in biological effects. The same goes for tissue effects, which could either be acute (soon after exposure) or delayed (chronic). A possible long term consequence of ionising radiation is leukaemia. Damage to germ cells (sperm/egg) might even result in genetic damages expressed in subsequent generations.

While imaging modalities utilising X-rays are designed to apply a dose as little as possible to keep effects of irradiation low, radiotherapy makes use of the lethal effects targeting cancer cells. [1], [2]

1.3 Imaging modalities

The imaging of human body's interior has diametrically changed medicine. It has its use in almost all medical disciplines. Currently, there are many ways to acquire section images (or also volumes) of our organism without causing serious and sustained side effects. They differ not only in size of the depicted volume and the image quality, but also in what additional information they provide besides purely morphologic data. These other features can be functional, for example describing effectiveness of a metabolic process; or even molecular, revealing pathways of a certain molecule's distribution. In the next chapters, X-ray planar imaging and the imaging modalities used for this thesis (computer tomography and magnetic resonance imaging) will be explained in more detail.

1.3.1 X-ray projection imaging

A widely used imaging technique based on photon interactions is X-ray projection. Its setup is made up by a radiation source, the object of interest and a detector. Since the technique is about projection, a patient needs to be placed between an X-ray tube and the detector (usually a film-cassette or digital sensor). In the first stage of the imaging process, X-ray photons emitted by the tube enter the body. Next, while travelling through human tissue, they interact with its atoms in various ways as described above (see 1.1). These processes govern how much radiation is absorbed or scattered. Finally, photons which make it through the patient are recorded as they reach the detector on the opposite side. This results in a negative greyscale image, where brightness values correspond to the intensity reduction. Low intensity (= high absorption) leads to bright spots on the image and vice-versa. The whole process could also be described as 'the projection of attenuation shadows onto the detector', since the radiation absorption directly depends on the attenuation coefficient. The attenuation, on the other hand, depend on the tissue's properties (e.g. atomic number Z, density, etc). Consequently, the attenuation shadows depict a projection of the patient.

Soft tissue contrast

Soft tissue such as brain matter and muscles absorb only little radiation, casting a lighter shadow (dark areas on image) than bone which absorbs more photons (bright areas). Practically, in the human body, anything other than bone differs only slightly in attenuation, owing to the relatively small difference in atomic numbers and density. For this reason, X-ray projection imaging is considered reliable when it comes to diagnose bone fractures, while at the same time, it is not suited to clearly delineate soft tissue structures. The use of contrast agents, which effectively increase the density (atomic number) of certain structures or fluids, can help tackle this shortcoming. Such substances fill e.g. the bloodstream with heavier atoms, which can be clearly seen against the dark background of surrounding soft-tissue. In CT angiography, for instance, iodine is administered intravenously enhancing vessel to vessel-wall contrast. In studies of the abdomen a diluted iodine solution or barium compounds swallowed by the patient leads to improved visibility of the gastrointestinal tract. For some examinations, the patient inhales a contrast agent.

For patients allergic to those chemicals, a number of alternative agents have been developed. Unfortunately, most introduce minor, sometimes serious side-effects. There is ongoing research to find materials yielding enhanced contrast while at the same time minimising adverse reactions, a promising candidate being gold nano particles. [1], [2]

Other imaging modalities are potentially better suited for soft tissue imaging, like medical ultrasound and Magnetic Resonance Imaging (MRI), to name a few. They are preferred for non invasive soft tissue examinations. The choice of suitable imaging modality depends a lot on the particular diagnostic needs and capabilities. It is for the clinician to decide how detailed the information needs to be and how fast it has to be provided. Often less accurate and/or cheaper methods are used first and, if necessary, followed by more sophisticated ones.

1.3.2 Computer Tomography - CT

Computer Tomography (CT) is a three-dimensional (3-D) imaging modality based on the measurement of X-ray planar projections. The technique has evolved from 2-D X-ray scanning. By mounting source and detector on a rotary ring with a patient at the centre, projections from any angle can be obtained. However, in contrast to 2-D projection methods, the detector resembles an arc made up by several hundreds of neighbouring detector elements. A single 'image' taken by the detector is therefore only in 1-D. Yet, by repeating this process from a sufficient number of different angles and along the entire patient (z-axis) a 3-D model can be computed (based on 'Radon transformation'). In contrast to 2-D methods, where the patients interior is projected/compressed onto a flat image, CT preserves the exact location information. This feature led to a radical improvement in diagnostics.

Since its clinical introduction in 1971 by Godfrey Hounsfield, CT has become a widely used 3-D imaging modality for a range of applications including radiation oncology. Especially in radiation therapy, knowledge of the exact geometry is crucial, which is why CT plays such a pivotal role in treatment planning (see 1.4). [1], [2]

3-D image reconstruction

As a photon passes through the patient, it encounters different materials associated with characteristic linear attenuation coefficients. It is practical to think of the scanned body as a collection of $N = N_X \cdot N_Y \cdot N_Z$ finite size cubes (Δx cube length) called 'voxels' (analogous to pixels in a 2-D digital photograph). The entire model can then be regarded as a 3-D matrix, with the attenuation coefficients μ_i of the voxels as its entries. Figure 1.2 represents a $(4,4,1)$ matrix. It depicts the path an X-ray may follow passing through voxels with different values μ_i. This discretisation allows us to change equation 1.4 to:

$$I(x) = I_0 e^{-\sum_{i=1}^{N_X} \mu_i \Delta x} \tag{1.5}$$

The initial and final intensities can be read of the settings of the X-ray tube and the detected signal. Based on these values, image reconstruction algorithms derive the three-dimensional linear attenuation coefficient matrix. For convenience, the computed numbers are converted to Hounsfield Units which are displayed in the final image. [1], [2]

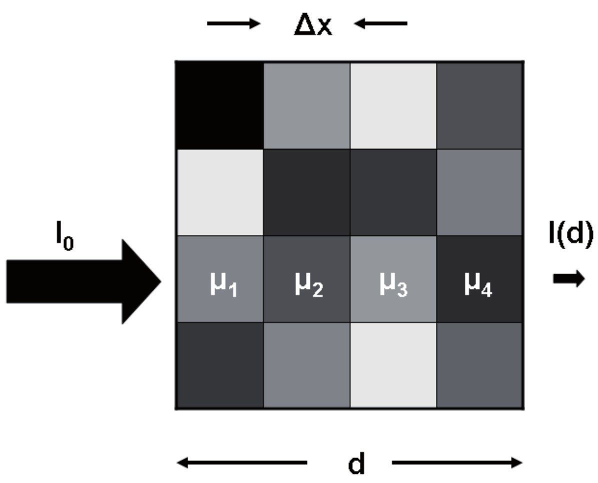

Figure 1.2: Simplified attenuation matrix (4,4,1); [image source: [2]]

Hounsfield Units

In a final CT scan, voxel values are recorded in Hounsfield Units (HU), which relate to the attenuation of water at room temperature:

$$HU_{material} = \frac{\mu_{material} - \mu_{water}}{\mu_{water}} \cdot 1000 \tag{1.6}$$

Table 1.1 lists types of human tissue and their values on the HU scale. Generally, HU values range from -1024 to +3071 (12 bit), but the upper limit can be extended to 15,359 (14 bit) if materials with even higher attenuation need to be visualised (e.g.

Table 1.1: Average HU values for various types of human tissue

Substance	HU
Air	–1000
Lung	–750 (–950 to –600)
Fat	–90 (–100 to –80)
Water	0
Muscle	+25 (+10 to +40)
Brain, white matter	+25 (+20 to +30)
Kidneys	+30 (+20 to +40)
Brain, grey matter	+35 (+30 to +40)
Blood	+55 (+50 to +60)
Liver	+60 (+50 to +70)
Compact bone	+1000 (+300 to +2500)

implants).

Typically, CT scans are displayed on computer monitors, which imposes the need to map the HU values to a 8-bit greyscale (256 steps of luminosity). Since the number of possible values (dynamic range) on the HU scale is 16 times the shades of grey on a screen (12-8 = 4 bit difference; equivalent to a factor of 2^4) the screen cannot convey all details at the same time. A linear mapping would result in 16 neighbouring HU values being compressed to the same brightness on the sreen. This way, the brightest (bone) and darkest parts (soft tissue) of the image would be clearly distinguishable. At the same time small differences (<16 HU) would appear to have exactly the same intensity. However, most of the time, the doctor's focus might lie either on soft tissue or bone material. Bearing in mind that soft tissue values range only from 10 HU to 70 HU at most (see table 1.1), such a compression would make distinguishing tissues using CT very unreliable. Instead of showing detail from the lowest to the highest value, a range of values - a so called window - can be chosen. Let's assume, for example, a range from -100 to 155 HU to be of interest. This selected range can be mapped directly and uncompressed to a 8-bit greyscale. Any values above 155 HU will be assigned the brightest value (white = 255), below -100 the darkest (black = 0). While showing very good soft tissue contrast, all bones would be depicted with exactly the same brightness (255), even though they might have a varying HU values. For bone structures, a range from 300 to 2500 HU might show sufficient contrast. Standard computer programs used to display CT images allow the user to change the window interactively to any value range. [1], [2]

Image acquisition

The time necessary to collect 1-D attenuation projections from sufficient angles is called 'acquisition time'. In 2-D X-ray scanning only one picture is taken, while a 3-D CT model is made up of a photo sequence. If the patient moves during the imaging process, the final model would show motion artefacts which might lead to wrong conclusions. Consequently, CT scanners are designed to minimise acquisition time while ensuring sufficient image quality. Very fast CT protocols result in smaller resolution, because less images are taken. It has to be said, though, that CT acquisition time is usually already significantly shorter than MRI. [1], [2]

Image quality

Additionally to the relatively short acquisition time, CT scans show little distortion compared MRI (see 1.3.3), which is why they are often used as 'gold standards' (reference scans used for MRI distortion assessment).

While bone structures are clearly visible in CT scans, 'soft tissue contrast' is relatively low compared to MRI. In other words, parts of the body which are considered as 'soft tissue' (intestines, brain, blood vessels, etc.) differ little in brightness and are therefore hard to distinguish. See 1.3.1 for more information.

Another aspect of image quality is the 'low contrast resolution' of the scan. It directly relates to how much structures and their surroundings have to differ in signal intensity to be clearly distinguishable by doctors. The quality of the 'low contrast resolution' is mainly limited by noise. Noise is a random pattern underlying the actual signal and is always present to some extent. It's prominence in the final image is described by the Signal to Noise Ratio (SNR). If the SNR is too low, fine structures blend with the noise and cannot be distinguished. Strategies to achieve a high SNR include raising the initial photon flux (intensity) or employing contrast agents. The intensity is governed by the tube current, which is limited by the heat capacity of the tube and health considerations regarding the patient dose.

Alternatively, the spatial resolution can be decreased, effectively combining neighbouring image slices. This way the SNR for the combined slices is increased, but fine structures along the z-axis might be lost due to the reduced resolution. [1], [2]

Health considerations

CT scans describe the attenuation throughout a patient, which is directly related to how much energy is transferred from photons to matter. Only because X-rays are absorbed by the human body, this imaging modality gives insight in the density distribution of a body's interior. However, this transferred energy is capable of causing biological damage. (see 1.2.2)

While the radiation dose administered during a single CT scan is relatively small (typically not more than 15 mSv) and almost negligible compared to the dose administered during a potential radiation therapy, patients receiving this dose regularly end up with a potentially harmful accumulated amount of radiation. Cancer patients, for instance, need to be imaged frequently during treatment planning. However, patients might die before those consequences come into effect. Therefore, it is typically children (who received a great number of CTs) to suffer from induced cancer occurring up to 40 years later. So while the benefit from using CT for diagnostics far outweighs the damage, there have been major efforts to reduce dose while maintaining reasonable image quality. [5]–[10]

1.3.3 Magnetic Resonance Imaging - MRI

Magnetic Resonance Imaging (MRI) is a 3-D imaging modality based on Nuclear Magnetic Resonance (NMR), a phenomenon discovered by physicist Isidor I. Rabi in 1938. Atomic particles such as protons have an inherent quantum mechanic feature called 'spin', which is associated with a magnetic moment μ. Without an external field, a proton's spin is oriented in a random direction in space and so is its magnetic moment. The sum of magnetic moments belonging to a number of protons results in a net magnetisation. Due to their random orientation, the net magnetisation will be zero for a sufficiently high number of particles. This is because, on average, for every proton's spin there is always another particle's spin oriented exactly the opposite way cancelling its magnetic moment.

In the case of an applied external magnetic field (this static field is often called B0), the spins will either align parallel (pointing in the same direction) or anti-parallel (opposite direction) to this field, where their energy reaches a local minimum. Parallel protons have an even lower energy than those pointing the other way. In a collection of many spins, the number of parallel spins will therefore slightly dominate, resulting in a net magnetisation greater than zero (see figure 1.3). In other words, only the amount of protons that is not compensated by those looking in the opposite direction contributes to a detectable magnetic field.

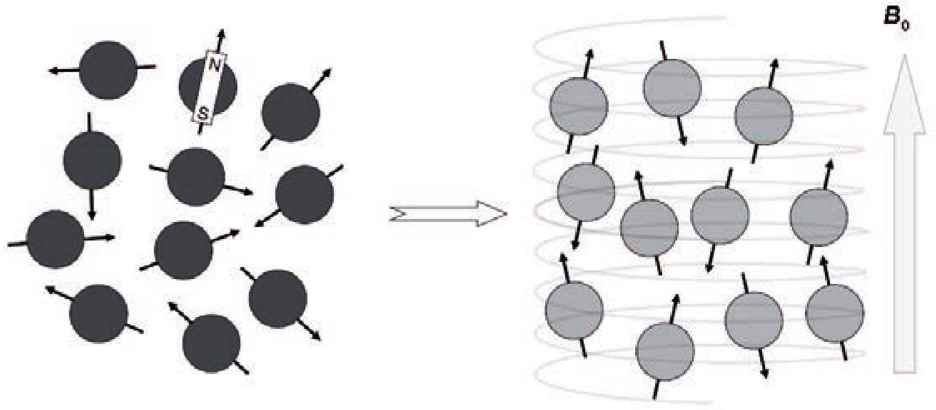

Figure 1.3: The spins, initially oriented randomly in space, become aligned either parallel or antiparallel to an externally applied magnetic field B_0. [image source: [2]]

By applying a short radio frequency pulse (often referred to as B1), the total external magnetic field changes and the magnetic moments start precessing around that new external field. The pulse duration is usually chosen as to flip the spins by a 90^o angle. They are now oriented in the transverse plane to the original external field, and so is the resulting net magnetisation. Similar to how a spinning top rotating at an angle to the direction of gravity precesses, the magnetic moments will now precess about the direction of the external field with a frequency linearly proportional to the external field strength. This precession movement can be detected as induced current in a receiver coil, because the net magnetisation still follows the spins' orientation. Again, the particles would like to minimise their energy by aligning their spins to the external field, but in order to do so they need to give away the surplus energy, transferring it to the surrounding lattice. Those spin-lattice interactions happen with different efficiency depending on the tissue. The time it takes the spins to align is expressed in a material specific time constant T_1. Shortly after applying the radio frequency pulse, regions of the body where magnetic moments align quickly (short T_1) have a stronger net magnetisation (in the direction of the external field) than those where energy is being transferred slowly (long T_1).

At the same time, the spins interact with each other, affecting the local magnetic field and spins in their vicinity. The magnetic moments, which started out precessing in phase directly after the radio frequency pulse flipped them, will precess at slightly different frequencies, due to the small fluctuations of the local magnetic field. The differences cause the collection of magnetic moments to 'de-phase' and the net magnetisation in the transverse plane to vanish. This process caused by spin-spin interactions is described by the material specific time constant T_2. Eventually, all spins will be again aligned either parallel or anti-parallel to the external field, just as they were before the RF-pulse.

Applying the RF pulse with a homogeneous field strength along the whole body would excite all spins simultaneously. In order to localise differences in tissue magnetisation, the RF pulse is instead combined with a linear magnetic gradient field 'selecting' a slice to be imaged at a time. The rest of the body is unaffected, the signal measured directly after such a pulse was applied originates only from the chosen slice. Eventually, by collecting data on the net magnetisation throughout the body in different locations ('scanning' the patient slice by slice), a 3-D image can be computed.

Depending on the information required from the examination, Doctors can choose to create images that reflect spin-lattice interactions (T_1 weighted) or spin-spin interactions (T_2 weighted).

Governed by the chosen settings, particular tissues will displayed varying contrasts. For example, areas with increased water level will be dark on T1 weighted (T_1w) MRI whereas the same areas will be bright on T_2w MRI. Additionally, certain types of materials (tissues) can be intentionally not imaged (suppressed) to reveal others that are in their close proximity. This is often done with fatty tissue that can cover relevant parts of the field of view. There are various methods how this can be achieved. MR imaging gives practically endless possibilities in terms of selective imaging and is mostly limited to imaging time and technical characteristics of the scanner. Medical physicists and scanner vendors are incessantly working on new MR imaging methods and applications.

The set of parameters governing how the tissue is excited and data acquired is called 'image sequence'. Delineating tumours or lesions is often accomplished by looking at both T_1w and T_2w weighted images and drawing the right conclusions.

Soft tissue contains a lot of water, which is made up by oxygen and hydrogen. Hydrogen nuclei are single protons and their nuclear magnetic resonance is what MRI is tuned to visualise. This is why soft tissue appears as bright areas in MRI, whereas bone material has only little contrast. [11]

Most the scanners are build to house a receiver coil in the gantry and they are able to measure the signal using only this one coil. However, in practise, to obtain a stronger signal, a smaller coil is typically placed closer to the source of the signal, the patient.

As the region of interest (ROI) is usually limited to a specific organ, receiver coils are available in different sizes and shapes, often designed to fit the patient with a comfortable but narrow space in between. To get even closer, so called 'surface coils' can be placed on the patient. 'Spine coils' are sometimes hidden in the table on which the patient lies during the examination. Typically, for creating images of a patient's head, coils with a fixed arc-like geometry are used. This type of coil was also used for the data acquisition of this thesis.

Studies have shown that delineating certain types of tumours, for example prostate cancer, is more accurate using MR images than using CT. [12]–[14]

In diagnostics, MR images prove to be very useful. Also for radiation therapy treatment planning, the superior soft tissue contrast is exploited during the definition of organs at risk and targets. Unfortunately, due to the physical principles of MRI, it indirectly provides the information about the proton density, whereas CT can provide information about electron density. It is the knowledge of the electron density which is necessary in the treatment planning process. During this, the dose distributions are calculated based on the applied beam geometry and the distribution of matter on its way.

Image Quality

Contrary to CT, MRI is prone to distortion due to field inhomogeneities. Organs might appear shifted, elongated or shrunk. The effect is most prominent along the outer edges of the scanner's field-of-view (FOV). In the isocentre (middle) of the scanner, the distortion is smaller, because here the field is least aberrant. For most applications, small position shifts and deformations are of minor importance. MRI scanners usually come equipped with an internal distortion correction algorithm. Figure 1.4 shows the unmodified and the corrected version of an image coming from such a scanner. Those methods are developed by the company designing the scanners. Knowing the technical details enables them to write tailor-fit scripts which drastically reduce the distortion.

However, for radiotherapy treatment planning this might not be enough and it is necessary to additionally monitor the distortion and, if necessary, take additional corrective measures.

While its soft tissue contrast is superior to CT, a relatively long acquisition time is necessary to achieve a sufficiently high SNR. This leads to the risk of motion artefacts (patients moving during the scanning procedure). To tackle this issue, resolution can be reduced, effectively combining signal from several voxels to create a single voxel, reducing the overall noise. The trade-off is that fine structures might get lost.

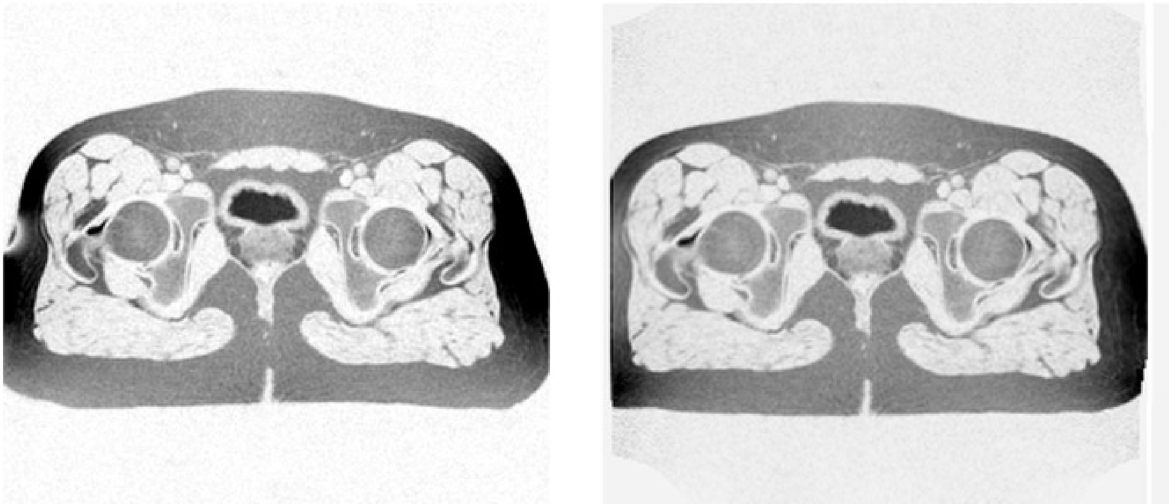

Figure 1.4: On the left is the original image, on the right the automatically corrected version of the same MR image (inverted colours) [image source: Courtesy Piotr Andrzejewski (unpublished data)]

Health considerations

Strong, static magnetic fields (typically up to $3T$) are present around MRI scanners at all times, and precautions have to be taken to ensure safety for patients and medical personnel. Ferromagnetic materials (such as steel and iron) can become dangerous projectiles in vicinity of the MRI scanner. They must be excluded from the room housing the magnet without exception.

The RF pulses repeatedly put spins in excited states, transferring energy to the human body. MRI scanners are designed to limit the rise of a patient's body temperature to 0.5^oC during standard imaging. Only combined with either medical or appropriate psychological monitoring the limit can be raised to 1^oC. An ethics committee approval is necessary for even higher values. In general, patients should be exposed to RF fields only as strong as their thermoregulatory system is capable to cope with.

Finally, magnetic field gradients are applied together with the RF pulse. They are switched at high frequencies leading to induced currents in conducting body tissue. In principle, those currents stimulate nerves which might result in muscle twitching or pain. However, gradient levels are set to avoid stimulation. During have reported some subtle biological effects, but there was no evidence pointing towards harm caused by short term exposures. At the same time, patients suffering from epilepsy might show increased sensibility to induced electric fields in the cortex and should be imaged with caution. [2] Some patients might be allergic to contrast agents used for specific MRI examinations. Here, safety procedures are similar to those performed during administration of regular drugs.

Open bore MRI scanners

The radiation oncology department of the Vienna General Hospital (AKH) is equipped with an $0.35T$ open-bore, c-arm MRI scanner (see Section 2.1.3 for more details). This open design has proven to drastically improve the well-being of patients experiencing anxiety in closed-bore scanners. For this reason, the number of incomplete MR examinations due to a claustrophobic events is relatively low. [15], [16] Besides, patients who would not fit in closed designed scanners can be imaged. Furthermore, brachytherapy patients can be placed in the scanner with applicators attached. Brachytherapy is a form of radiation therapy in which radiation sources are typically inserted into the human body to perform the irradiation from close distance; imaging is performed for dose distribution planning as well as verification of applicators position after their insertion (for more information see section 1.4).

This scanner's magnetic field is weaker than the fields of closed-bore scanners that are widely used (typically 1-3 Tesla). High field strengths result in greater resolution, better SNR ratio and faster imaging time. Generally, diagnostics benefit from greater image quality. However, at some point, diagnostic accuracy stops increasing with field strength. At the same time significant improvements can be achieved at low fields. A "combination of field independent polarisation [...] with frequency optimized MRI detection coils [...] results in low-field MRI sensitivity approaching and even rivalling that of high-field MRI." [17]

Low field MRI scanners are also typically characterised by less distorted images. [18]

Apart from the often satisfactory image quality, there are considerable cost advantages to the use of lower field MRI. The initial purchase price and the ongoing maintenance expenses are considerably lower than those of high field scanners, which often use superconducting magnets cooled with liquid helium. [19] Permanent magnets might be weaker, but do not require constant cooling. Also, low fields allow facilities to build smaller rooms and magnetic objects are less dangerous.

Diffusion Weighed Imaging - an example for non morphologic Imaging

Despite the fact that this type of MR imaging was not used for this thesis, it will be mentioned here as an example of the vast range of measurements possible with MRI techniques.

Diffusion weighted (DW) imaging quantifies molecular diffusion in the body. This imaging technique uses MRI technology differently: Additionally to the gradients needed to select a slice (strength $3-5\,mT/m$, duration $2-4\,ms$), the sequence for DW imaging applies two long, strong, consecutive and opposite gradients (strength $30-50\,mT/m$, duration $20\,ms$) during which molecules may move due to diffusion. After those two gradients (which, usually, will be applied in all three Cartesian directions), the remaining signal (net magnetisation) is measured by the receiver coil.

Molecules which are restricted in their movement will experience two equally strong but opposite magnetic fields. The first will cause them to precess with a certain speed (linear with field strength), effectively changing their phase. The second will cause them to precess exactly the other way around (same strength, but other direction), returning them to their initial state. Now they will again be in phase and result in a net magnetisation which is not zero, but visible as bright areas on the scan.

Those molecules which are free to move, however, will not experience a constant field strength, because the field has a gradient. As they move through the body they will precess at varying speeds during the first and then at different speeds during the second gradient. As a result, they will be out of phase when the net magnetisation is measured by the receiver coil, and will not cause bright areas in the scan.

DW imaging can be used to diagnose acute strokes (brain infarct), because areas with restricted diffusion (blocked blood flow) show a strong signal compared to healthy tissue with normal diffusion. Another interpretation of low diffusion (high measured signal) can be the increased cellular density (so dense that free diffusion of water molecules is suppressed) which is characteristic for cancerous tissue.

Since the time necessary to allow the molecules to move during the two gradients is relatively long, the image will naturally be T_2 weighted. This is taken into account by creating a second image which is also T_2 weighted, but does not apply two consecutive opposite gradients. oThe difference between the DW and the not DW weighted sequences reflects the actual contribution of diffusion (apparent diffusion coefficient - ADC). [20]

1.4 Radiation therapy

Radiation therapy utilizes ionising radiation to damage or kill cancer cells in order to stop them from multiplying. This prevents the growth of tumours, makes them shrink in size and hopefully cures the patient.

During radiotherapy treatment planning (RTP), 3-D models of the patient are used to define targets (regions where the dose should be delivered to) and organs at risk (where the dose should be delivered to). This ensures that vulnerable organs are spared from radiation while making sure the tumours receive sufficient dose. Moreover, methods to quantify the amount of radiation that different body parts absorbed are needed, because the actual treatment might differ from the plan.

While travelling through matter most types of radiation release energy mainly due to coulomb interactions with the outer shell electrons of atoms. Knowing the electron density of the targeted tissue area is therefore essential. In order to reach a specific penetration depth, the particles' initial energy has to be chosen accordingly. The necessity to treat the tumour with a required amount of radiation leads to a radiation therapy treatment plan.

There are two well established methods for applying the radiation. External beam radiotherapy (EBRT) is performed from afar: Gantries are able to position the radiation source around the patient in a way covering virtually any possible angle. During a treatment session, fractions of the total dose are administered from many different angles (or continuously with alternating gantry angle). The sum of those individual treatments results in the required dose distribution. Figure 1.6 shows an example of two differently calculated treatment plans.

In conventional EBRT, photons (X-rays) in the range of 4MeV to 20MeV are used to deposit the necessary dose at the location of the tumour. Unfortunately, radiation interacts with all cells it passes until it is fully absorbed. It releases its energy along its entire path while travelling through the patient. This behaviour may result in dose being delivered to cells all the way from the point of entry to the point where the (weakened) ray leaves the patient. Other types of ionising radiation are also used, but less common. Electrons and low energy X-rays are favoured for superficial tumours; rare methods using neutrons and even muons also exist. Charged particle therapy (using e.g. protons or carbon ions) is on the rise, but far from reaching the availability of X-rays. This type of radiation minimises the damage done to healthy tissue due to its distinctive behaviour in energy loss called “Bragg Peak”. They release most of their energy only shortly before being stopped completely. [21] This effect can be used to spare tissue lying behind the tumour from radiation entirely and also reduce the amount of energy transferred to organs located before. [22] A comparison between the behaviour of X-rays and protons is shown in figure 1.5.

Brachytherapy, on the other hand, is when the radiation source is placed close to or inside of the patient. The source is either moved close to the target area using applicators (temporary treatment) or implanted permanently. The latter method is done by inserting so called "seeds" (sealed metal containers with radioactive material) directly into the target area where they release high amounts of radiation. Over time they become less active and eventually the treatment stops automatically. These rice grain sized implants can remain in the body without causing any harm. Treatment of prostate and cervix cancer is often done with this technique. In comparison to EBRT, Brachytherapy allows higher doses while at the same time minimising the radiation reaching organs at risk; precise dose distributions can be achieved. At the same time, not all cancer types can be treated this way. For some, a non-invasive method (e.g. EBRT) is a better alternative.

[2] image source: by Cepheiden - `https://commons.wikimedia.org/wiki/File:Dose_Depth_Curves.svg`, [GFDL (`http://www.gnu.org/copyleft/fdl.html`)], via Wikimedia Commons

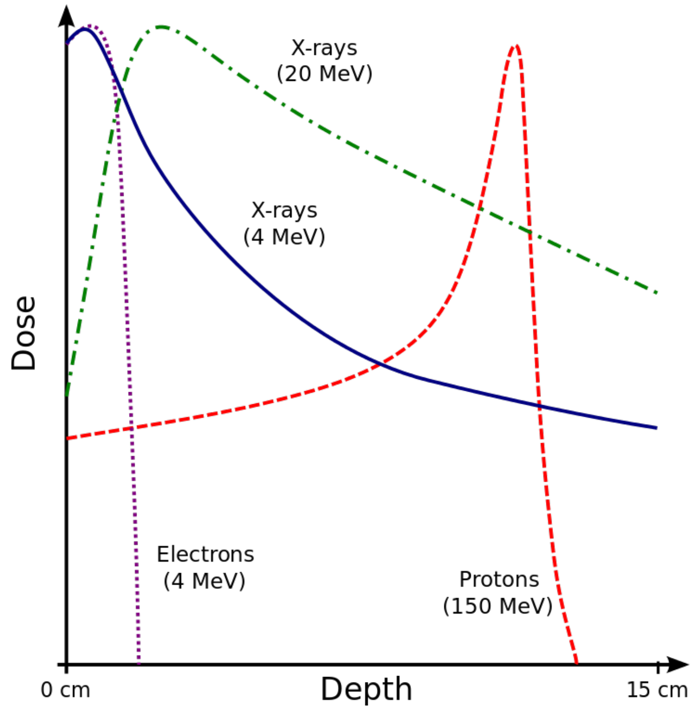

Figure 1.5: Energy release of ionising radiation [2]

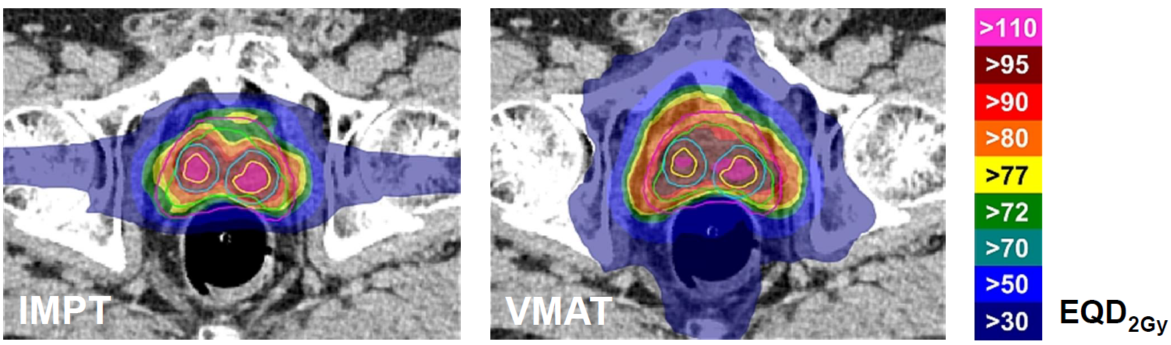

Figure 1.6: Example of Radiotherapy treatment plan: coloured areas represent dose values deposited during treatment. The plans were calculated using different treatment techniques: with protons (IMPR) and photons (VMAT). (image source: [23])

1.4.1 Role of CT

Until recently, RTP relied almost entirely on CT. There are two main reasons for this:

Firstly, calculating the electron density using data obtained with CT is an straightforward task. Secondly, CT images generate 3D images with little distortion. Exact geometries are needed for correct RTP. It is the most reliable approach to create precise radiotherapy treatment plans. [24], [25]

1.4.2 Role of MRI

MR images also record luminosity values, but they do not correspond to radiodensity. Due to the better visibility of tumours on MR images, RTP often uses combined data from both imaging modalities. Additional information derived from DW MRI, for instance, can also support response prediction and assessment. However, there are some difficulties arising from combining CT and MRI for EBRT: in order to profit from separately acquired data, the resulting images must be aligned (registered) either manually or automatically. This is a hard task since non-rigid objects (organs) change their shape and location between measurements which may lead to inaccuracies. Algorithms supporting non-rigid registrations are already under development, but there is still room for improvement. For now, only local rigid registration is capable of reliable target and organ at risk definition.

Alternatively, MRI-only radiation therapy protocols are being developed: one way of doing this is to use MRI data to create a Pseudo-CT, which contains information about electron density. Comparisons to using CTs and MRI-based pseudo CTs have shown acceptable deviations for X-ray therapy. In charged particle therapy the resulting dose gain in healthy tissue and dose loss in cancer regions owed to inaccurately assigned electron density values is bigger. However, further improvement of accuracy promises to reduce time and money needed for RTP when CT is no longer needed. Furthermore, patients would be spared the additional dose of CT examinations. [26]–[30]

1.5 Aim of this work

The idea of only using MRI for treatment planning is approaching the clinics, but there are still some issues that need to be addressed.

Due to the possible image distortion, great care needs to be taken and the MR images must be verified before they are used for RT target definition and dose calculation. The available MRI scanner at the AKH is equipped with an on board correction algorithm which is supposed to reduce distortion. See figure 1.7 for an example of how this correction affects an image. Distorted images might lead to wrong calculations of how much energy is needed for the radiation to accumulate exactly at the target region. If, for example, bone structure is depicted as thicker than it really is, RTP would suggest a treatment which would deposit more energy behind the tumour than intended. The opposite holds for cases where tissue appears to be thinner, which would result in areas lying before the tumour being irradiated.

The goal of this work is to: find an optimal (providing satisfactory image quality and convenience of use) liquid filling for the rod cavities in an already existing custom designed distortion phantom provided by the Medical University of Vienna to be able to acquire the reference CT image and test MR acquisitions.

Develop and implement a method to assess and illustrate the distortion of the MR image based on tracking of the distortion of one of the phantom rods, with an option to further extend the tool for mutli-rod tracking.

Therefore, this work focuses mainly on the assessment of the acquired imaging data (using the implemented software tools), choosing which liquids to fill the phantom with, but not its entire design. However, possible fillings have to be produced and tested. Similar approaches are being used for distortion correction by other facilities. [31]–[36]

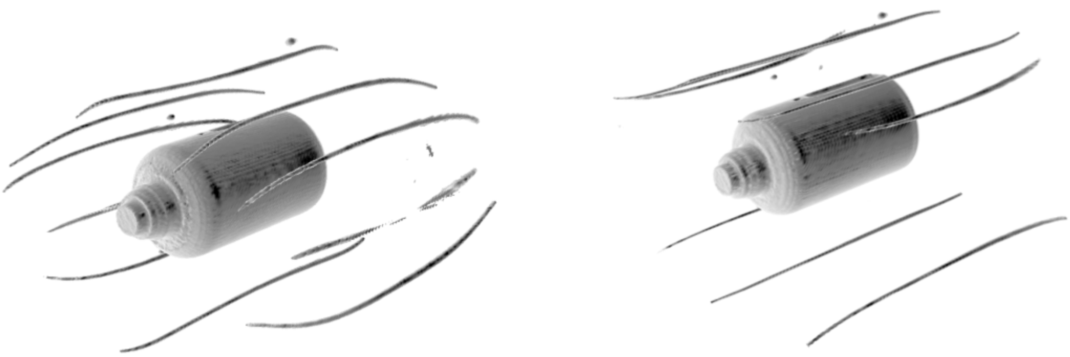

(a) MR scan with no distortion correction

(b) MR scan after internal distortion correction

Figure 1.7: Rendered MR scan showing the difference before (a) and after (b) applying the build-in distortion correction. [image source: Courtesy Piotr Andrzejewski (unpublished data)]

2 Material and methods

2.1 Scanners and Imaging protocols

The radiation oncology department of the Vienna General Hospital (AKH) owns a CT scanner and a open-bore, c-arm MRI scanner.

2.1.1 MR

Following the general practice of phantom measurements, and the AAPM recommendations on phantom filling materials [AAPM 1990 and 2010]/ [37] oils or water with addition of paramagnetic substances (to reduce the spin-lattice relaxations times) were chosen (generally short T1 time of 200-400 ms). This, combined with a T1-weighted test sequence, improves the efficiency of the measurements assuring relatively high SNR in short time. To further improve image quality, the averaging parameter of the test sequence was set to 4. This setting practically means the measurement is repeated and averaged n times by the scanners software. Remaining sequence parameters were optimized to yield a acceptable resolution for the chosen ROI setting (which is relatively large as it covers the whole phantom). The test sequence was chosen in a way, such as to deviate as little as possible from a typically used clinical imaging setting. However, to fully understand and investigate the possible image distortions, each clinically used sequence should be commissioned with a distortion phantom. Detailed sequence parameters are listed in table 2.1

system	MR
manufacturer	Siemens
product name	Magnetom C!
coil	Body/Spine Array Coil XL
[internal W x H]	[50 x 30.5 cm (19.7 x 12 in)]
orientation	axial
sequence	T1 weighted 3D-FLASH Vibe (Volumetric interpolated breath-hold)
slice thickness	2.3 mm
pixel spacing	2.3 mm
matrix	128 x 120
repetition time	7,07ms
echo time	2,7
bandwidth	240
flip angle	6 deg
averages n	4
acquisition time	17.5 min

Table 2.1: MR scanner and used protocol

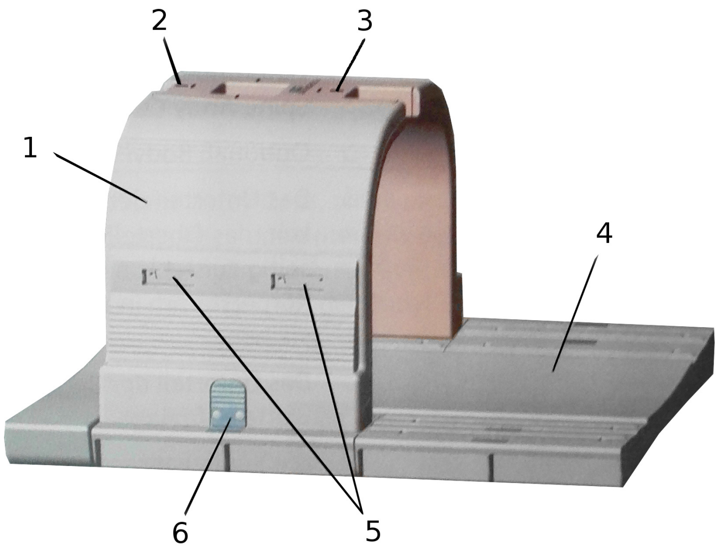

Figure 2.1: MR scanner coil: (1) upper part, Body/Spine Array Coil; (2,3) central positioning markers; (4) lower part, Body/Spine Array Coil; (5) connection ports; (6) colour label [image source: (with kind support of Siemens Healthineers)]

2.1.2 CT

To generate a reference CT image set a typically used clinical pelvis imaging protocol for radiation therapy planning (with increased resolution 0.6 mm) was used (see table 2.2).

system	CT
manufacturer	Siemens
product name	SOMATOM Definition AS
software version	syngo CT 2013B
protocol	Prostatae_VMATAdult
slice thickness	0.6 mm
row spacing	0.801mm; 512
column spacing	0.801mm; 512
kVP	120kV
x-ray tube current	19 mA
convolution kernel	I30f, 3

Table 2.2: CT scanner and used protocol

2.1.3 MRI scanner - field distribution

The Magnetom C! MRI scanner comes with a handbook which contains diagrams of the magnetic field strength (fig. 2.3) and its gradient (fig. 2.4, 2.6 and 2.5). Figure 2.2 shows an image and different views of the scanner and the planes along which the field strength and gradient are displayed. Patient are positioned as to place the ROI at the isocentre, the area where the B0 field is most homogeneous (where there is a low gradient).

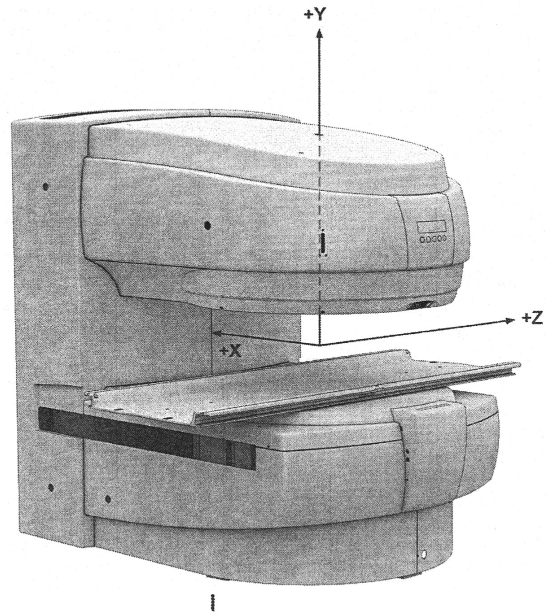

(a) Image of scanner
x,y, & z -axis

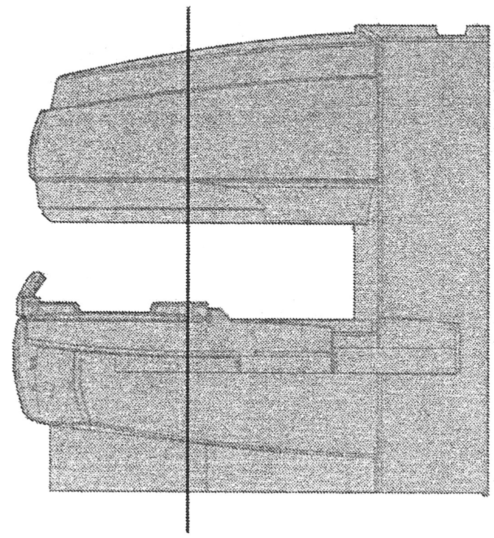

(b) side view along z-axis,
black line represents plane for front view (see fig. 2.5)

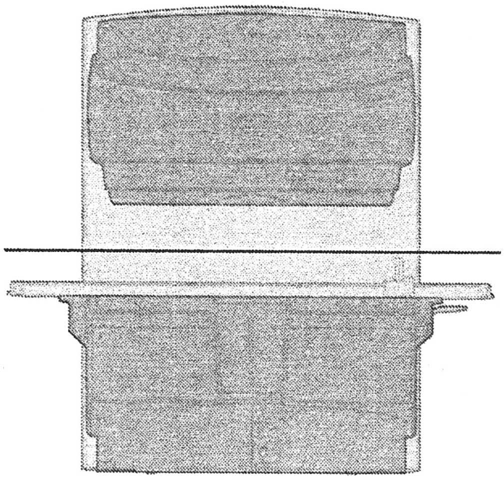

(c) front view along x-axis,
black line represents plane for top view (see fig. 2.6)

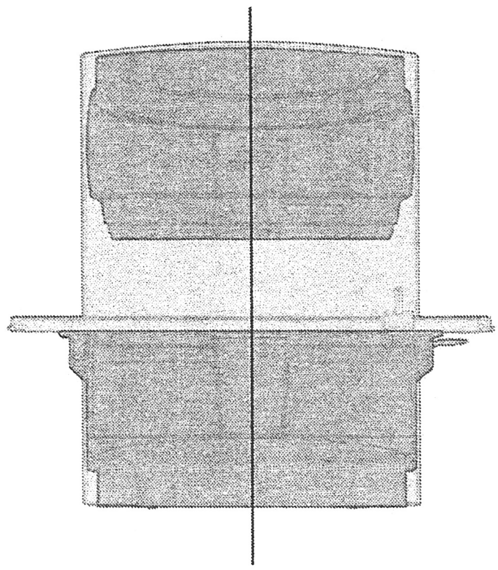

(d) front view along x-axis,
black line represents plane for side view (see fig. 2.4 and 2.3)

Figure 2.2: Magnetom C! [image source: [38] (with kind support of Siemens Healthineers)]

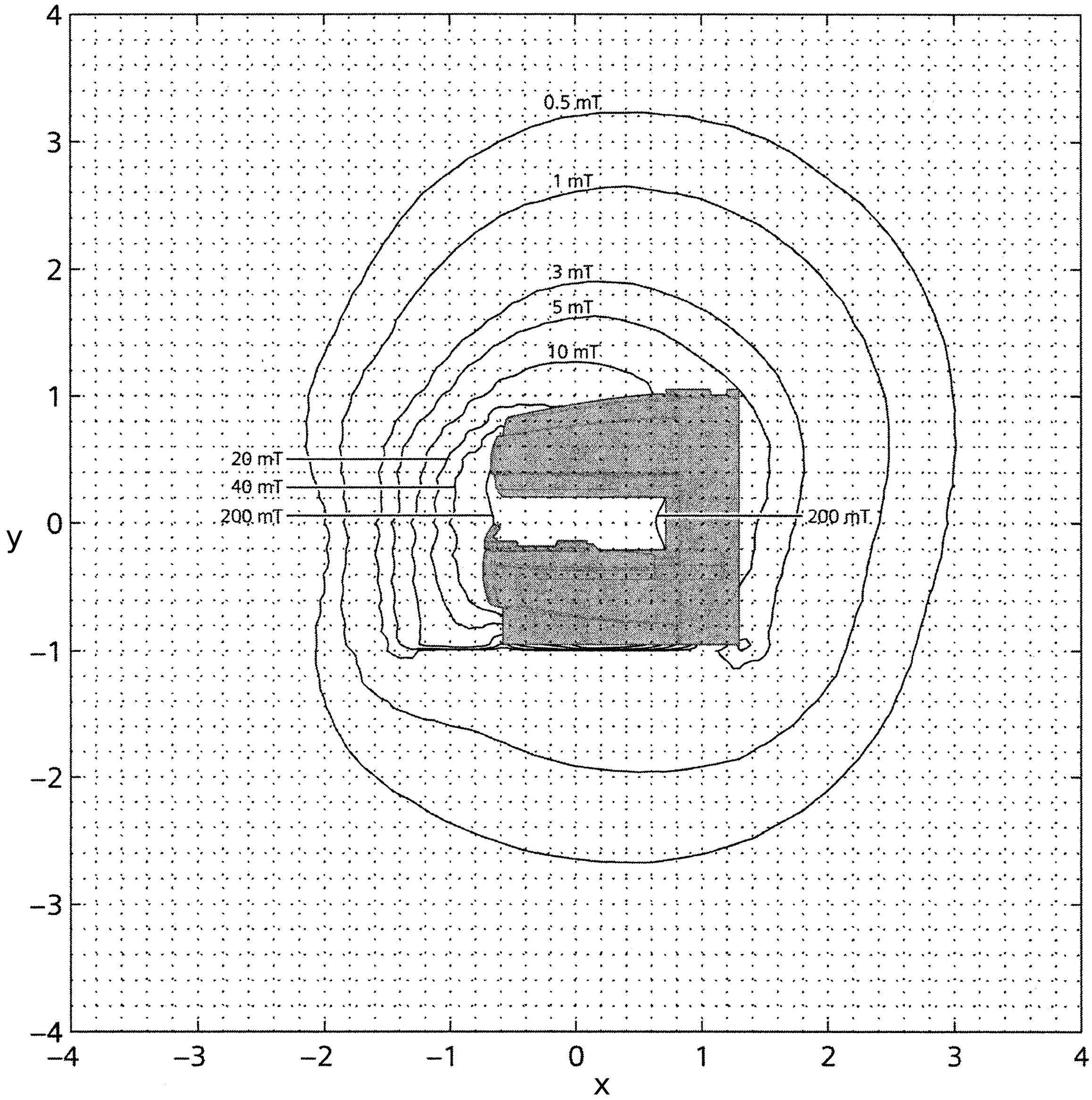

Figure 2.3: Magnetom C! field strength
side view along z-axis (see fig. 2.2d) [image source: [38] (with kind support of Siemens Healthineers)]

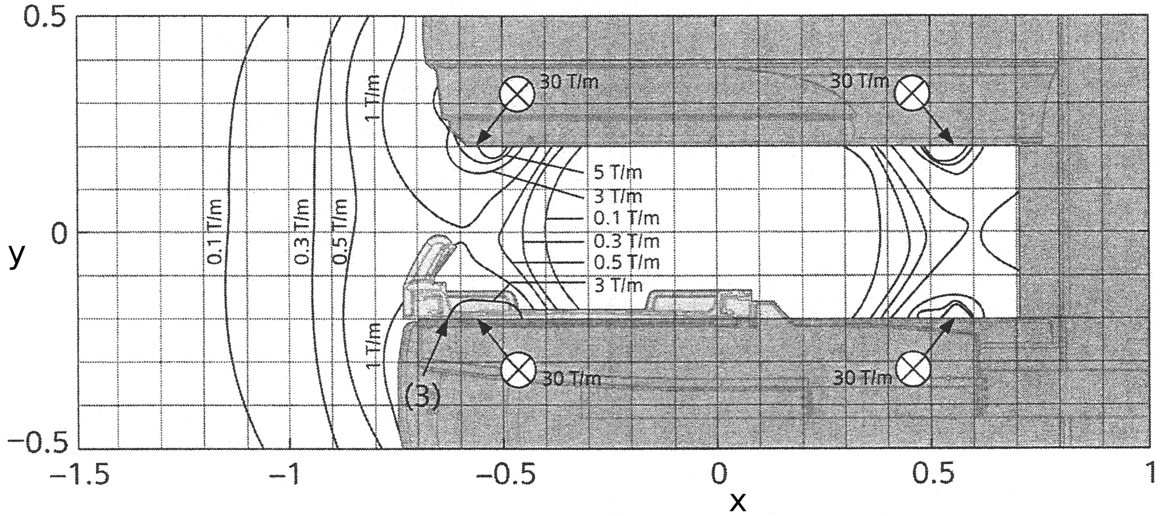

Figure 2.4: Magnetom C! field gradient
side view along z-axis (see fig. 2.2d) [38] (with kind support of Siemens Healthineers)

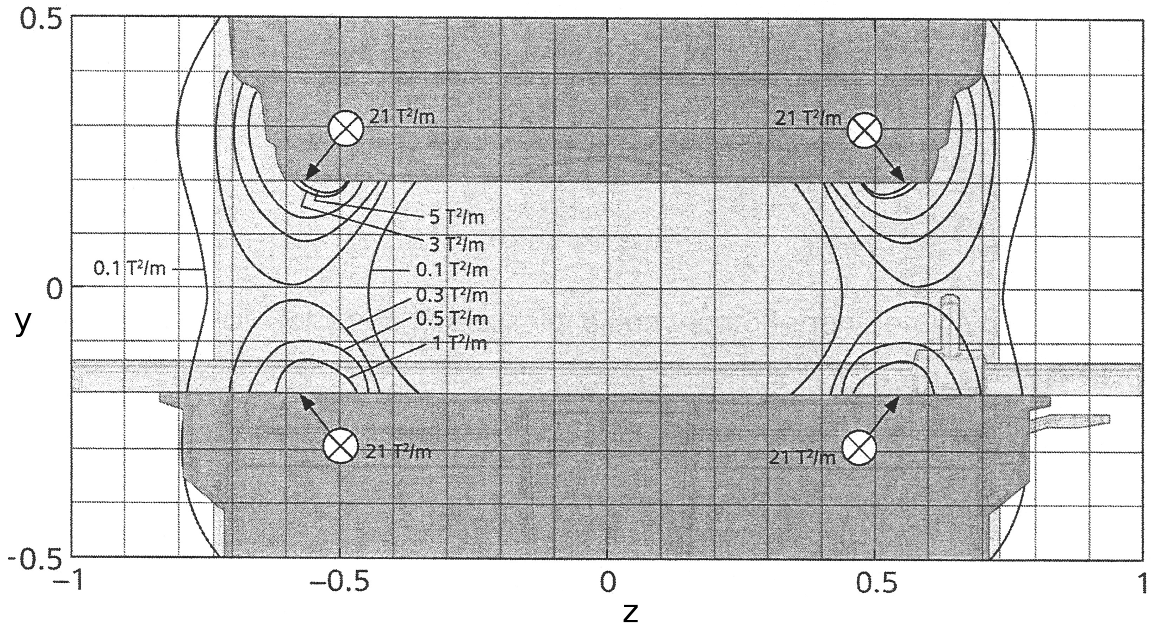

Figure 2.5: Magnetom C! field gradient
front view along x-axis (see fig. 2.2b) [image source: [38] (with kind support of Siemens Healthineers)]

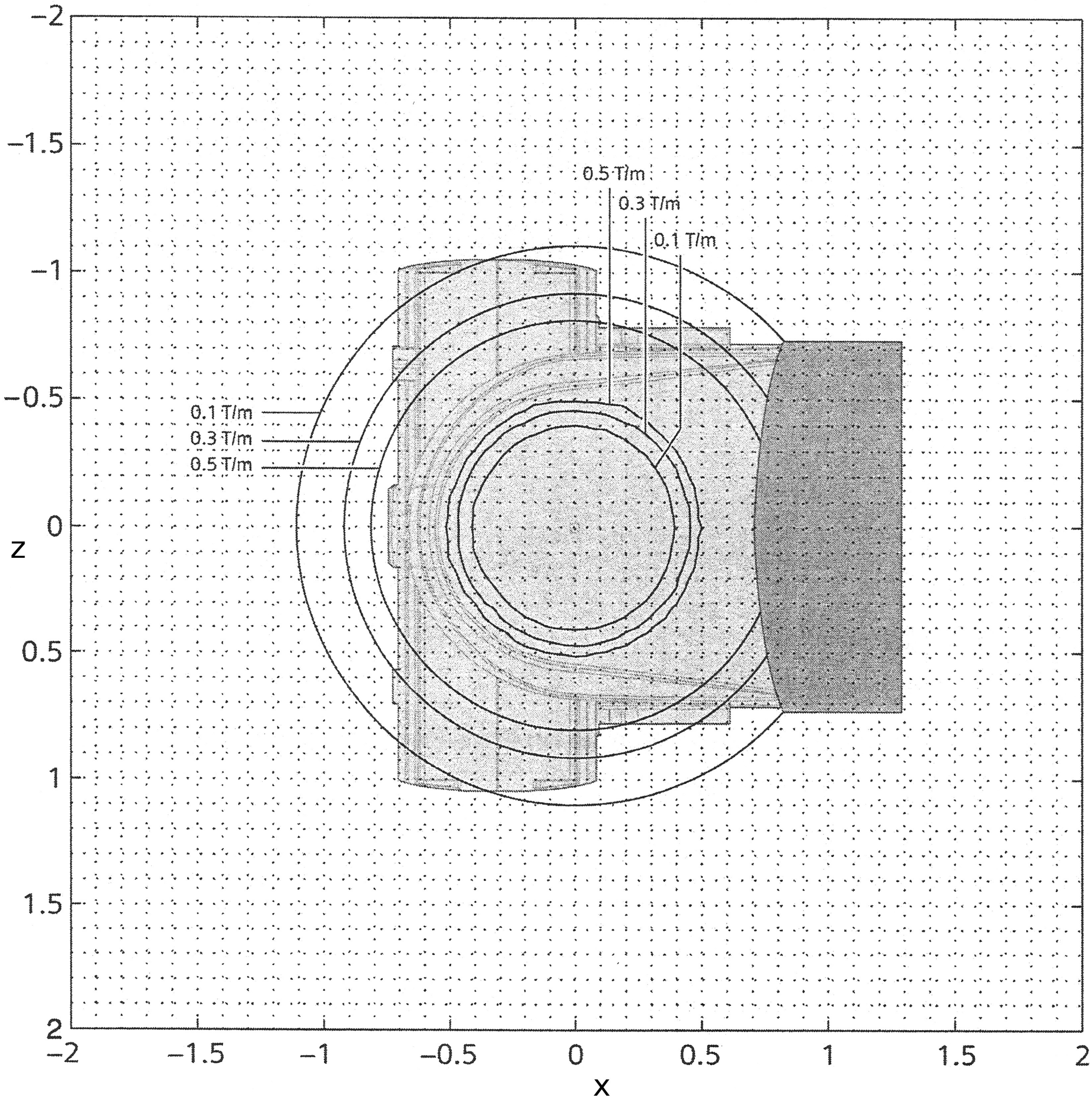

Figure 2.6: Magnetom C! field gradient
top view along y-axis (see fig. 2.2c) [image source: [38] (with kind support of Siemens Healthineers)]

2.2 Custom build phantom

To compare images from different scanners and asses occurring distortion, a rigid object with known dimensions is necessary. Such a 'phantom' is often made from plastics filled with liquids which are easy to handle and typically well seen on MR and CT images. The AKH's design is made up from an array of replaceable, fillable plastic rods.

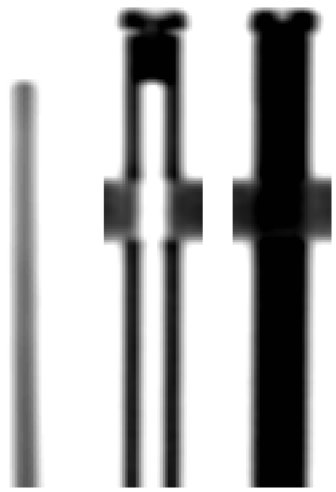

(a) MR (b) CT (c) CT

Figure 2.7: Comparison (inverted colours): MRI only shows liquid filling, CT also the plastic rod and pane (horizontal black bar crossing middle and right rod); (**a:**) *MRI* - filled rod, plastic not visible (field of view too small to show entire rod); (**b:**) *CT* - empty rod, plastic visible; (**c:**) *CT* - filled rod, plastic and filling visible

2.2.1 Frame and rods

The phantom was build to fit the largest available rigid coil for the MRI scanner. Three parallel acrylic glass panes in the shape of the coil serve as a frame for the plastic rods. In the middle an empty area was reserved for an optional additional smaller phantom (not used for this work). Figure 2.8 shows a rendered CT picture of the phantom. See also figure 2.9 showing a CT image of one pane (with no rods inserted).
More than 300 plastic rods (length: 50cm, outer diameter: 8mm, inner diameter: 4mm, volume: approx. 6ml) could be placed in the phantom. See figure 2.10 for a schematic sketch of one rod. The bottom part of each rod was sealed with a glued plastic plug,

the top could be closed with a plastic screw. Frame and rods were already build and assembled before the author started working on this project.

Additionally to the rods which would be used to assess the distortion, a number of vitamin-e pills were attached to the frame as reference markers (see figure 2.11). These pills are visible in both CT and MRI images and were used to align them (see section 2.3). This way there is another way of checking the alignment during the prototyping process in addition to the rods.

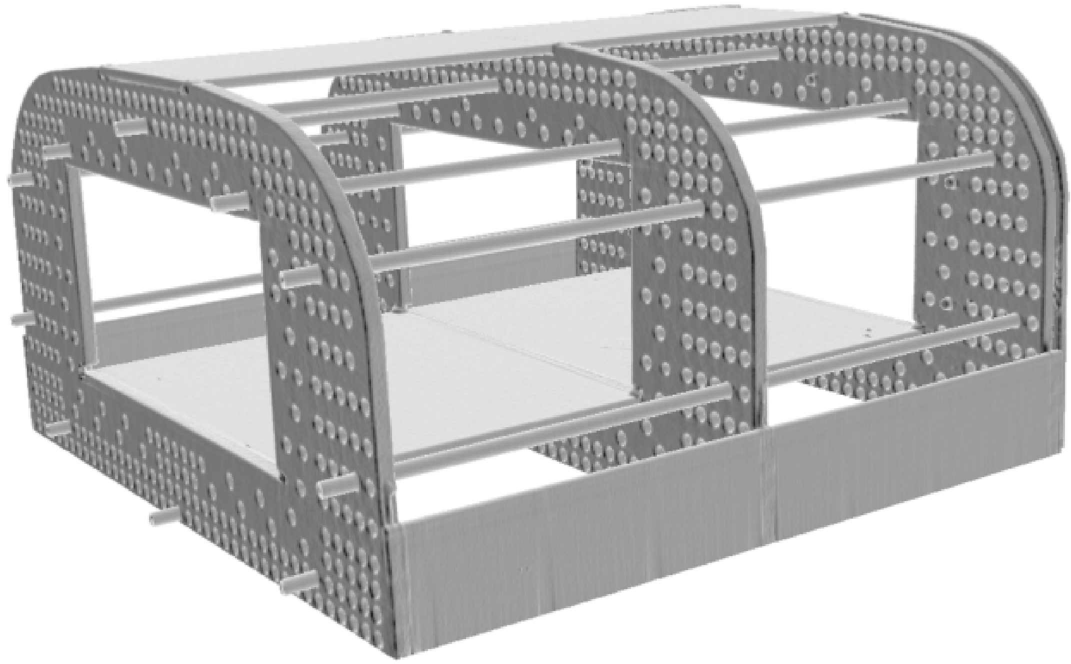

Figure 2.8: Rendered CT image of phantom [image source: Courtesy Piotr Andrzejewski (unpublished data)]

Figure 2.9: An axial view of one of three plastic panes that make up the frame of the phantom. This scan shows how the pane looks like with no rods inserted. A little 'x' in one of the holes slightly to the right of the lower part of the pane marks where rod #5 was inserted later for imaging (see section 3.3.1); a little 'z' in the centre of the upper area indicates where rod #16 was inserted for another imaging sequence (see section 3.3.2).

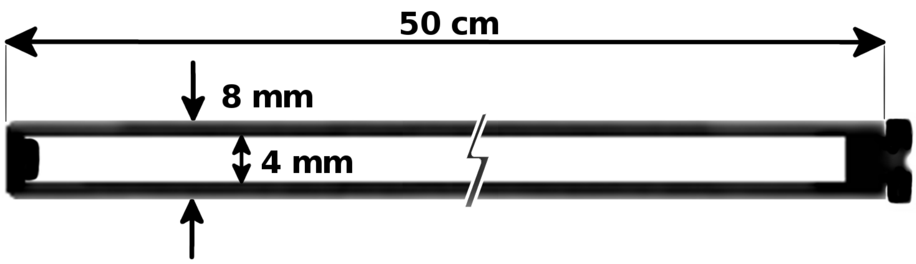

Figure 2.10: A schematic of an empty plastic rod as they are used for the phantom (inverted colours). On the left the rod ends with a glued plastic stopper, on the right hand side a plastic screw seals it. The figure does not show true proportions.

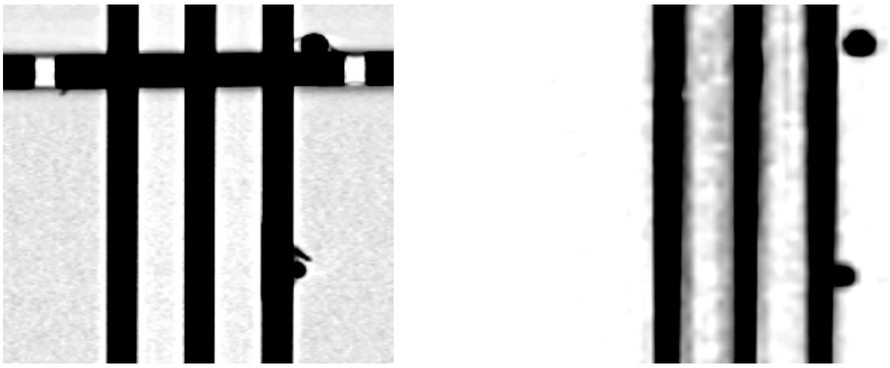

(a) CT scan (b) MRI scan

Figure 2.11: CT (a) MR (b) coronal images (inverted colours) showing rods and 2 attached vitamin-e pills visible on the right hand side of the rods. In the CT scan the plastic pane and adhesive tape used to hold the pills in place are also visible.

2.2.2 Rod fillings

For this study 17 different liquids were produced to be tested as possible fillings. They are listed in Table 2.3.

No.	$NaCl$	$CuSO_4 \cdot 5H_2O$	Soap	Ascorbic Acid	Agar	Primovist [volume-%]
#1						
#2	3.6	1.96				
#3	3.6	3.92				
#4	3.6	19.6				
#5	3.6	1.96	1			
#6	3.6	1.96	5			
#7	3.6	1.96	20			
#8	3.6	1.96		0.36		
#9	3.6	1.96		3.6		
#10	3.6	1.96		36		
#11	3.6					0.1%
#12	3.6					1%
#13	3.6					10%
#14	3.6	1.96			0.5	
#15	3.6	1.96			20	
#16		Motor Oil:	*Castrol Power1*			
#17		Silicon Oil:	*Charge: 15HLVY023*			

Table 2.3: The composition of all tested solutions.
(components in g/L; exception: Primovist in volume-%)

#1 *distilled water*
#2 $NaCl + CuSO_4 \cdot 5H_2O$
#3 increased concentration of $CuSO_4 \cdot 5H_2O$
#4 further increased concentration of $CuSO_4 \cdot 5H_2O$
#5 generic washing-up *soap* added to **#2**
#6 increased *soap* concentration
#7 further increased *soap* concentration
#8 *ascorbic acid* added to **#2**
#9 increased *ascorbic acid* concentration
#10 further increased *ascorbic acid* concentration
#11 *Primovist*
#12 increased amount of *Primovist*
#13 further increased amount of *Primovist*
#14 *agar*
#15 increased *agar* concentration
#16 synthetic motor oil
#17 silicon oil

Being closed at one end and having a capillary shape (small diameter) makes it impossible to fill the rods by simply pouring the liquid through the opening. Instead of adding the fluid at the top, it has to be injected starting at the bottom. This way the contained air is pushed out by the injected liquid through the opening at the top. A long, thin plastic tube was inserted and used for injection, leaving enough room for the gas to escape. Between injections of different liquids, the tube was flushed with **#1** (distilled water) or **#2** (main component of most solutions).

In order to minimise the amount of gas dissolved, the liquids were brought to boil shortly before injecting. Gas solubility generally decreases with rising temperature [39], [40]. After injecting the solution in the rods, they were left to cool down. Before closing, the rods were topped up completely (no trapped air bubbles). The oil based liquids, **#16** and **#17**, were not brought to boil.

2.3 Pre-processing MRI and CT scans

Prior to analysing the data, the scans had to be prepared. Figures 2.12, 2.13 and 2.14 show a few stages in the image processing work flow.

Step 1 After loading the CT and MRI scan into *MIRADA*, they were aligned using the vitamin-e pills, yielding maximum overlap in the centre of the image.

Step 2 Next, as the MRI image had a lower resolution than the CT scan, the MRI scan was resampled. Its voxel's size were changed to match the CT voxels and both scans exported.

Step 3 Both layers (MRI and CT) were loaded into *3D Slicer* (Versions: Slicer-4.5.0-1-linux-amd64, Slicer-4.6.2-win-amd64)

Step 4 Its module 'annotations' was used to set a new region of interest (ROI) to include only a single rod.

Step 5 With the module called 'crop volume' (setting: voxel based cropping) the scans were reduced to show only the selected ROI.

Step 6 Using the module 'resample scalar volume' a number of interpolated (setting: 'bspline') higher resolution pairs (CT/MRI) were created.

Step 7 All new pairs and the cropped original CT/MRI pair were exported with 'create a dicom series' and saved in a separate folder each.

After this procedure a number of pairs based on the original CT and MRI were available, all of which had the same number of slices along the z-axis parallel to the phantom's rods. They only differ in the number of pixels making up each slice, their resolution varying from the original up to a hundred times finer. Each pair (CT/MRI) has the same pixel spacing (and resolution) in x and y direction. See table 2.4 for more details. Figure 2.14 depicts 3 CT/MRI scans of a single rod (axial) with different resolutions. "x1" stands for the original CT scan resolution (MRI resampled to match). "x4" is a resolution caused by 1 pixel being split in 4 smaller pixels, "x9" in 9, and so on and so forth. For better visibility, images shown as figures in this work are printed with inverted colours. Dark pixels have a high density/intensity value, white pixels are equivalent to air (low density/intensity).

resample factor	z (not affected)	y (same as x)	x
x1	0.60	0.98	0.98
x4	0.60	0.49	0.49
x9	0.60	0.33	0.33
x25	0.60	0.2	0.2
x100	0.60	0.2	0.1

Table 2.4: pixel Spacing (rounded values) [mm]

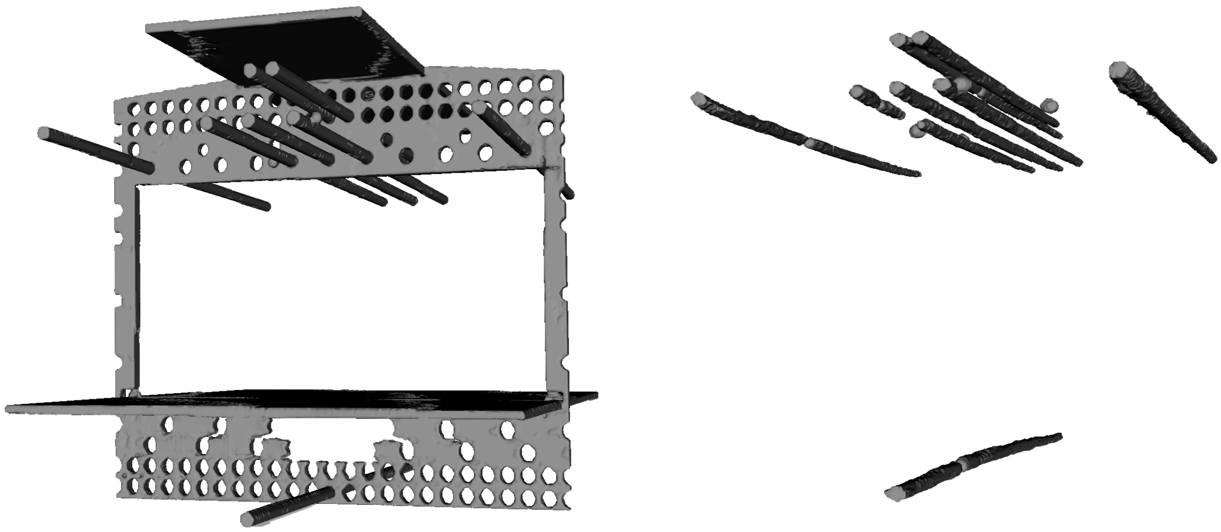

(a) CT (b) MR

Figure 2.12: rendered image, after steps 1-3

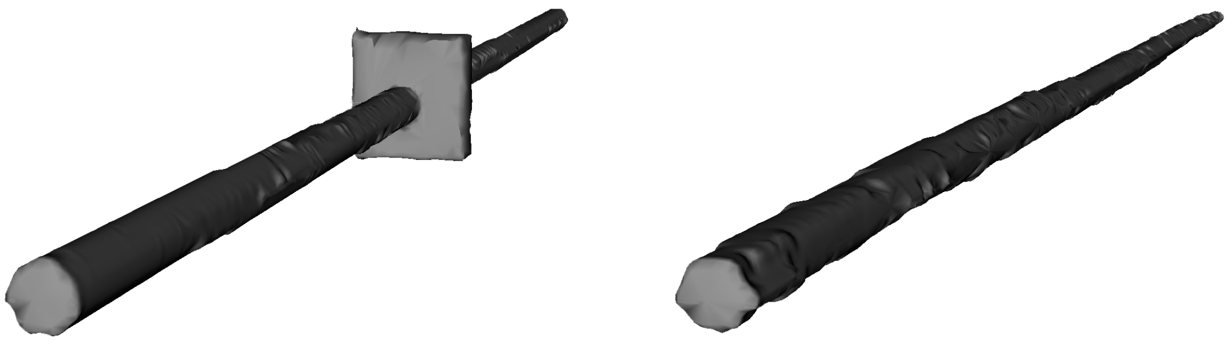

(a) CT (b) MR

Figure 2.13: rendered image, after steps 4 and 5

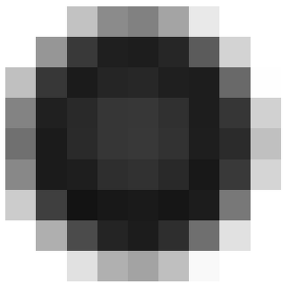

(a) CT x1

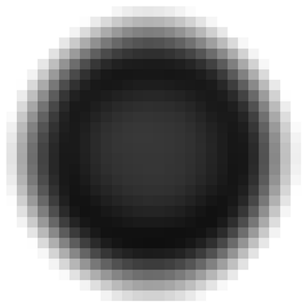

(b) CT x9

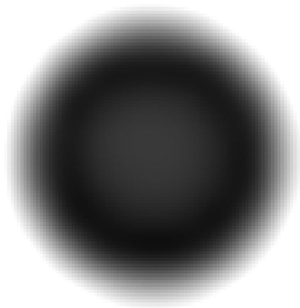

(c) CT x100

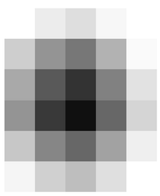

(d) MRI x1

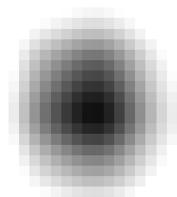

(e) MRI x9

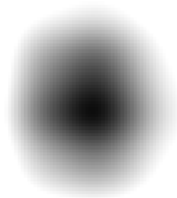

(f) MRI x100

Figure 2.14: CT/MRI axial images of the same rod (filling #5, inverted colours) after steps 6 and 7. The images on the very left show the original (CT) resolution, the resolution of those in the middle and the right were increased by resampling (9 times and 100 times finer)

2.4 Developed software tool

In order to asses the distortion of the MRI scanner, a software tool was programmed. It is written in Python 2.7 and uses the *SimpleITK* package to read and process *DICOM* ("*Digital Imaging and Communications in Medicine*") files. [41], [42] *SimpleITK* is a object-oriented "C++ library with wrappers for Python, Java, CSharp, R, Tcl and Ruby". [43], [44] It's versatility is one of the reasons why this approach was favoured. It is a simplified layer built on top of the National Library of Medicine Insight Segmentation and Registration Toolkit (ITK). SimpleITK is also used by Applications like *3D Slicer* , a "free and open source software package for visualisation and medical image computing". [45], [46] For this work 3D Slicer was used to crop and resample images, quickly read values and visualise the results. Documentation and code examples of SimpleITK can be found at [47], [48] An alternative way to handle DICOM data in Python would be Pydicom. [49], [50]

This is an extensive list of python packages used to process data after using 3D Slicer:

- SimpleITK
- numpy
- scipy
- matplotlib.pyplot [51]
- skimage.draw
- datetime
- os

Capabilities - Overview

The developed software tool is not able to automatically detect individual rods in a CT or MRI scan depicting the whole phantom. Instead the acquired 3D images have to be cropped so they include only a single rod (see section 2.3).

The python script can be used to:

- separate bright areas which are not connected ('masking' might be used as future method to automatically detect individual rods)
- find and mark slices which show irregularities
- calculate the centroid coordinates along the rod
- measure the local distortion described by the
  location shift (refered to as "warp")

dice coefficient (the "DC" refers to an object's roundness)

- visualise individual rod slices
- plot the average/peak brightness, warp, or `DC` along the rod
- write warp and `DC` for each slice in a combined ".txt" file
- export a rod shaped scan where the pixel values reflect the distortion occurring in each slice instead of their brightness as a ".mha" file (useful for visualisation, see figure 3.12).

2.4.1 Detection of irregularities

The method to find irregularities is described in figure 2.15. After loading the image data, the script calculates the mean brightness of a reference slice (which was chosen by the user) (**1.**). This reference slice will be used to decide if and which other slices might show irregularities, for example air bubbles, markers, or plastic panes. It is the user's responsibility to make sure the reference is free from any such objects. Ideally, it is located near the isocentre and has a brightness that is representative for the whole image.

The script will compare each slice of the volume to the reference slice individually, starting at one end (**2.**). To decide whether a particular slice is "irregular", it's average brightness will be compared to the reference slice's (**4.**). If the difference exceeds a certain value (**5b.**), the current slice will be marked as irregular and consequently won't be used to calculate its `DC` or centre of mass (COM). A value of 40 was found to be yield good results for CT scans. In the future a more sophisticated approach should be implemented where the script chooses a suitable value based on the image modality and the image size.

Irregular slices and their COM and DC values

As irregular slices cannot be used to asses distortion caused by the scanner, numbers describing their distortion are not of interest. Instead of calculating `DC`, `COM` and warp numbers, they will all be set to "-1". The `COM` cannot lie outside the image, yet coordinates "$(-1,-1)$" would indicate this. Similarly, the value referred to as `warpMagnitude` and the `DC` are defined to be positive numbers. All three are therefore easily understood to be invalid, indicating that the particular slice was marked as "irregular". The values representing x- and y-shift, on the other hand, are allowed to be negative or positive.

To be consistent, they are still set to "-1". It is essential to bear this in mind when interpreting the script's output.

Measuring distortion

Since the rods have a cylindrical shape, distortion can only be assessed in radial direction. The z-axis is parallel to the rods, x and y are radial. Ideally, each slice (z = const.) should depict the bright circular profile of the liquid (and of the plastic rod in CT) surrounded by black pixels (air).
Two phenomena were chosen to reflect the amount of distortion occurring in each slice of the MRI scans. The distance which the rod appears to be shifted in the MRI slice compared to the CT slice is referred to as "warp". The rod's deformation (deviation from circular profile) is described using the dice-coefficient "DC" (also known as Sorensen-Index).

2.4.2 Calculation: dice coefficient (DC)

The `DC` was chosen as indicator for the deviation from a circular profile. The implementation as python function is based on the open source python package "Medpy". [52] A part of it's module called "metric" was adapted. [53]

The calculation of the `DC` is performed for each slice individually. Additionally, to asses the overall distortion occurring along the rod, the average of all those values is also saved. As this aspect of distortion does not need a reference scan, the `DC` is measured for CT and MRI images separately. The dice coefficient or Sorensen index [54] is defined as:

$$DC = \frac{2|A \cap B|}{|A| + |B|} \tag{2.1}$$

Figure 2.16 describes the process of calculating the DC. It compares a binary image (input A) to a circle (reference B). In a binary image there are only 2 possible pixel values: "0" and "1". However, in the original image, values lie in a range between 0 (or -1024 in CT) and 1000 or higher. In order to reduce the true image to a binary image A, the script needs to split the pixels in 2 groups. A copy of the original picture is created where all pixels with a value above a certain `threshold` are set to the value of "1". These are regarded as part of the rod. Those which are darker are set to "0". (See

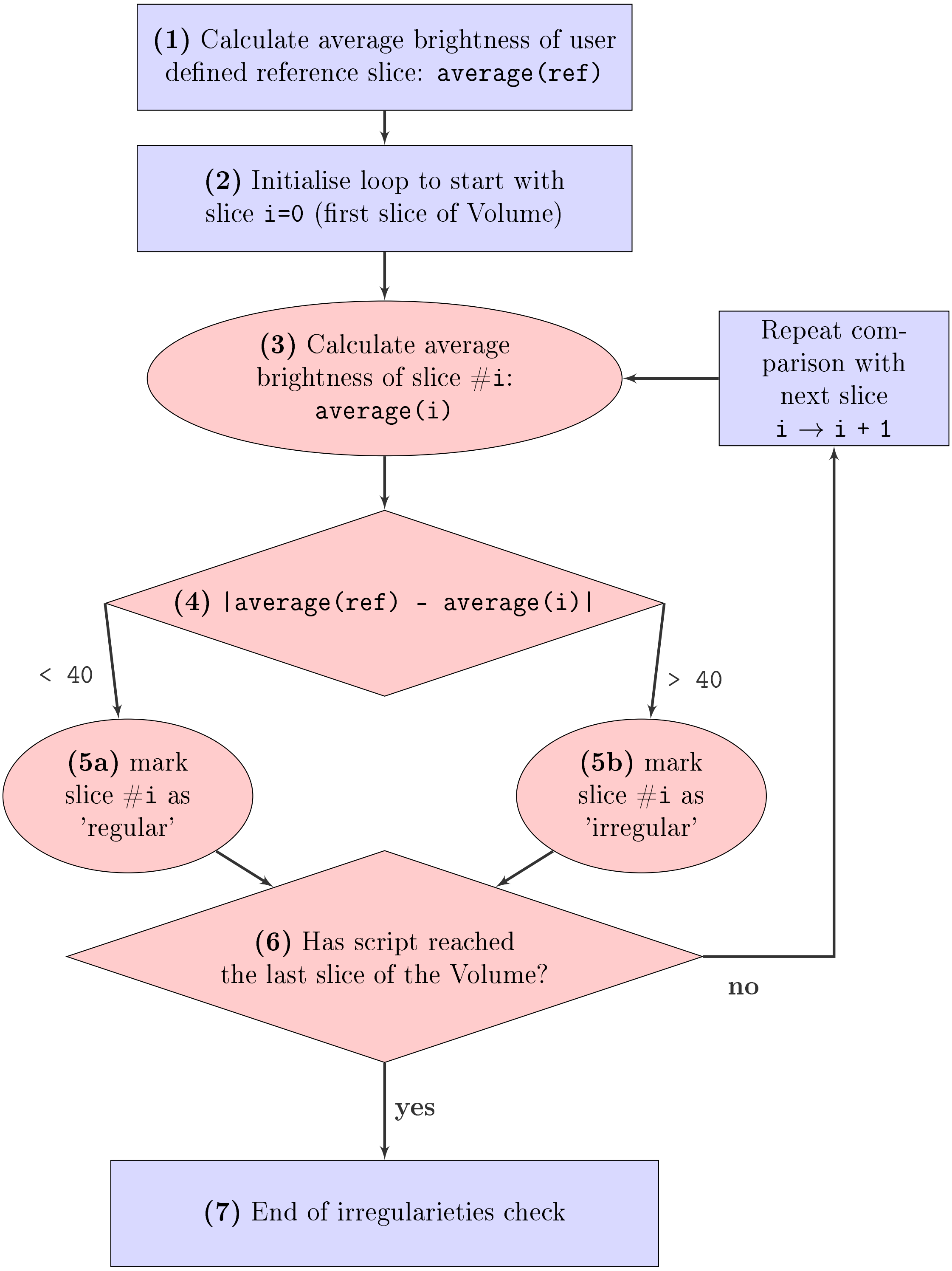

Figure 2.15: Check for irregularities

section 2.4.3 for details on how the `threshold` is calculated). Ideally, this procedure separates the surrounding dark area from the bright rod. This way the new binary image A still shows were the rod is, but it lost all information on the actual brightness.

Reference B is a circle with its midpoint typically placed at the centre of mass (COM) of the rod. The `COM` is usually calculated using those pixels which exceed the `threshold`, but weighted with their actual brightness (not using the binary image)

This way the script is supposed to place the reference circle B in the centre of the input image A. The position of the circle's centre and its radius highly influence the outcome. If the COM coordinates used to position the reference circle B lie outside of the image (e.g. '-1,-1'), the DC is set to '-1', indicating that no meaningful result could be obtained.

The `DC` ranges from 0 to 1. A value of 1 indicates a perfect circular shape. A low `DC`, on the other hand, means the shape differs greatly from a circle and could be caused by many things such as: little overlap (e.g. a ring or crescent shape); a very dark image hindering delineation of the rod from background; a small circle with a radius close to a only a few pixels.

The obvious choice for the radius of the reference circle B is to use the true size of the physical rod. For CT images this would be 4mm, for MRI images it would be 2mm. The script calculates the `DC` using various radii close to those values and returns the result yielding in the highest average `DC` for the whole rod.

Using the CT COM

Alternatively, the DC fo the MR scan can be calculated with the reference circle B placed in the COM of the corresponding CT image. This value could be regarded as a combined distortion guide number as it is influenced by the COM shift and the deformation simultaneously. One should bear in mind, though, that the meaning of it is neither equivalent to a real `DC` nor to the warp and should be interpreted with caution.

If the CT COM is far from the MR image, A and B have little overlap resulting in a small `DC`. As the implemented `DC` calculation tries a variety of radii, the circle B could, theoretically, always be chosen big enough to have some overlap with the binary image A. However, as B grows, A will stay the same. Therefore, only a fraction of B will contribute to the overlap and the rest will counter-act the benefits (see equation 2.1). Consequently, the DC would become so small that the script will choose a smaller radius for B.

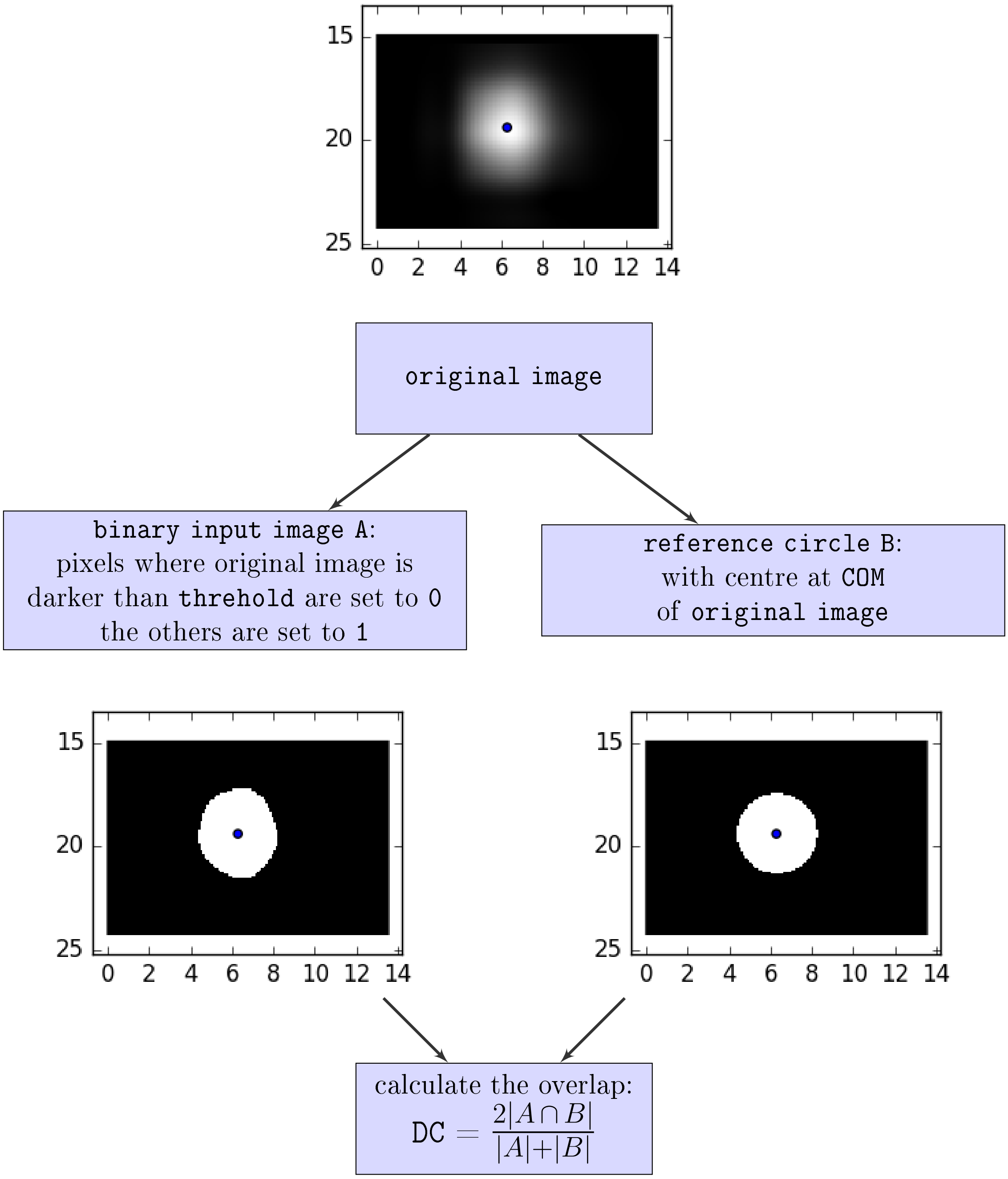

Figure 2.16: DC calculation for a MR scan (rod #5 @ slice 200) yielding a value of 0.9454

2.4.3 Calculation: warp & centre of mass (COM)

To calculate the location shift between rods shown in CT and MRI, the coordinates of the centre of mass (COM) were subtracted. The x- and y-shift (`warpXY`) measured in each slice was saved in an array. Furthermore, the absolute value of the coordinate shift (`warpMagnitude`) was calculated.

The calculation of the `COM` is done with help of the "scipy" python package. Its module "ndimage" contains the function "$center\_of\_mass()$", which returns the `COM`'s coordinates of a given input array. Only pixels representing the rod or the liquid should be used for the calculation. Otherwise the almost black voxels surrounding the rod would influence the result. To be regarded as part of the rod, the pixels' value has to reach a certain `threshold`. In order to find the relevant pixels two methods were developed:

1. a simple method calculating the number of pixels based on rod size

2. an iteration method finding a `COM` resulting in a good `DC`

Both methods rely on a single reference slice to calculate the `threshold`. This reference should be representative for the whole scan, because the `threshold` deduced from it will be used to find pixels belonging to the rod in all other slice, too.

1. Simple Method

The inner ($2mm$) and outer ($4mm$) radius of the plastic rods are known. So is the pixel `spacing`, the size of a voxel in real space (mm). Calculating the number of pixels which make up the more or less circular profile of the rod in a slice is calculated as follows:

$$pixelNumber = (radius^2 \cdot \pi) \,/\, (spacing^2) \tag{2.2}$$

For CT images the $radius = 4mm$, in MRI scans the $radius = 2mm$. $spacing$ is the pixel spacing in x and y direction. Next, the pixels are sorted by brightness. The top $pixelNumber$ pixels are then used to calculate the `COM`. The value of the darkest pixel that is still counted as part of the rod is saved as `threshold` for future calculations (e.g. finding the `DC` associated with the `COM`, see section 2.4.2).
The method is summarised in figure 2.17. Now, the DC can be obtained as described earlier using the now known `threshold` and COM coordinates.

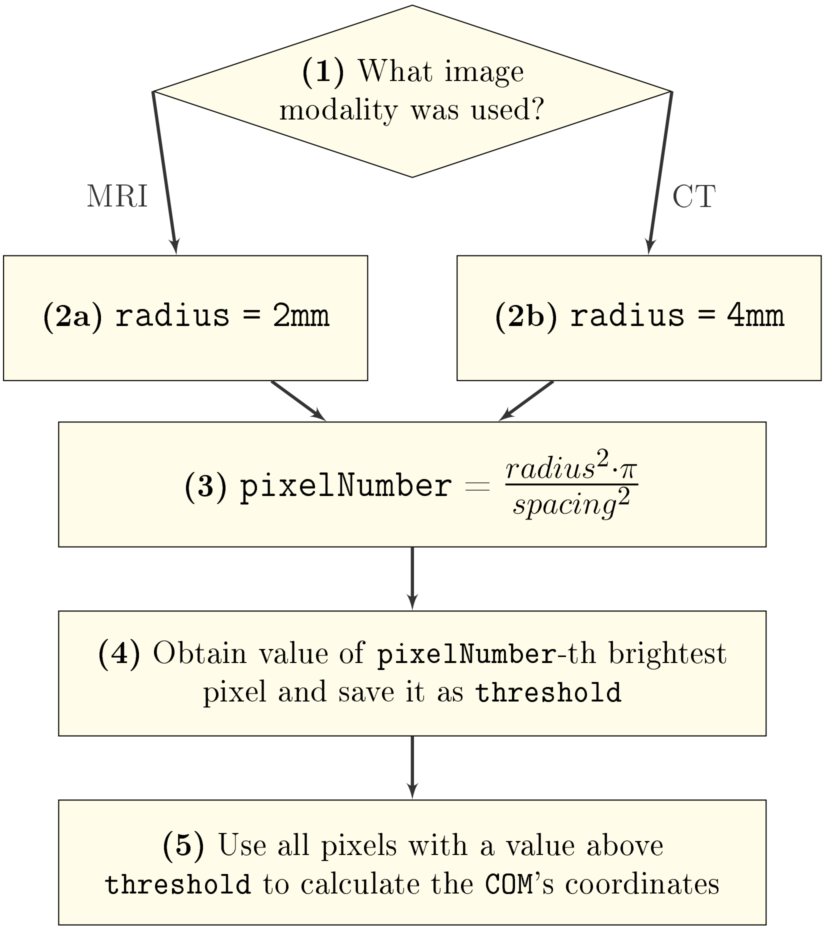

Figure 2.17: Simple method to find `threshold` for `COM` calculation based on real rod size

2. Iteration Method

This algorithm is an iteration method. Figure 2.18 shows in what order the scripts executes individual steps during the iteration.

To begin with, it looks at the whole range of possible pixelNumbers, from 0% to 100% (**1**). As a reasonable first guess it assumes that 50% of all pixels belong to the rod (**2**). Now, in the first iteration (**3**), to find out whether more or less pixels would result in a better `DC`, it considers two new guesses: One halfway from the lower limit (0%) to its current guess (50%) which is:

$$\frac{0+50}{2} = 25\% \tag{2.3}$$

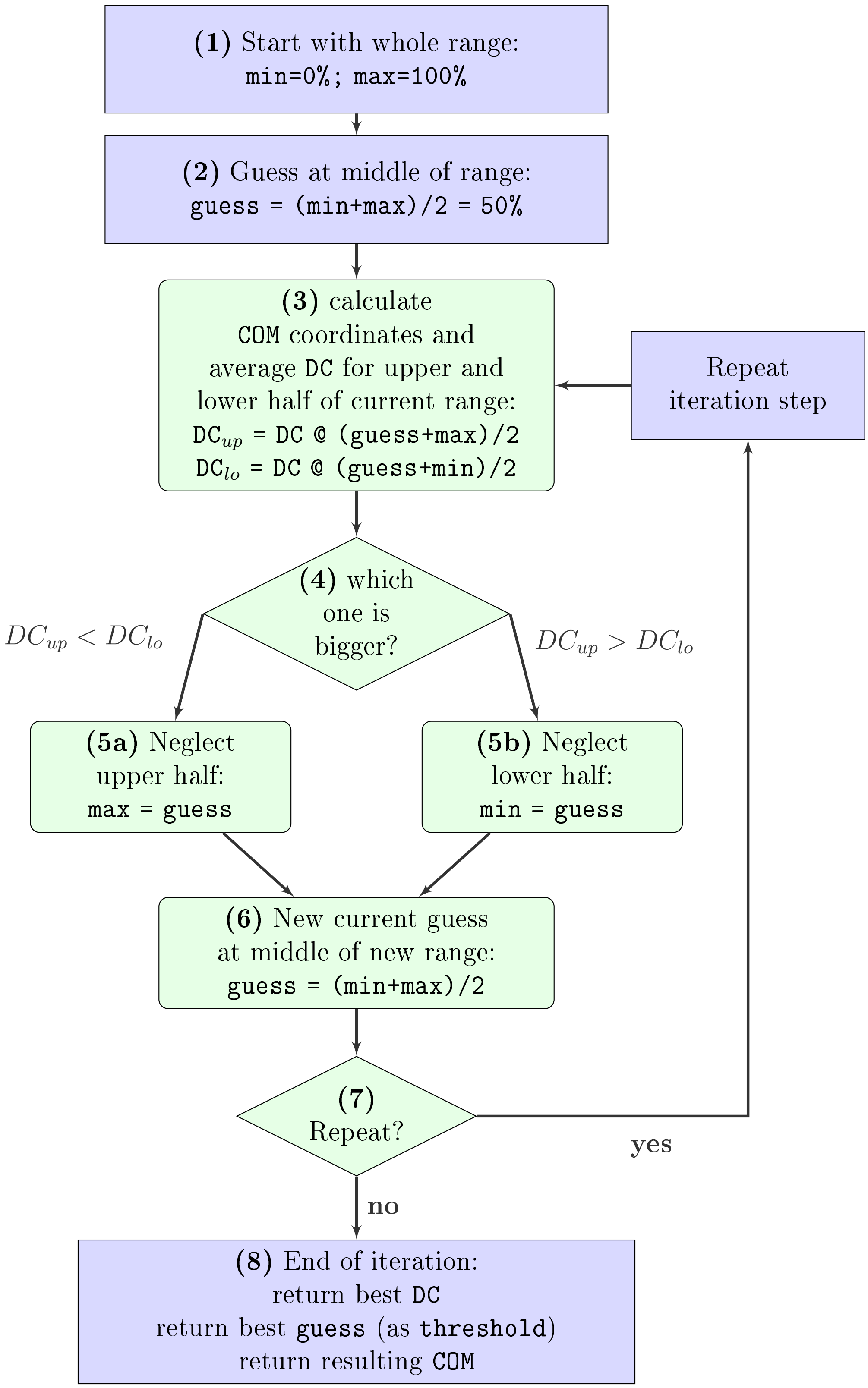

Figure 2.18: Iteration method to find `threshold`, `DC` and `COM`

and one halfway from the upper limit (100%) to its current guess (50%) which is:

$$\frac{100 + 50}{2} = 75\% \tag{2.4}$$

Those numbers correspond to a `threshold` each, separating the chosen percent of brighter pixels from all darker pixels in the slice. Using the `thresholds`, the script calculates the `COM` and `DC` for both possible guesses. Comparing the average over the whole rod for both `DC`s will decide which guess is closer to representing the rod better (**4**). If the lower number of pixels yields a better average `DC` (**5a**), the upper half of the range will be neglected in the next iteration or in other words, the new upper limit takes the value of the former guess (50%). If the higher percentage yields a better average `DC` (**5b**), the lower half of the range will be neglected in the next iteration, the new lower limit takes the value of the former guess (50%). At the end of the iteration (**6**), the percentage resulting in the higher average `DC` is saved as the new current guess. After this first iteration (**7**) the script can either repeat steps 3-6 or end it by returning the best guess and its (average) `DC` (**8**).

To get a better understanding, let's suppose the iteration is repeated. At the start of the second iteration, the range is smaller (half of the entire range) and the current guess is set exactly in its middle. If, for example, the average `DC` for 25% was higher than for 75%, the next guess will be 25%, because the new range goes from 0% to 50%. In that case, `DC`s for the lower half of that range ($12,5\%$) and the upper half ($18,5\%$) will be calculated and compared to decide which half to eliminate in the third iteration. If, on the other hand, the average `DC` for 75% was higher, the next guess will then be 75%, because the new range goes from 50% to 75%. In that case, `DC`s for $62,5\%$ and $82,5\%$ will be compared.

The iteration continues until further steps yield no better average `DC` or a set number of steps has been performed. After the iteration process, the algorithm will return the `COM` which resulted in the best DC. The percentage of pixels that led to this `DC` is equivalent to a `threshold` which is saved for future calculations. Figure 2.19 shows the `DC` found in the course of trying different percentages during the iteration method.

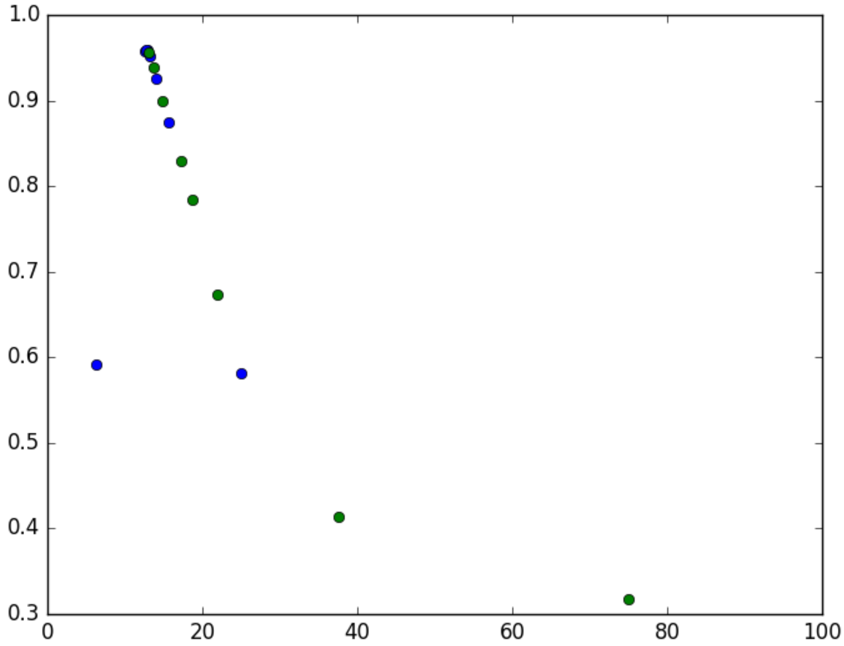

(a) full iteration process

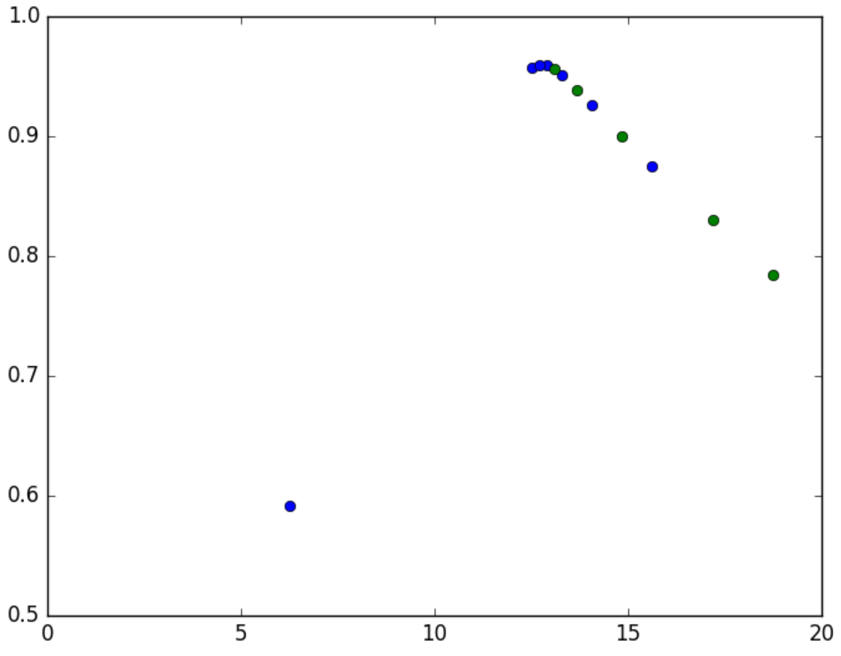

(b) close up of same iteration as in (a)

Figure 2.19: COM iteration method, 8 repetitions; green dots correspond to upper guesses, blue to lower guesses

3 Results

On the second day of working with the filled rods the one containing liquid #**6** broke (leakage). It happened when delicately knocking it against on the table while standing upright. This was intended to mobilise bubbles that sticked to the wall and make them travel vertically to on end of the rod. (see table 3.2) The plastic stopper on the lower end came loose. The rod containing filling #**6** was not replaced. Consequently, all CT/MRI images used to asses signal intensities of the tested solutions show only 16 rods.

3.1 Obtained MRI and CT scans

Figure 3.1 shows a coronal view of the 16 rods filled with the tested liquids and a reference rod on either side. In Figure 3.1b a trapped air bubble is clearly visible at the lower half of rod #5. Figure 3.2 shows an axial view of the tested rods and some surrounding rods. In figure 3.2b a water filled plastic bottle placed in the middle of the phantom is also visible. This was necessary, because the MRI scanner needs sufficient signal for shimming prior to the start of imaging. Without the bottle, the limited number of rods used for this scan would not have created enough signal. During a future distortion assessment where all available rods (over 300) are used, they will result in the required signal strength on their own.

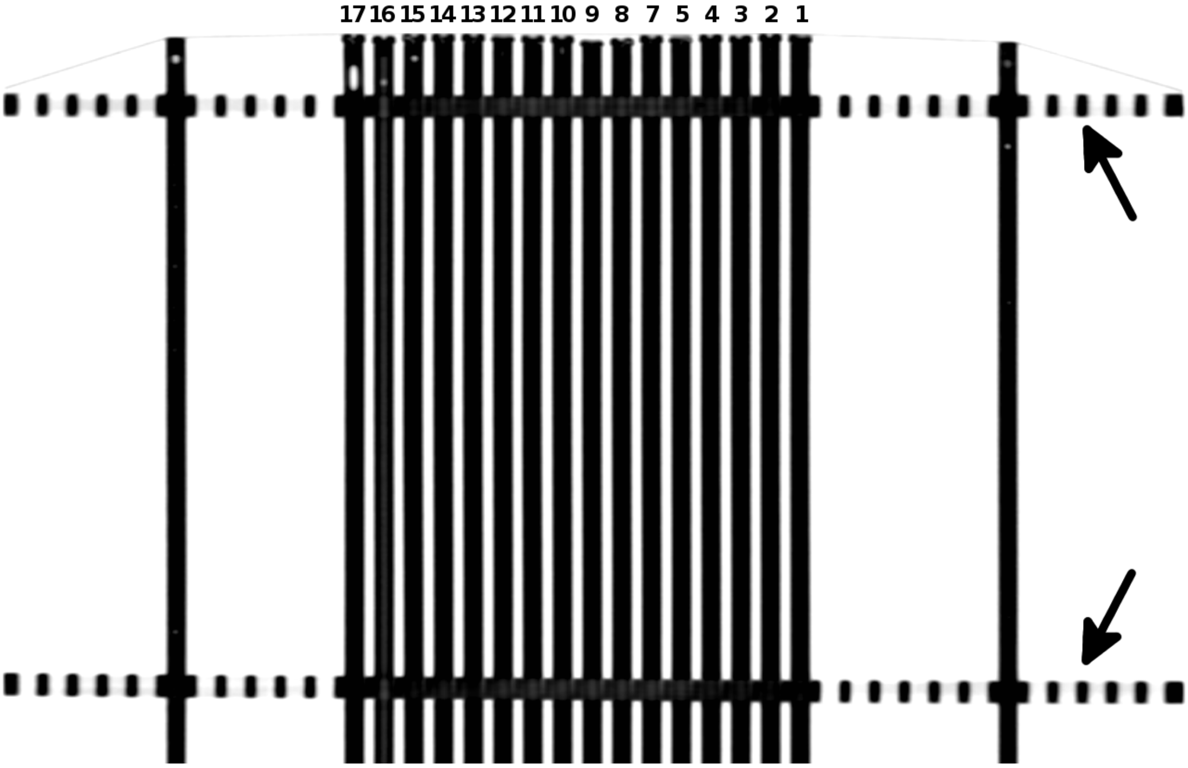

(a) CT: The periodic black lines in upper and lower part of image (indicated with arrows) depict the plastic panes and their holes from above; the faint line across upper end of rods shows adhesive tape used to hold the rods in place; in rod #16 an air bubble is clearly visible close to the upper end.

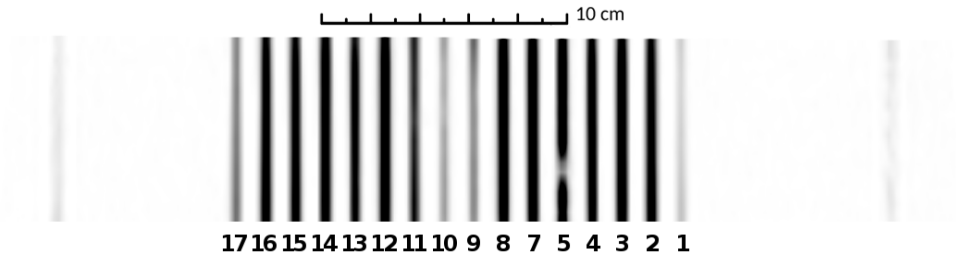

(b) MR: The rods appear to be thinner than in the CT scan, because only the liquid filling is visible. The tested liquids result in different signal intensity (brightness); all plastic parts (rods and panes) are not visible; there is a trapped air bubble visible in rod #5.

Figure 3.1: Coronal CT/MRI (inverted colours; same scale; cropped images) images of 16 rods (tested liquids, numbering starting from the right, #6 excluded) + 2 reference rods (filled with water) on the sides.

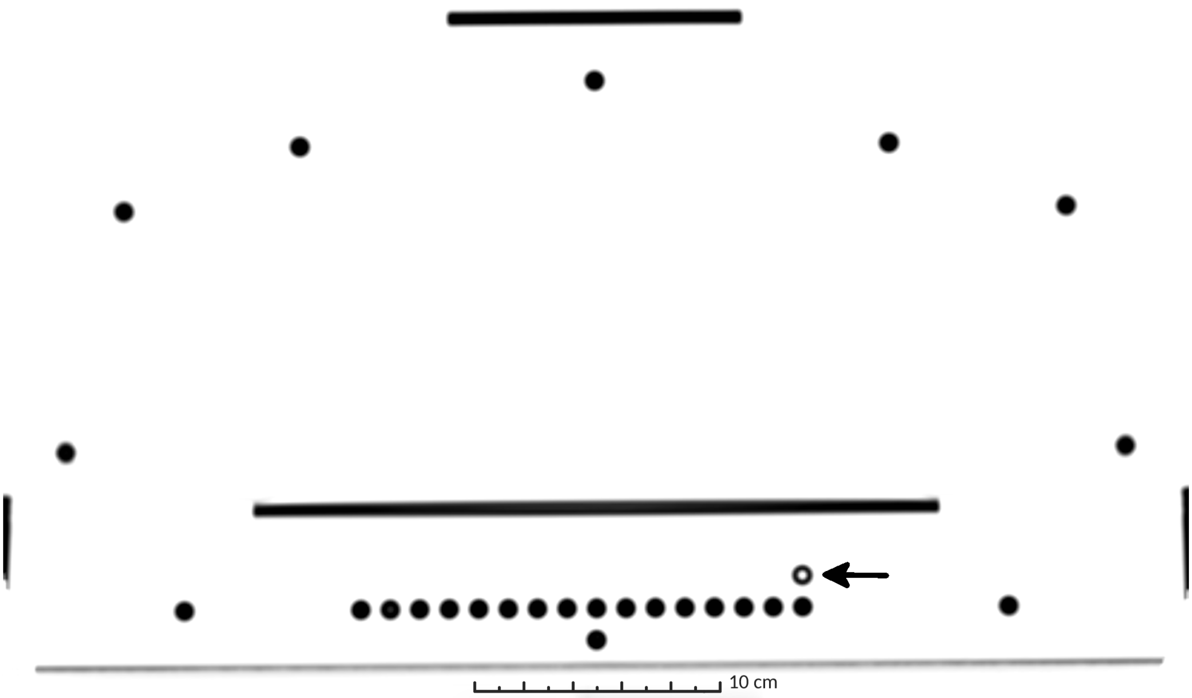

(a) CT: The black bars visible just above the 16 tested rods, at the very top, and to the sides show plastic parts of the phantom holding it together. The faint grey line running below the tested rods represents the table on which the phantom was positioned during imaging.

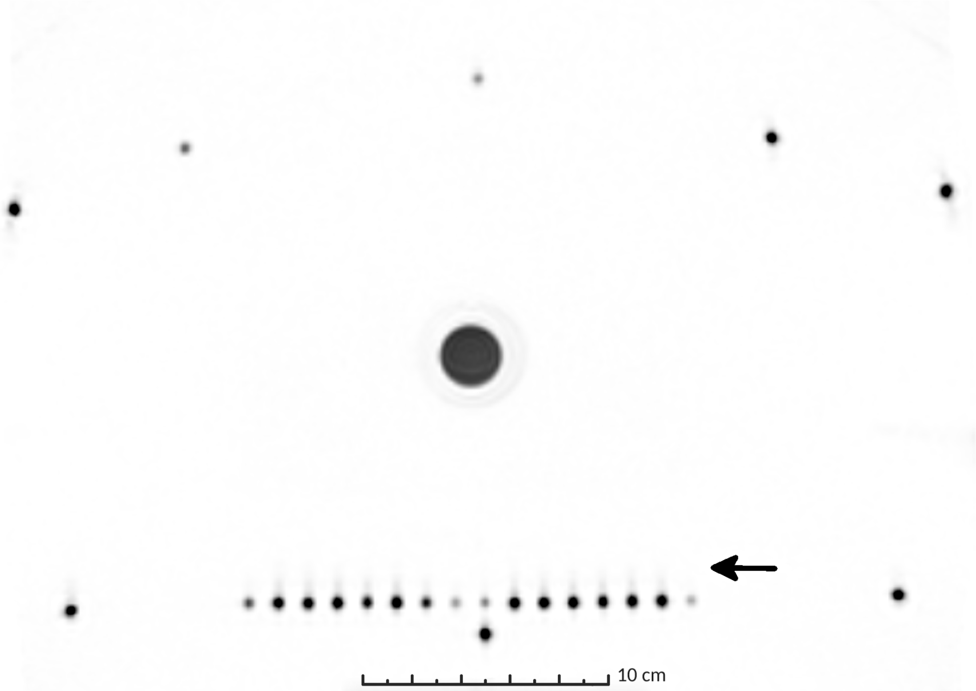

(b) MRI: The black circle in the centre depicts a water bottle which was placed in the middle of the phantom (necessary for MRI scanner to start imaging).

Figure 3.2: axial CT/MRI (inverted colours, same scale) images of the 16 rods filled with tested liquids (numbering starting from the right, #6 excluded); surrounded by reference rods (filled with water) and one empty rod (marked with arrow) which is not visible on the MRI scan

3.2 Tested solutions

3.2.1 Visibility on CT/MRI scans

It should be noticed that in the CT image there is little difference in brightness between the tested liquids. The plastic rods themselves result in brighter pixels than any of the tested solutions.

On MRI scans most liquids had a mean and a max brightness value above 1000 (see table 3.1).
Only #**1**, #**9**, #**10**, & #**16** resulted in significantly less signal (below < 1000).

No.	Min	Max	Mean	Median	σ
1	182	371	288	269	69,8
2	1044	1921	1443,8	1405	312,9
3	941	2075	1451,2	1394,5	413,2
4	1176	1709	1440	1437,5	232,5
5	1125	2111	1583,8	1549,5	355
7	971	2241	1466,8	1316	471,2
8	1459	1947	1704	1705	180,5
9	385	584	486,8	489	93
10	247	502	343,6	266	111
11	830	1268	1036,2	1023,5	163,2
12	1158	2211	1648,8	1613	394,2
13	836	1657	1146,8	1047	321,2
14	800	2062	1383	1335	473,1
15	1156	1829	1476,2	1460	272,7
16	1102	1967	1509	1483,5	325,8
17	356	938	629,6	602	223,6

Table 3.1: liquid visibility on MRI scan

3.2.2 Mechanical properties of solutions

The liquids were filled in a rod each and observed for several months. Number #**14** could be injected without problems, the solution remained fluid even after reaching room temperature. Number #**15** on the other hand changed to a gel like consistence and clogged the injection tube at the quickly after the rod was filled. The tube could not be used again.

Each rod was free of bubbles directly after sealing. All rods containing water based solutions contained some air after 2 months and the amount of liquid continued to decrease further (see table 3.2). After 6 months the volume of air further increased (proportionally to the behaviour observed until then). Figure 3.5 shows the rods after a time of over 6 months. In some of the tested rods, the occurring air bubbles would stick to the wall. Only after gently hitting the rod they would start moving. Knowing the inner diameter d of the rods and measuring the length l of trapped air bubbles, their volume can be estimated:

$$V = \frac{d^2}{4} \cdot \pi \cdot l \tag{3.1}$$

While adding generic washing soap (#**5**, #**6** and #**7**) did not hinder air bubbles from forming, it significantly improved their mobility. Not only did they move quickly when the rod was tilted, large quantities of air also did not block the entire diameter of the rod. Instead they formed large but cohesive bubbles that could be moved to one end of the rod easily and at no point sticked to the plastic wall.

The ascorbic acid present in #**8** (concentration of 0.36 g/L corresponds to approx. 0.00204 mol/L), #**9** (3.6g/L), and #**10** (36g/L) seemed to have held back the formation of air bubbles for up to one week. After two months of observation, however, the rods also contained some air. It should be noted that all three liquids turned brown, the colour being more saturated for higher concentrations of ascorbic acid.

The rods filled with Primovist (#**11** to #**13**) were filled with some air bubbles after at least two days. Moreover, the bubbles sticked to the walls of the rod and only shaking it violently made them move to one side of the rod.

It took more than a week until the rod containing the low concentration of agar (#**14**) contained an air bubble. The viscous consistency made it impossible to coerce it to either end of the rod. Liquid #**15** on the other hand did not form bubbles at the middle of the rod, but seemed to have dried starting at the end with the plastic stopper.

No.	*after 1 day* bubbles	hit req.	*after 2 days* bubbles	hit req.	*after 1 week* bubbles	hit req.
#1	yes	no	no		no	
#2	yes	yes	no		no	
#3	yes	yes	no		no	
#4	yes	yes	no		no	
#5	yes	no	yes	no	no	
#6	yes	no	——— *rod was leaking* ———			
#7	yes	no	yes	no	yes	no
#8	no		no		no	
#9	no		no		no	
#10	no[1]		yes	yes	yes	yes
#11	no		yes,	*sticked to wall*	yes	yes
#12	yes	yes	yes,	*sticked to wall*	yes	yes
#13	yes	yes	yes,	*sticked to wall*	yes	yes
#14	no		yes	no	yes	yes
#15	no		no		no	
#16	no		no		no	
#16	no		no		no	

No.	*after 2 months* length of trapped bubble l [mm]	approx. volume V [mm^3]
#1	2	25.13
#2	1.8	22.62
#3	1+1 (air blockage, at lower end)	25.13
#4	4	50.27
#5	1.5 (many small bubbles)	18.85
#6	——— *rod was leaking* ———	
#7	2 (many small bubbles)	25.13
#8	2.3	28.90
#9	3	37.70
#10	2.4	30.16
#11	2	25.13
#12	2	25.13
#13	2.3	28.90
#14	1.5+0.5 (big immobile bubble, at center)	25.13
#15	3.4 (agar gel dried)	42.73
#16	0	0.00
#17	0.5	6.28

Table 3.2: Observations regarding the mechanical properties of the tested solutions.

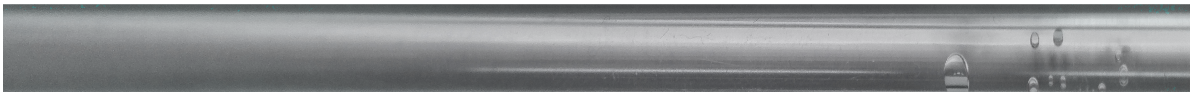

Figure 3.3: Rod #5 showed some bubbles after 2 months.

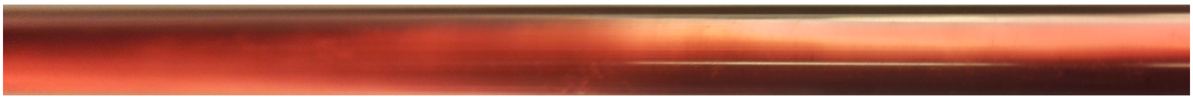

Figure 3.4: Rod #16 contained no bubbles after more than 6 months.

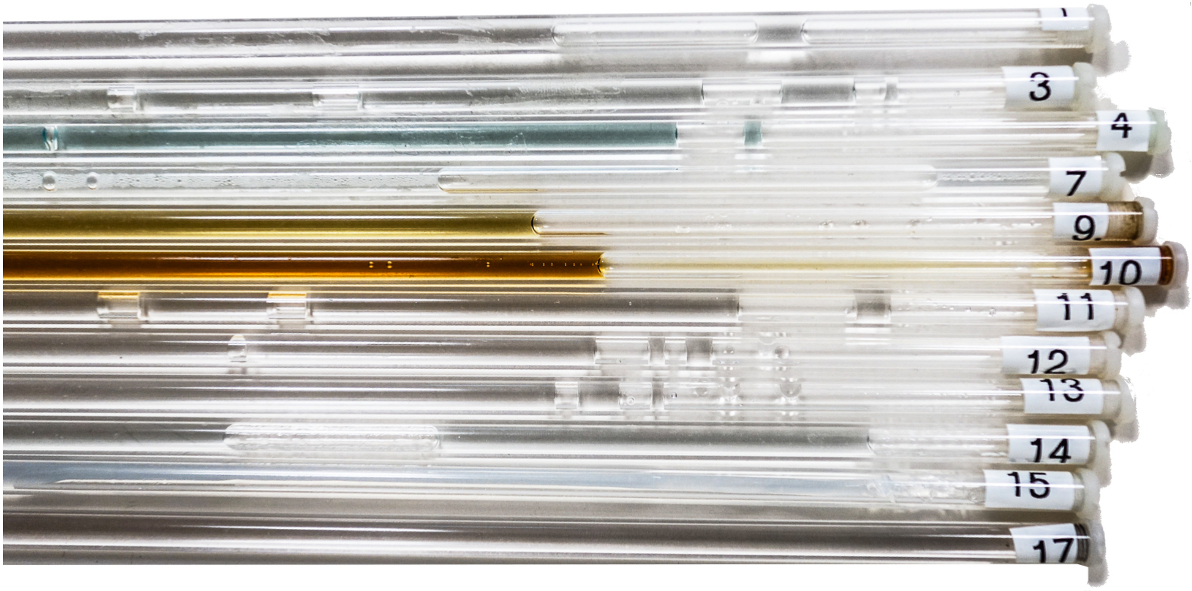

Figure 3.5: The rest of the tested rods (all except #5 and #16) after more than 6 months.

3.3 Distortion assessment

Two sets of images were taken using CT and MRI. For the first, all possible liquids were scanned to find their signal intensity in MRI. A few months later, in the second imaging, one of the most promising candidates was imaged again on its own. Varying resample rates of both sets were used to test the developed software tool. If not mentioned otherwise, results and discussion refer to the scans resampled to a 100-times finer resolution (x100).

The output generated by the script is attached in the appendix. Tables 3.3 and 3.4

summarise the most interesting regions along the rods. They contain the calculated centroid shift in x and y direction and its magnitude ($warp_x$, $warp_y$, $warpM$); the DC for CT using the CT-centroid (DC_{CT}); MRI using the MRI-centroid (DC_{MR}); and MRI using the CT-centroid ($DC_{MR(CT-COM)}$). These six numbers were generated using the simple method (see figure 2.17) and the iteration method (figure 2.18) of finding COM and DC. The latter are marked in the table with a * (e.g. $warpM^*$).

3.3.1 First Set, Rod #5

From the first MRI and CT scans, only the rod containing liquid #5 was analysed. The hole in which it was placed is marked with a little 'x' in figure 2.9. It was decided to use this rod, because it had a reasonably good signal strength and it contained a small air bubble. This situation provided data containing a irregularity (bubble) and was therefore well suited for testing some of the software tool's capabilities and limitations. Figure 3.6 and 3.7 show the brightness of the rod on CT and MR scans. Figures 3.11, 3.8, 3.9 and 3.10 visualise the calculated output. All plots were created using the data obtained with the iteration method.

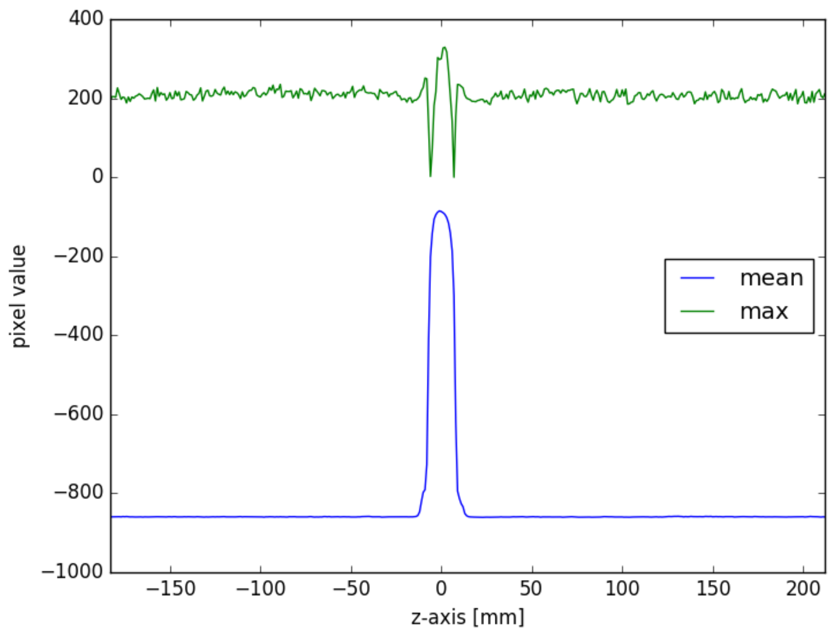

Figure 3.6: Rod #5: brightness of all pixels at a certain slice, CT x100; the plastic pane fills the area from $-10mm$ to $10mm$.

slice	dist	$warp_x$	$warp_y$	$warpM$	DC_{CT}	DC_{MR}	$DC_{MR(CT-COM)}$	$warp^*_x$	$warp^*_y$	$warpM^*$	DC^*_{CT}	DC^*_{MR}	$DC^*_{MR(CT-COM)}$
0	-183	-0.1046	-1.115	1.1199	0.983	0.8444	0.6102	-0.1047	-1.0571	1.0623	0.9945	0.9504	0.7546
1	-182	-0.1205	-1.1132	1.1197	0.9807	0.8547	0.6091	-0.1199	-1.0527	1.0595	0.9929	0.9496	0.7573
2	-181	-0.1278	-1.1107	1.1181	0.9819	0.8666	0.6135	-0.1334	-1.0472	1.0556	0.9925	0.9501	0.7583
:													
:													
171	-12	0.0025	-0.6891	0.6891	0.9786	0.9421	0.7848	-0.0261	-0.6921	0.6926	0.9941	0.9528	0.8437
172	-11	0.0089	-0.6825	0.6825	0.9723	0.9425	0.7862	-0.026	-0.6869	0.6874	0.9898	0.9527	0.8445
173	-10	-1	-1	-1	-1	0.9421	-1	-1	-1	-1	-1	0.9529	-1
174	-9	-1	-1	-1	-1	0.9433	-1	-1	-1	-1	-1	0.9535	-1
:	:	:	:	:	:			:	:	:			
:	:	:	:	:	:			:	:	:			
192	9	-1	-1	-1	-1	0.9468	-1	-1	-1	-1	-1	0.9517	-1
193	10	-1	-1	-1	-1	0.9472	-1	-1	-1	-1	-1	0.9525	-1
194	11	0.0379	-0.709	0.71	0.9707	0.9481	0.778	0.0072	-0.7123	0.7123	0.9878	0.9531	0.8349
195	12	0.0364	-0.7048	0.7058	0.9731	0.9465	0.7789	0.0053	-0.7131	0.7132	0.9905	0.9535	0.8345
:													
:													
301	118	0.2997	-0.8702	0.9204	0.9838	0.4306	0.409	0.1153	-0.7938	0.8021	0.9909	0.8851	0.7757
302	119	0.3943	-1.1317	1.1984	0.981	0.145	0.1459	0.1144	-0.8896	0.8969	0.9903	0.8631	0.7477
303	120	-1	-1	-1	0.9817	-1	0	0.1093	-1.0022	1.0081	0.9915	0.832	0.7129
304	121	-1	-1	-1	0.9809	-1	0	0.0979	-1.1751	1.1792	0.9928	0.7853	0.6619
305	122	-1	-1	-1	0.9826	-1	0	0.0881	-1.4076	1.4104	0.9918	0.7164	0.5901
306	123	-1	-1	-1	0.982	-1	0	0.0787	-1.5728	1.5748	0.9918	0.6762	0.5439
307	124	-1	-1	-1	0.9812	-1	0	0.0866	-1.5327	1.5351	0.9917	0.7164	0.5705
308	125	-1	-1	-1	0.9805	-1	0	0.0927	-1.5189	1.5218	0.9925	0.7516	0.5913
309	126	-1	-1	-1	0.9811	-1	0	0.0915	-1.4745	1.4773	0.9922	0.7849	0.6167
310	127	0.3786	-2.0028	2.0383	0.981	0.0755	0.0219	0.0792	-1.4414	1.4436	0.9915	0.8148	0.6361
311	128	0.3434	-1.9836	2.0131	0.9808	0.1647	0.0613	0.0819	-1.3987	1.401	0.9916	0.843	0.6576
:													
:													
393	210	0.1083	-0.2563	0.2783	0.9822	0.9527	0.9048	0.0989	-0.2569	0.2753	0.9943	0.9675	0.9294
394	211	0.1147	-0.263	0.2869	0.9808	0.9522	0.9024	0.1039	-0.2608	0.2808	0.9917	0.9681	0.9287
395	212	0.1214	-0.2454	0.2738	0.9815	0.9552	0.9089	0.1114	-0.2424	0.2668	0.9921	0.9691	0.9311

Table 3.3: rod #5: script generated data; dist and $warp$ in $[mm]$

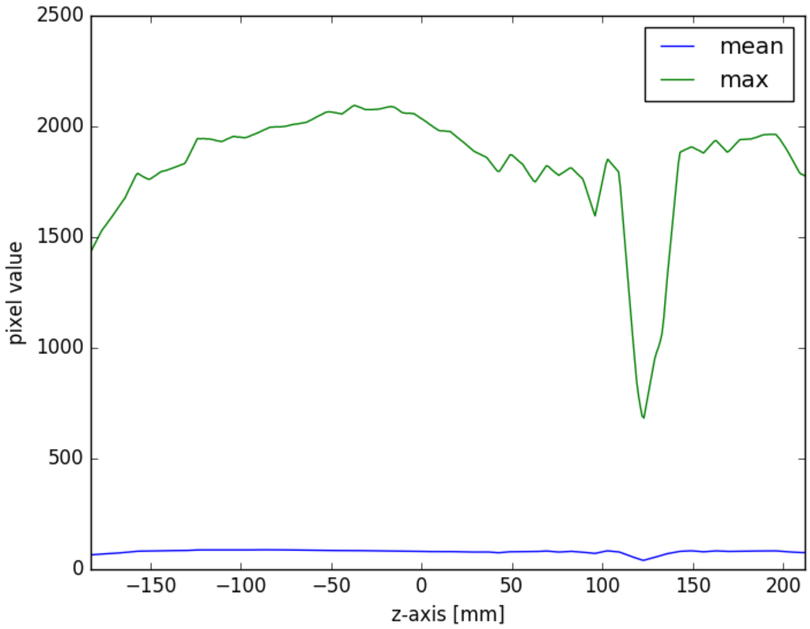

Figure 3.7: Rod #5: brightness of all pixels at a certain slice, MRI x100; drop of max brightness at around 110mm to 135mm is due to air bubble.

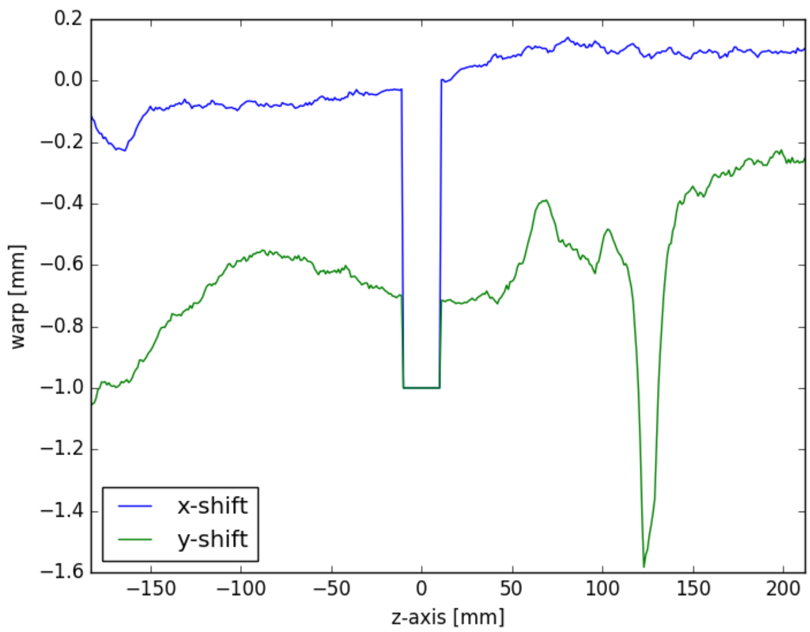

Figure 3.8: Rod #5: warp XY [mm] (iteration method), CT-MRI x100; plastic pane present from $-10mm$ to $10mm$, bubble at about 110mm to 135mm.

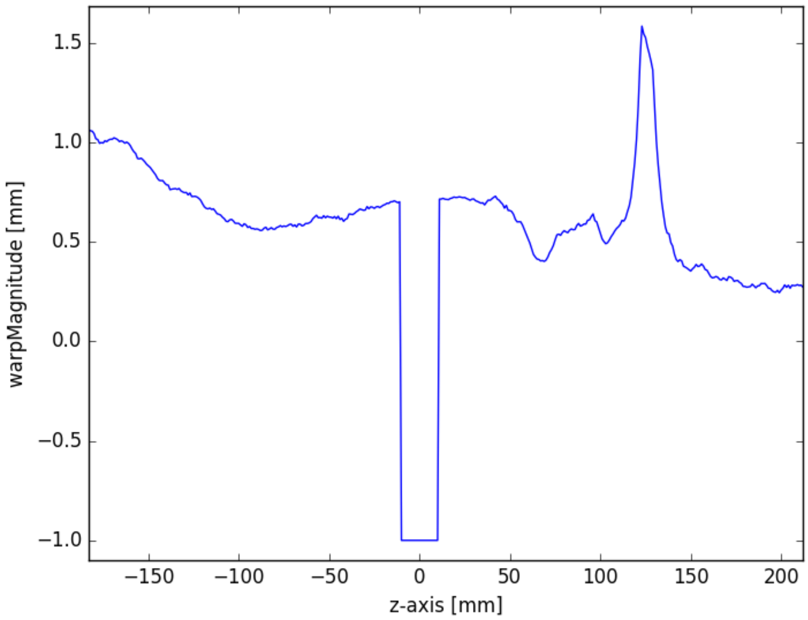

Figure 3.9: Rod #5: warp Magnitude [mm] (iteration method), CT-MRI x100; plastic pane present from $-10mm$ to $10mm$, bubble at about $110mm$ to $135mm$

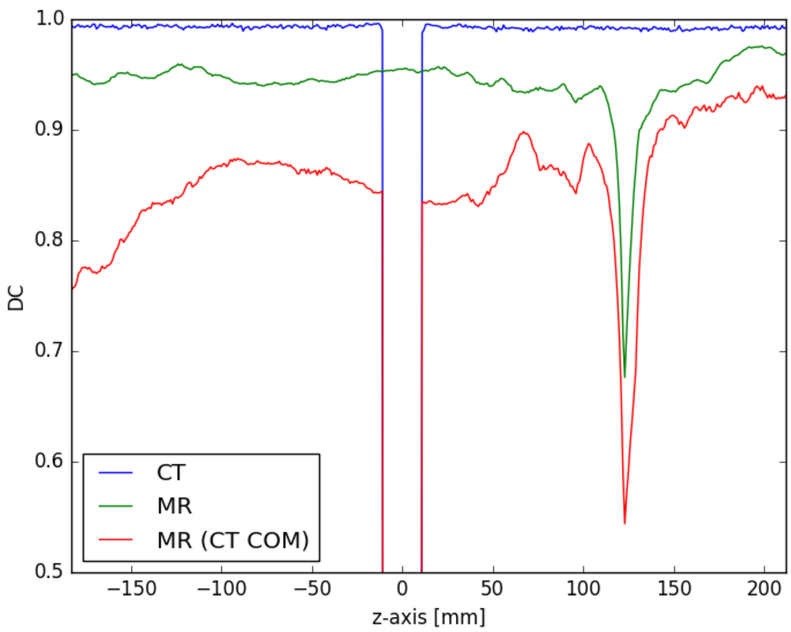

Figure 3.10: Rod #5: DC (iteration method) for CT & MRI & MRI (using CT COM), x100; plastic pane at $-10mm$ to $10mm$, bubble at about $110mm$ to $135mm$

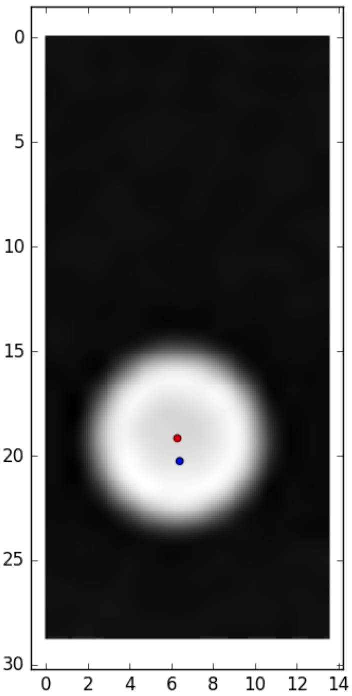

(a) CT @ 0

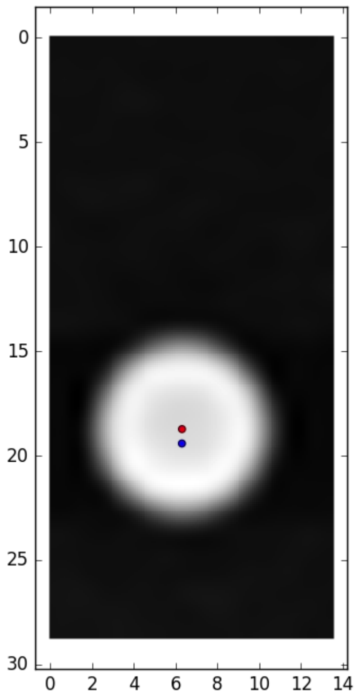

(b) CT @ 171

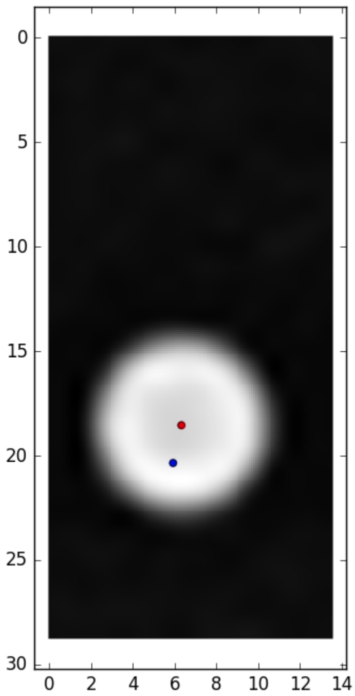

(c) CT @ 304

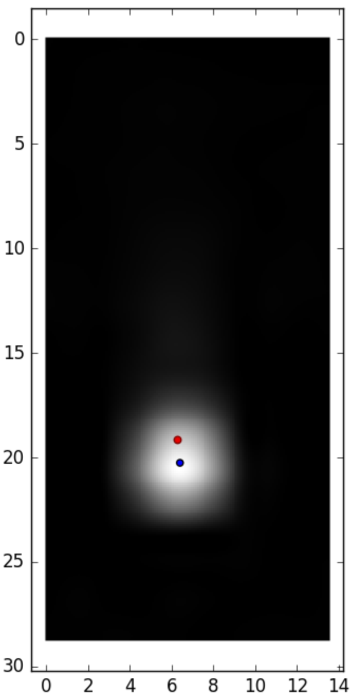

(d) MRI @ 0

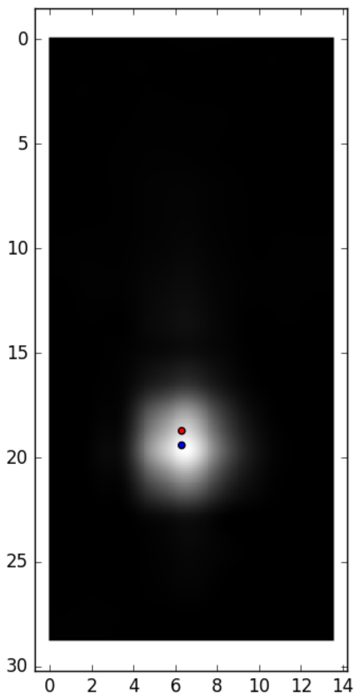

(e) MRI @ 171

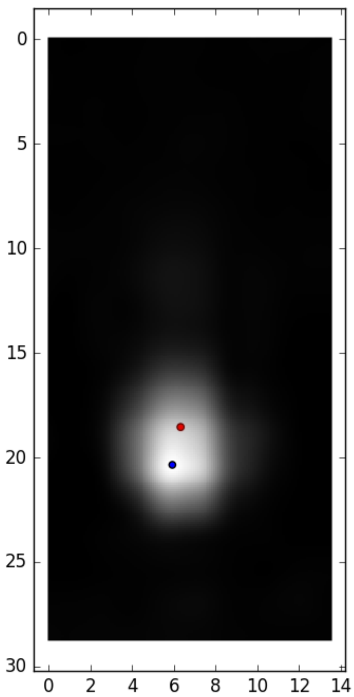

(f) MRI @ 304

Figure 3.11: MRI x100 scan of rod filled with #5 (true colours). The dark blue dot represents the MRI centroid, the bright red dot represents the CT centroid. Slice 171 is located approximately at the isocentre, 0 on the very end of the image, 304 on the other but also close to an air bubble.

3.3.2 rod #16

After deciding which of the possible liquids might be a suitable choice for the future use of the phantom, another set of MRI amd CT scans was taken. This second data set shows the rod containing liquid #16. The hole in which it was placed is marked with a little 'z' in figure 2.9. Figure 3.13 and 3.14 show the brightness of the rod on CT and MR scans. Figures 3.15, 3.16 and 3.17 visualise the spatial distortion assessed using the iteration method. All plots were created using the data obtained with the iteration method.

Figure 3.12: Rod #16: colour coded map; colours reflect *warpM**; based on x100

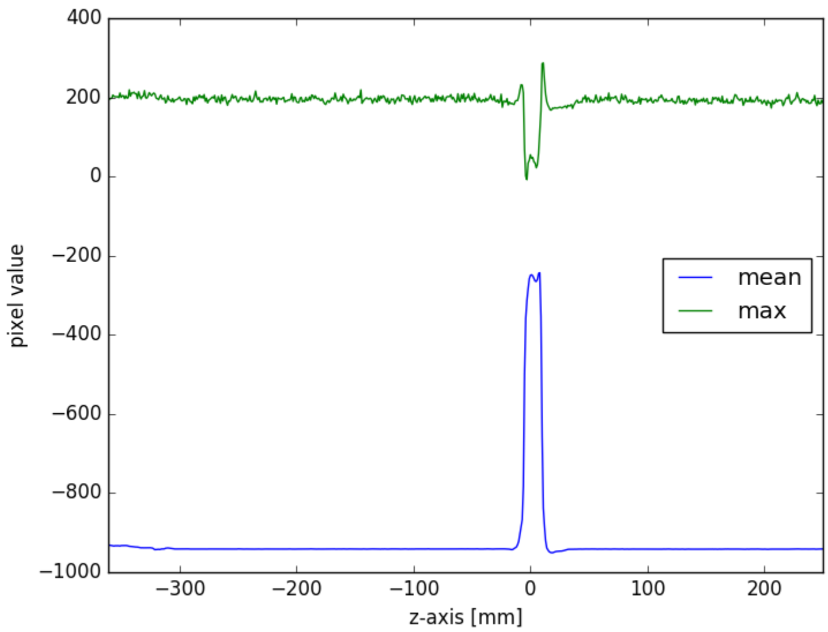

Figure 3.13: Rod #16: brightness of all pixels at a certain slice, CT x100

slice	dist	$warp_x$	$warp_y$	$warpM$	DC_{CT}	DC_{MR}	$DC_{MR(CT-COM)}$	$warp^*_x$	$warp^*_y$	$warpM^*$	DC^*_{CT}	DC^*_{MR}	$DC^*_{MR(CT-COM)}$
0	-361	2.9415	0.4286	2.9725	0.9676	0.033	0.0062	3.3112	0.8531	3.4193	0.944	0.6126	0.3313
1	-360	2.94	0.4294	2.9712	0.9706	0.0331	0.0062	3.3129	0.8427	3.4184	0.9456	0.6126	0.3308
2	-359	2.9441	0.4224	2.9742	0.9725	0.0391	0.0077	3.2904	0.8202	3.3911	0.9475	0.6121	0.3346
:													
:													
351	-10	-0.2049	-0.0356	0.208	0.9896	0.9165	0.9091	-0.2696	-0.1097	0.2911	0.9901	0.9294	0.9248
352	-9	-0.2217	-0.0174	0.2223	0.9937	0.916	0.9112	-0.282	-0.0942	0.2973	0.9834	0.9283	0.9251
353	-8	-1	-1	-1	-1	0.916	-1	-1	-1	-1	-1	0.9274	-1
354	-7	-1	-1	-1	-1	0.9144	-1	-1	-1	-1	-1	0.9258	-1
355	-6	-1	-1	-1	-1	0.912	-1	-1	-1	-1	-1	0.9229	-1
356	-5	-1	-1	-1	-1	0.9113	-1	-1	-1	-1	-1	0.9209	-1
357	-4	-1	-1	-1	-1	0.909	-1	-1	-1	-1	-1	0.9186	-1
358	-3	-1	-1	-1	-1	0.9079	-1	-1	-1	-1	-1	0.9156	-1
359	-2	-1	-1	-1	-1	0.9082	-1	-1	-1	-1	-1	0.9153	-1
360	-1	-1	-1	-1	-1	0.9088	-1	-1	-1	-1	-1	0.9131	-1
361	0	-1	-1	-1	-1	0.9112	-1	-1	-1	-1	-1	0.9102	-1
362	1	-1	-1	-1	-1	0.9102	-1	-1	-1	-1	-1	0.9042	-1
363	2	-1	-1	-1	-1	0.9096	-1	-1	-1	-1	-1	0.9013	-1
364	3	-1	-1	-1	-1	0.9088	-1	-1	-1	-1	-1	0.896	-1
365	4	-1	-1	-1	-1	0.9068	-1	-1	-1	-1	-1	0.8931	-1
366	5	-1	-1	-1	-1	0.9047	-1	-1	-1	-1	-1	0.8908	-1
367	6	-1	-1	-1	-1	0.907	-1	-1	-1	-1	-1	0.8967	-1
368	7	-1	-1	-1	-1	0.9079	-1	-1	-1	-1	-1	0.9006	-1
369	8	-1	-1	-1	-1	0.9077	-1	-1	-1	-1	-1	0.903	-1
370	9	-1	-1	-1	-1	0.9082	-1	-1	-1	-1	-1	0.9057	-1
371	10	-1	-1	-1	-1	0.915	-1	-1	-1	-1	-1	0.9105	-1
372	11	-1	-1	-1	-1	0.92	-1	-1	-1	-1	-1	0.915	-1
373	12	-1	-1	-1	-1	0.9268	-1	-1	-1	-1	-1	0.9187	-1
374	13	-0.2506	0.1242	0.2797	0.9911	0.9281	0.9168	-0.2511	0.0942	0.2682	0.9867	0.9212	0.9397
375	14	-0.2181	0.1166	0.2473	0.9858	0.9298	0.9225	-0.223	0.0966	0.243	0.9937	0.9231	0.9436
:													
:													
609	248	3.0734	0.7814	3.1712	0.9838	0.917	0.3481	3.0773	0.9077	3.2084	0.9967	0.9221	0.5231
610	249	3.1422	0.7546	3.2315	0.984	0.9269	0.328	3.1288	0.8802	3.2503	0.9967	0.9312	0.5192
611	250	3.2214	0.7399	3.3053	0.9834	0.9359	0.3064	3.1835	0.8563	3.2967	0.9971	0.9282	0.5145

Table 3.4: rod #16: script generated data; dist and $warp$ in $[mm]$

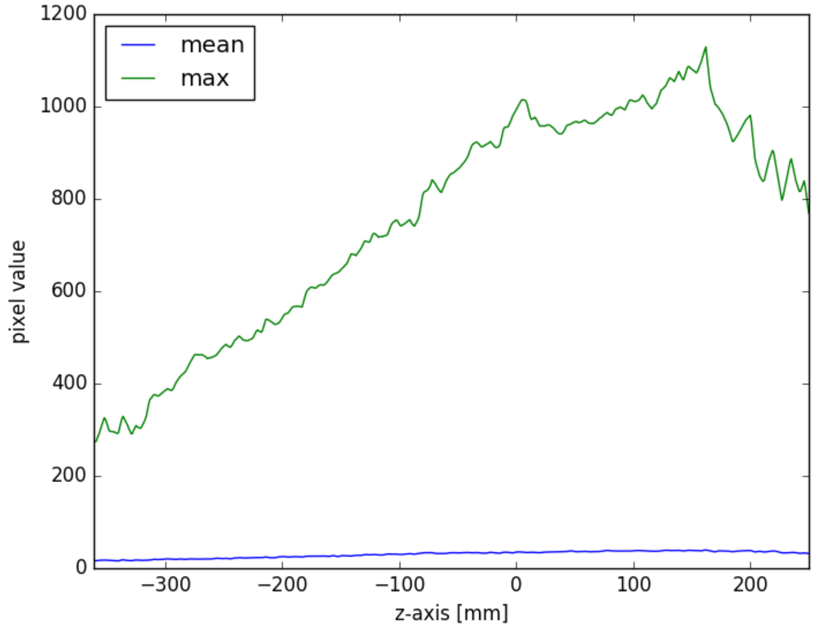

Figure 3.14: Rod #16: brightness of all pixels at a certain slice, MRI x100

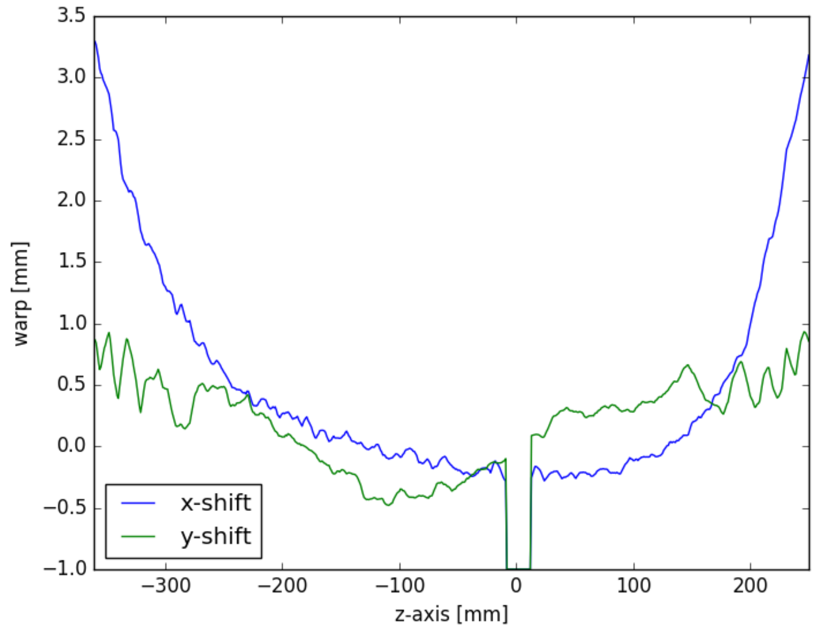

Figure 3.15: Rod #16: warp XY [mm] (iteration method), CT-MRI x100; plastic pane fills region from $-8mm$ to $12mm$

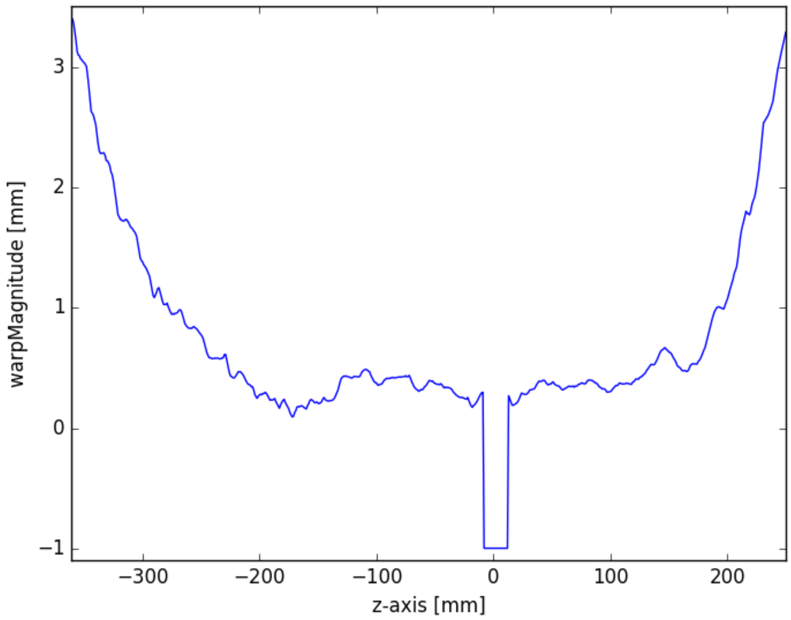

Figure 3.16: Rod #16: warp Magnitude [mm] (iteration method), CT-MRI x100; plastic pane fills region from $-8mm$ to $12mm$

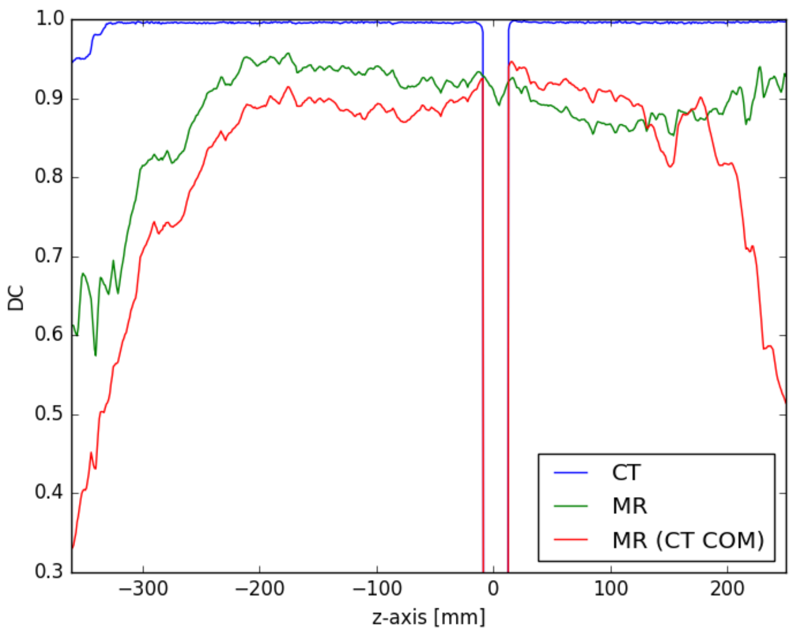

Figure 3.17: Rod #16: DC (iteration method) for CT & MRI & MRI (using CT COM), x100; plastic pane fills region from $-8mm$ to $12mm$

4 Discussion

4.1 Phantom design

To be able to assess the spacial distortion of an MRI scan, a rigid object with known dimensions needs to be scanned so the cross referencing to the ground truth can be performed. Such phantoms are commercially available, but often expensive and designed for a specific calibration protocol. Some institutions build their own to fulfil exactly the requirements of a given application. The scanner used at the AKH is a relatively rare model, which is why no off-the-shelf phantom that would fit its coil is available.

A previously used phantom did not fill the whole FOV, while at the same time weighing about 45kg. This was due to the fact that it resembled a cuboid water tank with a thin filled or solid plastic rod construction inside. As the peripheral zones of the FOV are those where distortion is most pronounced, a bigger phantom was needed to assess those regions. The new design deals reaches the outer regions and weighs much less at the same time.

Due to the underlying physics, plastics are not visible in MR scans, but CT scans visualize them. See figure 2.7 for a comparison (MRI/CT visibility). Therefore, it was decided to use plastic rods with a suitable fluid filling. Such a liquid should be easily produced, non-toxic and yielding sufficient signal in MRI scans.

Commercially available phantoms often resemble water filled tanks containing plastic grids as a reference. This design results in stronger signal, but exceeds practical weight. There are few brands offering solutions utilising liquid fiducial markers in the shape of pellets. They are arranged in a regular pattern surrounded by air or plastic. The AKH's design however relies on replaceable rods, which makes it a novelty.

4.1.1 Observed issues

Interestingly, all water based solutions seemed to have evaporated partly. As the rod filled with liquid **#15** has dried starting at the end with the plastic stopper, it seems likely that, at least in this particular case, the plastic stopper did not effectively close the rod. It might also be that the rod itself does not prevent volatile liquids from escaping slowly. This was tested in a small experiment where a filled rod with only both its ends submerged in water, but the middle part in contact with air was observed over a period of some months (upright rod placed in a glass of water so that the lower end was surrounded by water, a plastic cup of water with a hole in its bottom through which the rod was stuck, glued to seal the hole). Just like in all other rods which were not partly submerged in water, air bubbles formed along its wall. This indicates that not (only) the plastic stopper, but the wall (which was the only part of the rod that was in contact with air) is too thin to keep the filling from evaporating. An airtight container might have led to other conclusions regarding the formation of air bubbles. It is hard to tell if they were caused by evaporation only or if dissolved gases played a role, too. Whatever the reasons are, the use of water based liquids seems to be suboptimal. Despite this, the observed behaviour will still be discussed as different phantom design might benefit from drawn conclusions.

4.2 Tested solutions

For measuring the position of the rods in the CT scans, the plastic rods without filling would be enough already. That is why the visibility of the liquids on CT is not important at all. Hollow plastic rods would not be visible on the MRI scans, though. From now on 'signal (strength)' or 'visibility' will refer to MRI scans only (see table 3.1).

4.2.1 Thoughts about choosing possible candidates

The tested solutions were chosen for a number of reasons:

- Generally, imaging techniques aims for a high signal-to-noise ratio. Therefore, Liquids resulting in brighter pixels are favoured.
- The amount of gas in the rods should be minimised.
- If air bubbles form, tilting the entire phantom slightly should be enough to move them to one side. The FOV of the MRI scanner is too small to show the entire

phantom anyway.

- Most tested fluids are based on water, because this makes them easy to empty and clean. They could then be filled again with a different liquid if needed.
- Preferably, the components which are chosen to be used for the entire phantom should be non-toxic.

Rod #**1** was filled with plain distilled water and intended to be used only as a reference. It was clear from the beginning that it would not result in high signal and was never considered a possible filling.

Aiming for high SNR

To achieve a better SNR, liquids #**2** to #**10** and #**14** to #**15** are based on a solution of sodium chloride ($NaCl$ concentration of $0.36\,g/L$) and copper(II) sulfate pentahydrate ($CuSO_4 \cdot 5H_2O$ concentration of $1.96\,g/L$ as suggested by AAPM MR Subcommittee [37]; #**3** and #**4** contain double and ten-fold the concentration) in distilled water. Most of these liquids resulted in an about 5 times brighter signal than plain distilled water. Regarding the toxicity of $CuSO_4 \cdot 5H_2O$, the minimum dose to have caused acute toxic effects in humans is reported to be $11mg/Kg$.

Primovist (#**11** to #**13**) is a common contrast agent used for MRI scans [55]–[57] intended to yield an even stronger signal than $CuSO_4 \cdot 5H_2O$ based liquids. The major drawback is its tendency to separate from the water and stick to the container's wall. This results in low signal at the centre and high signal along the wall, which would not necessarily pose a problem, but as the liquid forms bubbles, it is not guaranteed that the walls would be covered homogeneously. The uneven distribution might result in wrong calculations, especially if the software tool is not programmed to cope with this behaviour. At the same time the removal of such a solution would be hardly possible.

Handling dissolved gas

Unfortunately, dissolved gases may eventually leave the liquid and form air bubbles trapped in the rod. To improve the mobility of trapped air bubbles, generic washing-up soap was added (#**5**, #**6**, and #**7**; suggestion by Data Spectrum Corporation [58]).

The higher concentrations of soap were tested as reference. If the liquid should happen to leak from the rod, the relatively low concentration of soap would not add to its toxicity. For those reasons, and because the liquid is cheap and easy to produce, it appears to be a promising candidate.

Liquids #**8** ($0.36g/L$), #**9** ($3.6g/L$) and #**10** ($36g/L$) contain ascorbic acid. Adding this was supposed to reduce forming of air bubbles by binding dissolved oxygen and eventually degrade to dehydro-ascorbic acid and water. The amount suggested by [59], [60] is 0.00204 mol/L which corresponds to approx. ($0.36g/L$).

In an attempt to limit the forming of gas, *agar* was used in solutions #**14** and #**15**. Agar and agarose are commonly used as basic reference material for MRI phantoms [61], [62]

Non water-based liquids

As an alternative to water based solutions, two oils were proposed. Since oil is neither soluble in air, nor able to evaporate, a rod completely filled with oil should stay free from air bubbles. Yet, oil is not as easily removed from a rod as a water based liquid. At the same time, it might not be necessary to ever replace the oil. Once filled, the rods could be used until the surrounding plastic breaks or starts leaking. Using vegetable oil would be a non-toxic solution, but has been ruled out as a filling from the beginning, because it would eventually rot. Synthetic oil on the other hand does not rot, however, it might be toxic if consumed.

4.2.2 Choosing a promising candidate

As all rods containing water continued to lose liquid due to evaporation, only the early forming of air bubbles might indicate whether solutions effectively hinder dissolved gases to result in trapped air bubbles. Apart from the solutions containing ascorbic acid (#**8** ($0.36g/L$), #**9** ($3.6g/L$)) all water based liquids produced some air bubbles after at least two days (see table 3.2.2). Considering the low visibility of #**9**, the only suitable water based liquid capable of staying free from air bubbles might be #**8**. At the same time, long-term observations performed in an airtight container might have shown that even

#**8** only delays the process. In the case of the used rods, such a conclusion cannot be drawn with certainty.

The rod containing the highest concentration of ascorbic acid showed a yellow colouring, caused by dehydroascorbic acid which is the result of a oxygenation process. However, as the high concentration in #**9** and #**10** led to a radical reduction in signal with the tested MRI sequence, this solutions is not considered a suitable filling anyway.

Primovist (#**11** to #**13**) lead to a good signal, but its limited mobility of air bubbles; its tendency to accumulate along the wall; and the difficulty of cleaning the rods rule it out as a candidate.

If the forming of a small amount of gas is not considered a problem, adding soap appears to be a reasonable solution. The smallest tested amount of soap (#**5**, 1 g/L) was already enough to result in sufficient mobility of air bubbles, and an even lower concentration might also be acceptable. Interestingly, the rod filled with this solution contained the least amount of gas after 2 months, but this might be because the particular rod closed better than the others. The visibility recorded was among the higher candidates, too. For those reasons, and because the liquid is cheap and easy to produce, it is a promising candidate.

Solutions containing *agar* (#**14** and #**15**) are even harder to remove from rods if not impossible. As they might lead to air bubbles, too, which cannot be moved to either side of the rod, agar is not suited for this phantom.

Finally, the synthetic motor oil (#**16**) resulted in the highest signal intensity of all candidates. Besides the question of its toxicity, it seems to be a good alternative to water based liquids. The silicon oil (#**17**) on, the other side, had a low signal compared to most candidates and is therefore not suited.

4.3 Distortion

4.3.1 Calculation Methods

`DC` and warp calculated with the simple and iteration method do not differ much. Moreover, both methods choose very similar thresholds for their calculations (see header of appended '.txt' output file) As the simple method uses additional information on the rod's true dimension, it is supposed to yield accurate, reliable results. The iteration process, oblivious to the imaging modality, supports this claim as it produces very similar numbers.

The biggest difference in the results obtained with both methods are the values in the region of the air bubble in rod #5: Slices 303-310 in table 3.3 mark the area where the maximum brightness dropped significantly due to the absence of liquid (see figure 3.7). The simple method for finding the COM did not manage to calculate coordinates in this region, due to the lack of pixels above the threshold based on the reference slice (which was 827; see appendix). Consequently, warp and DC for MRI were set to '-1'. However, the iteration method tried various thresholds and settled for the one resulting in the highest average DC for the whole scan. As slices with values of '-1' influence the average dramatically, the chosen threshold is low enough (339; see appendix) to include some of the brightest pixels in slices 303-310.

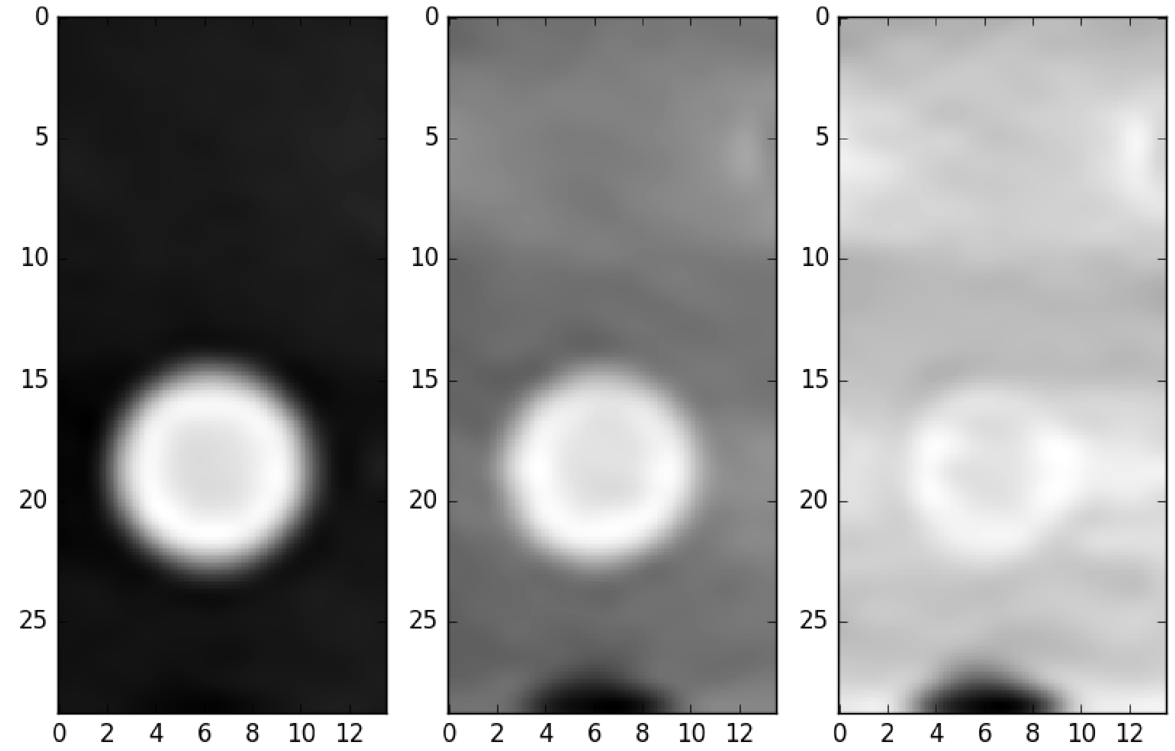

(a) slice 175 (b) slice 176 (c) slice 177

Figure 4.1: Slices at edge of plastic pane in CT image showing rod #5 (true colours): a black crescent remains at the bottom where there is a hole in the pane that is not filled with a rod at the moment

4.3.2 Irregularities

All obtained CT scans include a region where the plastic panes are visible. Figure 4.1 shows how the plastic pane makes it impossible to define the rod on the CT image. These areas cannot be used for distortion assessment as the COM cannot be calculated reliably. Figures 3.6 and 3.13 exhibit spikes in the average brightness where the image shows a plastic pane. The script recognised this difference and marked all affected slices as 'irregular'. Consequently, in table 3.3 and 3.4, the values of the COM shift ($warp_x$, $warp_y$, $warpM$); the DC for CT using the CT-centroid (DC_{CT}); and the DC for MRI using the CT-centroid ($DC_{MR(CT-COM)}$) are all set to '-1'.

4.3.3 Measured distortion - Rod #5

Figure 3.11 visualises the centroid shift at interesting slices of rod #5. It is clearly visible that the shift is bigger at the end of the rod (slice 0) compared to a slice close to its middle (slice 171). The values of $warpM^*$ in table 3.3 verify this (1.0623mm $>$ 0.6926mm). Furthermore, the distortion measured at the location of the air bubble (slice 304) shows a maximum for the COM shift ($warpM^* = 1.5748$mm) and a minimum for the DC ($DC^*_{MR} = 0.6762$). These values originate not from true spatial distortion, but are caused by the presence of gas in the rod. Since the bubble floated on top of the liquid, the COM shift is most pronounced in the y direction (up-down) as shown by figure 3.8. The overall impact on the area of 110mm to 140mm is clearly visible in figures 3.9 and 3.10. In conclusion, it is imperative for the distortion assessment to exclude bubbles from the FOV.

4.3.4 Measured distortion - Rod #16

Similar to the findings for rod #5, the distortion is bigger in the peripheral regions of the FOV (see figure 3.17). Interestingly, the y shift changes its orientation around the centre (see figure 3.15). This might be a local feature of the distortion and cannot be put in relation, because no distortion map of the entire FOV is available yet.

As rod #16 does not contain any air bubbles, the brightness plotted in figure 3.14 shows no sudden drops. However, the left hand side has a drastically lower signal strength than the right. A closer look revealed that rod #16 contained oil of two different colours. It seems that some residue of the other oil, which was injected into rod #17, was still present in the syringe when rod #16 was filled. To avoid this, the injecting syringe and the capillary were flushed with the next liquid before injection. This procedure was not enough to clean it thoroughly. The liquids separated into parts with different density while the rod was stored upright and were still distributed unevenly during imaging. To avoid this problem in the future, a new and unused syringe should be used for filling.

It is likely, that this influenced the calculated warp and DC as the lighter oil (which results in a different signal strength) floated on top of the other, resulting in an unwanted shift of the calculated COM. This might explain why the y shift changes its orientation close to the isocentre as this is the point where the signal intensity starts to change, too. To be sure of the actual impact of the oil mix on the distortion assessment, a new rod should be filled and the imaging repeated. For now, the already gained results will be used as no new measurement could be obtained in the limited time that the scanner is available for such experiments.

In the region beyond -330, there is a drop of the DC for the CT. Investigations revealed that this is caused by adhesive tape attached to the rod to hold it in place during transport from the CT scanner to the MRI scanner. The values calculated for this area are most likely influenced by this.

4.3.5 Effect of resampling

Figures 4.2 and 4.5 depict the measured $warpM^*$ of rod #5 and #16 for x1 and x100 resample rates. The location shift calculated with x1 and x100 resample rate are relatively close (see tables 4.1 and 4.2).

The calculated DCs for the scans in original CT resolution (x1) are shown in figures 4.3 and 4.6 and for a x4 finer resolution in figures 4.4 and 4.7. Compared to the DCs of the x100 resampled scans (figures 3.10 and 3.17), the low resolution x1 yields significantly less smooth curves. A resample rate of x4, on the other hand, is already much closer to the quality of the x100 scans.

While the original resolution might be sufficient for the calculation of the COM shift, the DC calculation benefits a lot from a interpolated image. It is easier to spot significant changes as the plot shows less jumps. At the same time, the computing time for calculations scales with the resolution of the images and should be kept minimal, because a future assessment would include more than 300 individual rods.

Now that the appearance of the curves has been addressed, it will be discussed how the calculated distortion varies with increased resample rate.

Rod #5

Table 4.1 lists the expectancy and standard deviation (σ_Δ) of the difference between the calculated distortion for x1 and x100 resample rate of rod #5:

The expectancy value E was calculated as the sum of the difference in each slice over the number of slices; it is the average difference. A random deviation should result in some slices with positive and some with negative local differences. Therefore, the average should be close to zero. Otherwise, an increased resample rate would either result in an overall drop or rise of measured distortion. Indeed, E is relatively small compared to the typical COM shift (even smaller than σ_Δ), which indicates that the increased resample rate does only result in a smoother curve, but not in very different values overall.

The COM shift mostly lies in a range of 0.5 to 0.7mm; σ_Δ is approximately one order of magnitude smaller. To verify whether this hints at increased accuracy or not, an external reference would be needed. In any case, a difference of less than $0.1mm$ would not influence treatment planning and can be regarded negligible.

The value of the MRI DC lies between 0.9 and 1 (except for the air bubble region); σ_Δ is roughly a 45th of the average DC value $(0.9/0,02)$. This is small enough to be neglected, too.

	E	σ_Δ
$\Delta warpM^*$ [mm]	0.038	0.058
ΔDC^*_{MRI}	0.000518	0.019070
$\Delta DC^*_{MRI(CT-COM)}$	-0.008905	0.022050

Table 4.1: Expectancy and standard deviation of difference between calculated distortion for x1 and x100 resample rate; rod #5

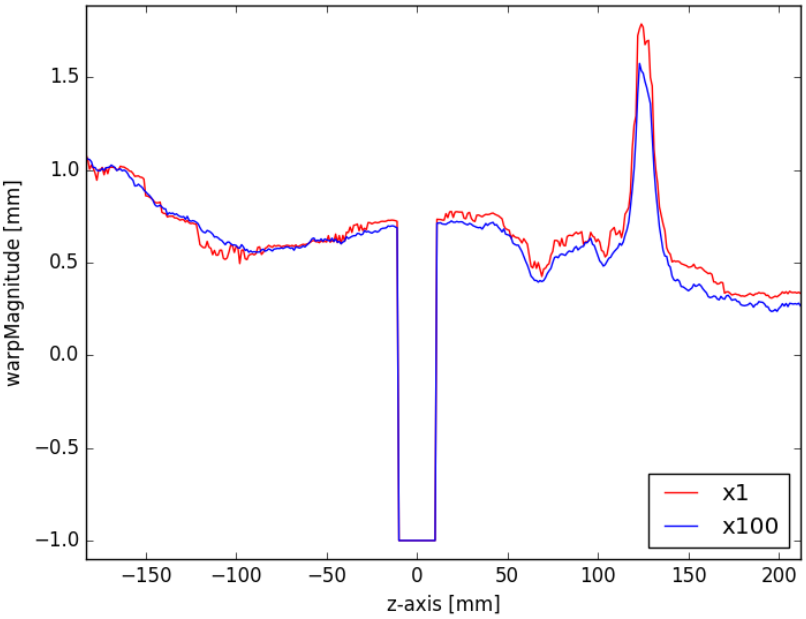

Figure 4.2: Rod #5: warp Magnitude [mm] (iteration method), CT-MRI x1 and x100; plastic pane from $-10mm$ to $10mm$, bubble at about $110mm$ to $135mm$

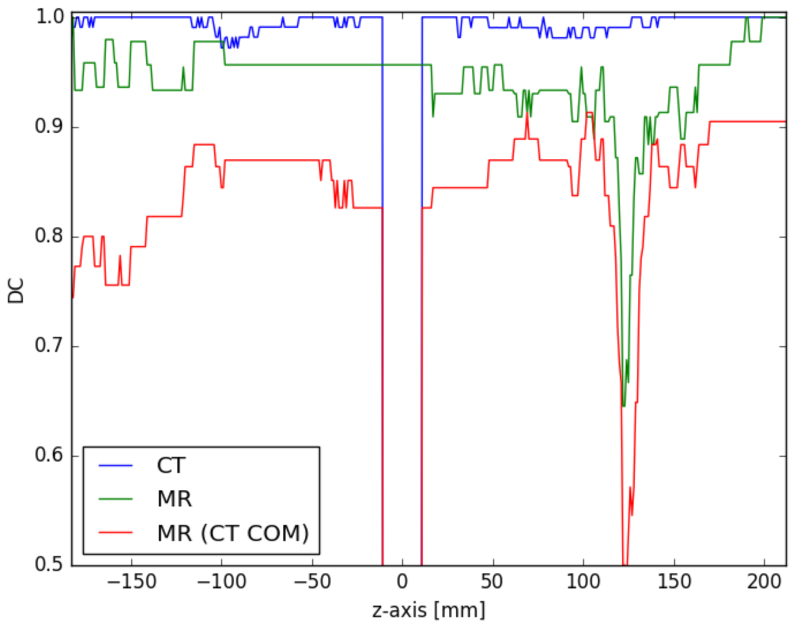

Figure 4.3: Rod #5; x1: DC (iteration method) for CT & MRI & MRI (using CT COM); plastic pane from $-10mm$ to $10mm$, bubble at about $110mm$ to $135mm$

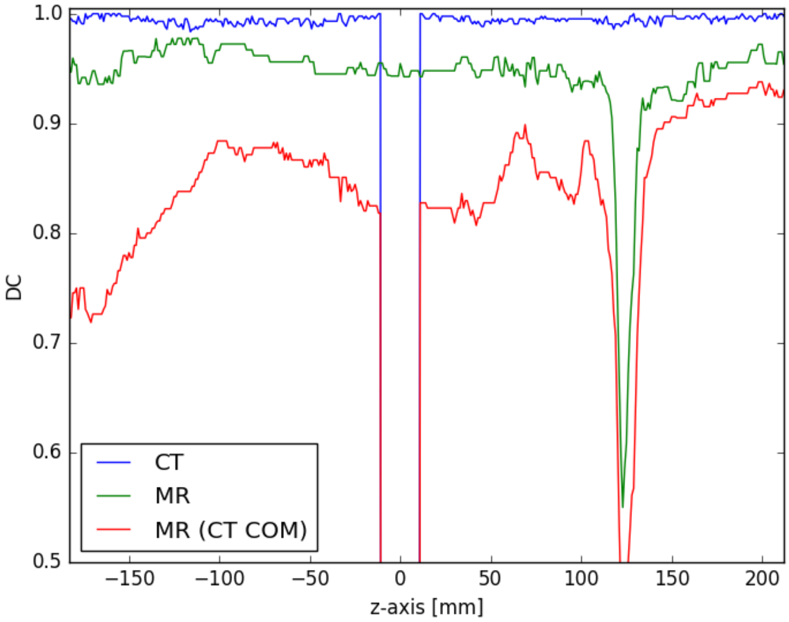

Figure 4.4: Rod #5; x4: DC (iteration method) for CT & MRI & MRI (using CT COM); plastic pane from $-10mm$ to $10mm$, bubble at about $110mm$ to $135mm$

Rod #16

Table 4.2 lists the expectancy and standard deviation σ_Δ of the difference between calculated distortion for x1 and x100 resample rate of rod #16:

Again, the expectancy E is relatively small; hinting at a low overall shift of the calculated values.

Just like with rod #5, σ_Δ for the COM shift is approximately one order of magnitude smaller than the occurring warp and can therefore also be regarded a negligible.

Similarly, σ_Δ for the MRI DC is approximately a 45th of the average DC value $(0.9/0, 02)$ and can be neglected.

	E	σ_Δ
$\Delta warpM^*$ [mm]	0.005	0.025
ΔDC^*_{MRI}	0.004835	0.019823
$\Delta DC^*_{MRI(CT-COM)}$	0.012554	0.019429

Table 4.2: Expectancy and standard deviation of difference between calculated distortion for x1 and x100 resample rate; rod #16

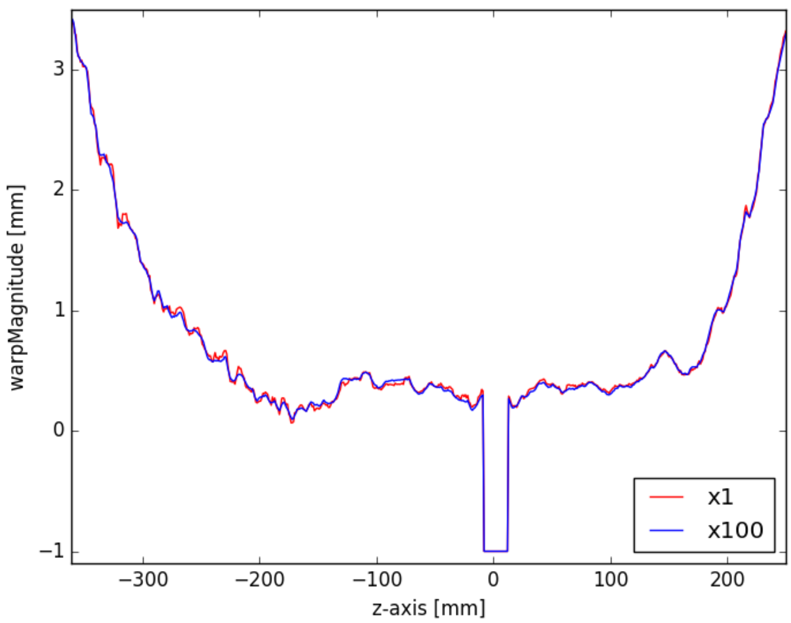

Figure 4.5: Rod #16: warp Magnitude $[mm]$ (iteration method), CT-MRI x1 and x100; plastic pane from $-8mm$ to $12mm$

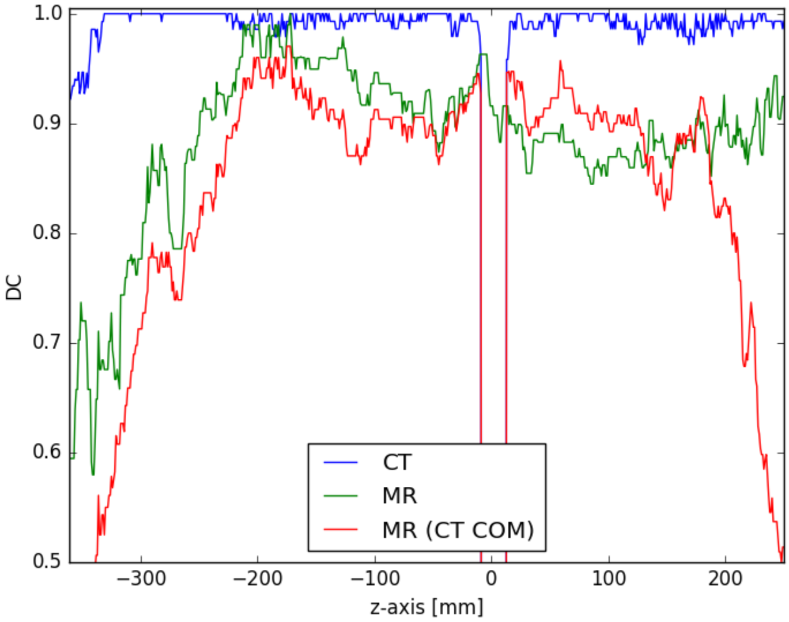

Figure 4.6: Rod #16; x1: DC (iteration method) for CT & MRI & MRI (using CT COM); plastic pane from $-8mm$ to $12mm$

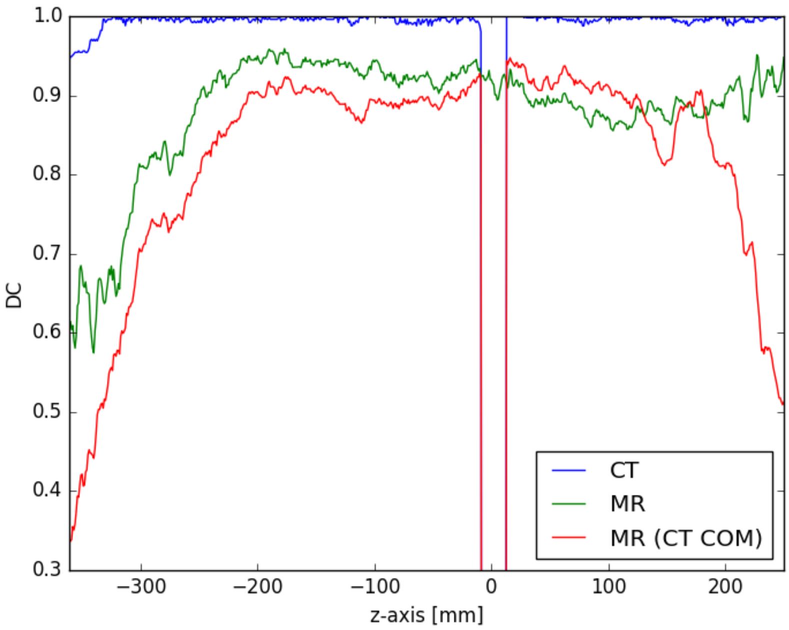

Figure 4.7: Rod #16; x4: DC (iteration method) for CT & MRI & MRI (using CT COM); plastic pane from $-8mm$ to $12mm$

5 Conclusion and Outlook

5.1 Filling for phantom

As topping up over 300 rods regularly is too time consuming, and all water-based liquids continued to evaporate, they are not long-term solution for this phantom. They are, however, useful for prototyping. For short time experiments with this phantom (not airtight rods) #**5** is recommended, because the soap allows the air to be moved out of the FOV. If another set of rods with airtight walls were obtained, adding ascorbic acid to the solution (a combination of #**5** and #**8**) might be an even better filling:

- distilled water
- $0.36\,g/L$ of $NaCl$
- $1.96\,g/L$ of $CuSO_4 \cdot 5H_2O$
- $1\,g/L$ of soap
- $0.36 g/L$ of ascorbic acid

In that case, the forming of air bubbles might be either avoided entirely (due to the ascorbic acid) or delayed and then easily taken care of by tilting the whole phantom slightly to move the bubbles out of the FOV. The long-term behaviour of the mix might lead to adverse properties and should be tested, though.

In the current set-up, it seems best to fill the rods of the phantom with the type of oil that does not rot and yields high signal. The tested synthetic motor oil (#**16**) fits those requirements.

5.2 Recommended resample rates

The accuracy of the distortion assessment, especially of the DC calculation, can be enhanced by using interpolated scans. Resample rates of x4, x9, x25 and x100 were used to create finer images which were all analysed using the same algorithms. The original resolution (x1) might be sufficient for the COM shift calculation, but the DC curve gains significant smoothness at already x4 finer resolution. This small interpolation could be already enough to increase accuracy while keeping necessary computing power low. A future distortion assessment of the whole FOV with 300 individual rods would profit from a effective procedure at low resolution. Using the simple method to find the COM would use less time, too.

5.3 Future improvement of software tool

The developed tool took a simplified approach to the problem by looking only at a single rod. Distortion assessment can be performed using the generated tool, however, it needs to be implemented on more general scale to be able to measure the distortion for all the rods automatically. This could be done by a auto-trace function which detects individual rods and applies the already implemented algorithms to each of them separately.

The two implemented methods of finding COM and DC need to be assessed themselves. In order to tell which of the two gets closer to the absolute truth, additional checks should be performed. A possible accuracy test could look like this: two CT scans of the phantom which differ only by a known displacement of one rod are registered and resampled. The software tool is used to calculate the COM shift between the images which can be compared to the real displacement.

At the moment the iteration method does not take into account the steepness of the DC curve. In some cases this might result in neglecting the left hand side close to very low percentages. This happens when the maximum lies roughly in the middle of the current range, but a little bit to the left. Because the slope is steeper on the left (close to 0%), a value representing the left hand side (also close to 0%) yields a much lower result than the value on the right hand side (flat slope). This should be taken into account during further improvement of the method.

In the current version of the software tool, only changes in the mean brightness are used to characterise irregularities. It might be usefull to consider drops in the peak brightness as irregularities, too. This way, the distortion would not be calculated in the region of an air bubble. For the time being, running the script over those regions might aid troubleshooting and give better understanding how to improve the code.

5.4 Scale of distortion

For the investigated position of the rod (rod #16), the obtained values for the occurring spatial distortion report a COM shift below $1mm$ in a region of at least $40cm$ (from -283mm to 185mm; simple method). This does not rule out the possibility of using the MR scanner for radiotherapy planning. Whether the distortion is small enough to guarantee accurate treatment planning can only be discussed after a map for the entire FOV has been created.

Bibliography

[1] International Atomic Energy Agency, *Radiation Oncology Physics: A Handbook for Teachers and Students*, E. B. Podgorsak, Ed. International Atomic Energy Agency, 2005, ISBN: 9201073046.

[2] A. Maidment and M. Yaffe, *Diagnostic Radiology Physics: A Handbook For Teachers And Students*. International Atomic Energy Agency, 2014, pp. 209–235, ISBN: 978-92-0-131010-1.

[3] K. Baumann, "Stem cells: a key to totipotency", *Nature Reviews Molecular Cell Biology*, vol. 18, no. 3, pp. 137–137, Feb. 2017, ISSN: 1471-0072. DOI: 10.1038/nrm.2017.9.

[4] M. Joiner and A. van der Kogel, *Basic Clinical Radiobiology*. Taylor & Francis Ltd., Apr. 11, 2009, 288 pp., ISBN: 9780340929667.

[5] A. Sodickson, P. F. Baeyens, K. P. Andriole, L. M. Prevedello, R. D. Nawfel, R. Hanson, and R. Khorasani, "Recurrent CT, cumulative radiation exposure, and associated radiation-induced cancer risks from CT of adults", *Radiology*, vol. 251, no. 1, pp. 175–184, Apr. 2009, ISSN: 0033-8419. DOI: 10.1148/radiol.2511081296.

[6] C. H. McCollough, A. N. Primak, N. Braun, J. Kofler, L. Yu, and J. Christner, "Strategies for reducing radiation dose in CT", *Radiologic Clinics of North America*, vol. 47, no. 1, pp. 27–40, Jan. 2009. DOI: 10.1016/j.rcl.2008.10.006.

[7] M. J. Murphy, J. Balter, S. Balter, J. A. BenComo, I. J. Das, S. B. Jiang, C.-M. Ma, G. H. Olivera, R. F. Rodebaugh, K. J. Ruchala, H. Shirato, and F.-F. Yin, "The management of imaging dose during image-guided radiotherapy: report of the AAPM task group 75", *Medical Physics*, vol. 34, no. 10, pp. 4041–4063, Sep. 2007. DOI: 10.1118/1.2775667.

[8] A. Smith, W. Dillon, R. Gould, and M. Wintermark, “Radiation dose-reduction strategies for neuroradiology CT protocols”, *American Journal of Neuroradiology*, vol. 28, no. 9, pp. 1628–1632, Oct. 2007. DOI: 10.3174/ajnr.a0814.

[9] A. R. Goldman and P. D. Maldjian, “Reducing radiation dose in body CT: a practical approach to optimizing CT protocols”, *American Journal of Roentgenology*, vol. 200, no. 4, pp. 748–754, Apr. 2013. DOI: 10.2214/ajr.12.10330.

[10] D. J. Brenner, C. D. Elliston, E. J. Hall, and W. E. Berdon, “Estimated risks of radiation-induced fatal cancer from pediatric CT”, *American Journal of Roentgenology*, vol. 176, no. 2, pp. 289–296, 2001, ISSN: 0361803X. DOI: 10.2214/ajr.176.2.1760289. arXiv: 01/1762âĂŞ289 [0361-803X].

[11] S. Currie, N. Hoggard, I. J. Craven, M. Hadjivassiliou, and I. D. Wilkinson, “Understanding MRI: basic MR physics for physicians”, *Postgraduate Medical Journal*, vol. 89, no. 1050, pp. 209–223, 2013, ISSN: 0032-5473. DOI: 10.1136/postgradmedj-2012-131342. eprint: http://pmj.bmj.com/content/89/1050/209.full.pdf.

[12] C. Rasch, I. Barillot, P. Remeijer, A. Touw, M. van Herk, and J. V. Lebesque, “Definition of the prostate in CT and MRI: a multi-observer study”, *International Journal of Radiation Oncology Biology Physics*, vol. 43, no. 1, pp. 57–66, Jan. 1999. DOI: 10.1016/s0360-3016(98)00351-4.

[13] M. Debois, R. Oyen, F. Maes, G. Verswijvel, G. Gatti, H. Bosmans, M. Feron, E. Bellon, G. Kutcher, H. V. Poppel, and L. Vanuytsel, “The contribution of magnetic resonance imaging to the three-dimensional treatment planning of localized prostate cancer”, *International Journal of Radiation Oncology Biology Physics*, vol. 45, no. 4, pp. 857–865, Nov. 1999. DOI: 10.1016/s0360-3016(99)00288-6.

[14] M. Roach, P. Faillace-Akazawa, C. Malfatti, J. Holland, and H. Hricak, “Prostate volumes defined by magnetic resonance imaging and computerized tomographic scans for three-dimensional conformal radiotherapy”, *International Journal of Radiation Oncology Biology Physics*, vol. 35, no. 5, pp. 1011–1018, Jul. 1996. DOI: 10.1016/0360-3016(96)00232-5.

[15] “Reduction of claustrophobia with short-bore versus open magnetic resonance imaging: a randomized controlled trial”, *PLoS ONE*, vol. 6, no. 8, J. Laks, Ed., Aug. 2011. DOI: 10.1371/journal.pone.0023494.

[16] C. Bangard, J. Paszek, F. Berg, G. Eyl, J. Kessler, K. Lackner, and A. Gossmann, "MR imaging of claustrophobic patients in an open 1.0 T scanner: Motion artifacts and patient acceptability compared with closed bore magnets", *European Journal of Radiology*, vol. 64, no. 1, pp. 152–157, 2007, ISSN: 0720048X. DOI: 10.1016/j.ejrad.2007.02.012.

[17] A. M. Coffey, M. L. Truong, and E. Y. Chekmenev, "Low-field MRI can be more sensitive than high-field MRI", *Journal of Magnetic Resonance*, vol. 237, pp. 169–174, 2013, ISSN: 10960856. DOI: 10.1016/j.jmr.2013.10.013. arXiv: NIHMS150003.

[18] A. Fransson, P. Andreo, and R. Pötter, "Aspects of MR image distortions in radiotherapy treatment planning", *Strahlentherapie und Onkologie*, vol. 177, no. 2, pp. 59–73, Jan. 2001. DOI: 10.1007/pl00002385.

[19] B. K. Rutt and D. H. Lee, "The impact of field strength on image quality in MRI", *Journal of magnetic resonance imaging : JMRI*, vol. 6, no. 1, pp. 57–62, 1996, ISSN: 1053-1807. DOI: 10.1002/jmri.1880060111.

[20] D. W. McRobbie, E. A. Moore, M. J. Graves, and M. R. Prince, *MRI from Picture to Proton*. Cambridge University Press, 2006, pp. 329–335, ISBN: 9780521865272.

[21] K. Nakamura and (. D. Group), "Passage of particles through matter", *Journal of Physics*, vol. G, no. 37, p. 075 021, 2010, ISSN: 1434-6044. [Online]. Available: http://iopscience.iop.org/0954-3899/37/7A/075021/media/rpp2010_0001-0007.pdf (visited on 09/29/2017).

[22] H. Paganetti, T. Bortfeld, and H. Kooy, "Proton beam radiotherapy - The state of the art", *Medical Physics*, vol. 32, no. 6Part13, pp. 2048–2049, 2005, ISSN: 2473-4209. DOI: 10.1118/1.1999671. [Online]. Available: http://www.aapm.org/meetings/05AM/pdf/18-4016-65735-22.pdf (visited on 09/29/2017).

[23] P. Andrzejewski, P. Kuess, B. Knäusl, K. Pinker, P. Georg, J. Knoth, D. Berger, C. Kirisits, G. Goldner, T. Helbich, R. Pötter, and D. Georg, "Feasibility of dominant intraprostatic lesion boosting using advanced photon-, proton- or brachytherapy", *Radiotherapy and Oncology*, vol. 117, no. 3, pp. 509–514, Dec. 2015. DOI: 10.1016/j.radonc.2015.07.028.

[24] C. Constantinou, J. C. Harrington, and L. A. DeWerd, "An electron density calibration phantom for CT-based treatment planning computers.", *Medical Physics*, vol. 19, no. 2, pp. 325–327, 1992, ISSN: 00942405. DOI: 10.1118/1.596862.

[25] U. Schneider, E. Pedroni, and A. Lomax, "The calibration of CT Hounsfield units for radiotherapy treatment planning.", *Physics in medicine and biology*, vol. 41, no. 1, pp. 111–24, 1996, ISSN: 0031-9155. DOI: 10.1088/0031-9155/41/1/009. arXiv: arXiv:1011.1669v3.

[26] C. M. Rank, N. Hünemohr, A. M. Nagel, M. C. Röthke, O. Jäkel, and S. Greilich, "MRI-based simulation of treatment plans for ion radiotherapy in the brain region", *Radiotherapy and Oncology*, vol. 109, no. 3, pp. 414–418, 2013, ISSN: 01678140. DOI: 10.1016/j.radonc.2013.10.034.

[27] T. Stanescu, J. Hans-Sonke, P. Stavrev, and B. G. Fallone, "3T MR-based treatment planning for radiotherapy of brain lesions", *Radiology and Oncology*, vol. 40, no. 2, pp. 125–132, 2006, ISSN: 13182099. [Online]. Available: http://www.scopus.com/inward/record.url?eid=2-s2.0-33746661222&partnerID=tZOtx3y1 (visited on 09/29/2017).

[28] J. H. Jonsson, M. G. Karlsson, M. Karlsson, and T. Nyholm, "Treatment planning using mri data: an analysis of the dose calculation accuracy for different treatment regions", *Radiation Oncology*, vol. 5, pp. 62–, 2010. DOI: 10.1186/1748-717X-5-62.

[29] P. Greer, D. Ph, J. Dowling, D. Ph, P. Pichler, J. Sun, M. Sc, H. Richardson, B. M. R. Sc, D. Rivest-henault, D. Ph, S. Ghose, D. Ph, J. Martin, C. Wratten, J. Arm, L. Best, J. Denham, and P. Lau, "Development of MR-only Planning for Prostate Radiation Therapy Using Synthetic CT", pp. 61–62, 2015.

[30] L. Chen, R. A. Price, L. Wang, J. Li, L. Qin, S. McNeeley, C. M. C. Ma, G. M. Freedman, and A. Pollack, "MRI-based treatment planning for radiotherapy: Dosimetric verification for prostate IMRT", *International Journal of Radiation Oncology Biology Physics*, vol. 60, no. 2, pp. 636–647, 2004, ISSN: 03603016. DOI: 10.1016/j.ijrobp.2004.05.068.

[31] R. G. Price, M. Kadbi, J. Kim, J. Balter, I. J. Chetty, and C. K. Glide-Hurst, "Technical note: characterization and correction of gradient nonlinearity induced distortion on a 1.0 t open bore MR-SIM", *Medical Physics*, vol. 42, no. 10, pp. 5955–5960, Sep. 2015, ISSN: 0094-2405. DOI: 10.1118/1.4930245.

[32] B. Petersch, J. Bogner, A. Fransson, T. Lorang, and R. Pötter, "Effects of geometric distortion in 0.2 T MRI on radiotherapy treatment planning of prostate cancer",

Radiotherapy and Oncology, vol. 71, no. 1, pp. 55–64, 2004, ISSN: 01678140. DOI: 10.1016/j.radonc.2003.12.012.

[33] T. Torfeh, R. Hammoud, M. McGarry, N. Al-Hammadi, and G. Perkins, "Development and validation of a novel large field of view phantom and a software module for the quality assurance of geometric distortion in magnetic resonance imaging.", *Magnetic Resonance Imaging*, vol. 33, no. 7, pp. 939–949, 2015, ISSN: 0730725X. DOI: 10.1016/j.mri.2015.04.003.

[34] D. Wang, D. M. Doddrell, and G. Cowin, "A novel phantom and method for comprehensive 3-dimensional measurement and correction of geometric distortion in magnetic resonance imaging", *Magnetic Resonance Imaging*, vol. 22, no. 4, pp. 529–542, 2004, ISSN: 0730725X. DOI: 10.1016/j.mri.2004.01.008.

[35] D. Wang, W. Strugnell, G. Cowin, D. M. Doddrell, and R. Slaughter, "Geometric distortion in clinical MRI systems: Part II: Correction using a 3D phantom", *Magnetic Resonance Imaging*, vol. 22, no. 9, pp. 1223–1232, 2004, ISSN: 0730725X. DOI: 10.1016/j.mri.2004.08.014.

[36] T. Mizowaki, Y. Nagata, K. Okajima, M. Kokubo, Y. Negoro, N. Araki, and M. Hiraoka, "Reproducibility of geometric distortion in magnetic resonance imaging based on phantom studies", *Radiotherapy and Oncology*, vol. 57, no. 2, pp. 237–242, 2000, ISSN: 01678140. DOI: 10.1016/S0167-8140(00)00234-6.

[37] E. F. Jackson, "MR Acceptance Testing and Quality Control : Previous MR Committee TG Reports MRI Acceptance Testing - E . Jackson Levels of Involvement MR Acceptance Test Reality Check MR Siting Issues", vol. 17, no. 1, pp. 287–295, 2009.

[38] S. AG, *System owner manual - mr compatibility data sheet - magnetom c!*, 2013, pp. 89–116.

[39] W. Henry, "Experiments on the Quantity of Gases Absorbed by Water, at Different Temperatures, and under Different Pressures", *Philosophical Transactions of the Royal Society of London*, vol. 93, no. 1, pp. 29–274, Jan. 1803, ISSN: 02610523. DOI: 10.1098/rstl.1803.0004.

[40] R. Sander, "Compilation of Henry's law constants (version 4.0) for water as solvent", *Atmospheric Chemistry and Physics*, vol. 15, no. 8, pp. 4399–4981, 2015, ISSN: 16807324. DOI: 10.5194/acp-15-4399-2015.

[41] (). Python 2.7.13, [Online]. Available: https://www.python.org/ (visited on 01/10/2017).

[42] (). DICOM: About DICOM, [Online]. Available: http://dicom.nema.org/Dicom/about-DICOM.html (visited on 01/08/2017).

[43] (). SimpleITK, [Online]. Available: http://www.simpleitk.org/ (visited on 12/19/2016).

[44] (). SimpleITK - Wiki, [Online]. Available: https://itk.org/Wiki/SimpleITK (visited on 01/10/2017).

[45] (). 3D Slicer, [Online]. Available: https://www.slicer.org/ (visited on 09/29/2017).

[46] R. Kikinis. (2012). Overview: functions of 3D Slicer, [Online]. Available: http://perk.cs.queensu.ca/sites/perk.cs.queensu.ca/files/2014-04-30-Kikinis-Slicer-reduced.pdf (visited on 09/29/2017).

[47] (). SimpleITK: IPython Notebooks, [Online]. Available: http://insightsoftwareconsortium.github.io/SimpleITK-Notebooks/ (visited on 12/19/2016).

[48] A. Kyriakou. (). Image Segmentation with Python and SimpleITK, [Online]. Available: https://pyscience.wordpress.com/2014/10/19/image-segmentation-with-python-and-simpleitk/ (visited on 09/29/2017).

[49] (). Pydicom, [Online]. Available: http://pydicom.readthedocs.io/en/stable/getting_started.html (visited on 01/10/2017).

[50] ——, (). DICOM in Python: Importing medical image data into NumPy with PyDICOM and VTK, [Online]. Available: https://pyscience.wordpress.com/2014/09/08/dicom-in-python-importing-medical-image-data-into-numpy-with-pydicom-and-vtk/ (visited on 01/10/2017).

[51] J. D. Hunter, "Matplotlib: a 2d graphics environment", *Computing in Science & Engineering*, vol. 9, no. 3, pp. 90–95, 2007. DOI: 10.1109/mcse.2007.55. [Online]. Available: https://matplotlib.org/ (visited on 09/29/2017).

[52] (). MedPy 0.2.2 : Python Package Index, [Online]. Available: https://pypi.python.org/pypi/MedPy (visited on 12/19/2016).

[53] (). medpy.metric.binary — MedPy 0.2.2 documentation, [Online]. Available: http://pythonhosted.org/MedPy/_modules/medpy/metric/binary.html#dc (visited on 12/19/2016).

[54] O. Maier. (2015). medpy.metric.binary.dc — MedPy 0.2.2 documentation, [Online]. Available: `http://pythonhosted.org/MedPy/generated/medpy.metric.binary.dc.html#medpy.metric.binary.dc` (visited on 12/19/2016).

[55] B. E. Van Beers, C. M. Pastor, and H. K. Hussain, "Primovist, eovist: what to expect?", *Journal of Hepatology*, vol. 57, no. 2, pp. 421–429, Aug. 2012, ISSN: 01688278. DOI: `10.1016/j.jhep.2012.01.031`.

[56] M. Rohrer, H. Bauer, J. Mintorovitch, M. Requardt, and H.-J. Weinmann, "Comparison of Magnetic Properties of MRI Contrast Media Solutions at Different Magnetic Field Strengths",

[57] Bayer-Group. (Jul. 7, 2007). Primovist: Physico-Chemical Properties, [Online]. Available: `http://www.medsafe.govt.nz/profs/Datasheet/p/primovistsol.pdf` (visited on 09/29/2017).

[58] Data Spectrum Corporation. (). Frequently Asked Questions - How do I eliminate air bubbles in the Mini, Micro and Ultra Micro line of phantoms?, [Online]. Available: `http://www.spect.com/faq.html` (visited on 09/29/2017).

[59] S. M. Abtahi, M. Shahriari, M. H. Zahmatkesh, H. Khalafi, S. Akhlaghpoor, and S. Bagheri, "A new approach to contrast enhancement in MAGICA gel dosimeter image with MRI technique", *Iranian Journal of Radiation Research*, vol. 6, no. 3, pp. 151–156, 2008, ISSN: 17284562.

[60] R. S. Bodannes and P. C. Chan, "Ascorbic acid as a scavenger of singlet oxygen", *FEBS Letters*, vol. 105, no. 2, pp. 195–196, Sep. 1979, ISSN: 00145793. DOI: `10.1016/0014-5793(79)80609-2`.

[61] M. Bucciolini, L. Ciraolo, and B. Lehmann, "Simulation of biologic tissues by using agar gels at magnetic resonance imaging", *Acta Radiologica*, vol. 30, no. 6, pp. 667–669, Jan. 1989. DOI: `10.3109/02841858909174735`.

[62] R. Mathur-De Vre, R. Grimee, F. Parmentier, and J. Binet, "The use of agar gel as a basic reference material for calibrating relaxation times and imaging parameters.", *Magnetic resonance in medicine : official journal of the Society of Magnetic Resonance in Medicine / Society of Magnetic Resonance in Medicine*, vol. 2, no. 2, pp. 176–179, 1985, ISSN: 0740-3194. DOI: `10.1002/mrm.1910020208`.

Appendix

The current version of the python script 'FunITK.py' with all functions described in this thesis used to calculate the presented numbers is available at:
`https://github.com/cyberspeck/mri-for-rt/blob/master/scripts`

The data of the cropped images showing rod #5 and #16, the created '.txt' and '.mha' files are stored at:
`https://github.com/cyberspeck/mri-for-rt/tree/master/data`

The following pages contain today's version of the python script 'FunITK.py' and the generated data for rod #5 & #16.

```python
# -*- coding: utf-8 -*-
"""
Created on Sat Jul 16 22:45:11 2016
@author: david

Volume class
custom FUNcitons using SimpleITK
https://itk.org/Wiki/SimpleITK/GettingStarted#Generic_Distribution

works only with cropped CT and MRI images (showing only one rod),
both Volumes should have the same PixelSpacing,
 and x and y PixelSpacing shoult be equal
sitk_write() creates .mha file with pixel values corresponding
 to distortion in pixel distance * PixelSpacing (mm)

important to remember:
    sitk.Image saves Volume like this (x,y,z)
    array returned by sitk.GetArrayFromImage(Image)
    is transposed: (z,y,x)

based on:
https://pyscience.wordpress.com/2014/10/19/image-segmentation-with-python-and-SimpleITK/

"""

import numpy as np
from scipy import ndimage
import SimpleITK as sitk
import matplotlib.pyplot as plt
import os
from skimage.draw import circle


class Volume:
    '''
    Create a Volume (SimpleITK.Image with convenient properties and functions)
    recommended use:
    create new Volume (optional use denoise=True)
    Volume.getThresholds()

    Parameters
    ----------
    path : string_like
        directory containing DICOM data
    method : string_like, recommended
        either "CT or "MR", used for automatic calculations
    denoise : bool, optional
        If true, the imported data will be denoised using
        SimpleITK.CurvatureFlow(image1=self.img,
                                timeStep=0.125,
                                numberOfIterations=5)
    ref : int, optional
        slice used to make calculations (idealy isocenter) e.g. thresholds
        all plots show this slice
        by default it is set to be in the middle of the image (z-axis)
    resample : int, optional
        resample rate, becomes part of title
    seeds : array_like (int,int,int), optional
        coordinates (pixel) of points inside rod, used for segmentation
        by default list of brightest pixel in each slice
    radius: double, optional
        overrides radius value (default CT:4mm, MR:2mm)
    spacing: double, optional
        by default SitpleITK.img.GetSpacing is used to find relation of pixels
        to real length (in mm)
    skip: int, optional
        neglecting first 'skip' number of slices
    leave: int, optional
        neglects last 'leave' number of slices
    rotate: bool, optional
        if True: mirrors x- & z-axis, effectively rotating the image by 180°
        (looked at from above), this is applied after skip&size
```

```
    '''
    def __init__(self, path=None, method=None, denoise=False, ref=None,
                 resample=False, seeds='auto', radius=0, spacing=0, skip=0,
                 leave=False, rotate=False):
        if(path is None):
            print("Error: no path given!")
        else:
            self.path = path
            self.method = method
            self.denoise = denoise
            self.resample = resample
            self.centroid = False
            self.mask = False
            self.masked = False
            self.title = method
            self.radius = radius
            self.bestRadius = 0
            self.lower = False
            self.upper = False

            file_no = len([name for name in os.listdir(path) if os.path.isfile(os.path.join(path,
name))])
            size = file_no - skip - leave
            if size <= 0:
                print("There nothing left to load after skipping {} file(s) and ignoring the last {}
files.".format(skip,leave))
                print("The directory only contains {} files!".format(file_no))
            else:

                print("Import {} DICOM Files from: {}\n".format(size, path))
                shortened_img = sitk_read(path, denoise)[:, :, skip:(file_no + skip - leave)]
                if rotate is True:
                    self.img = shortened_img[::-1,:,::-1]
                else:
                    self.img = shortened_img

                if (self.img and self.denoise):
                    a = self.title
                    self.title = a + " denoised"

                if resample:
                    a = self.title
                    self.title = a + ", x" + str(resample)

                self.xSize, self.ySize, self.zSize = self.img.GetSize()
                if spacing == 0:
                    self.xSpace, self.ySpace, self.zSpace = self.img.GetSpacing()

                if type(ref) == int:
                    self.ref = ref
                else:
                    self.ref = int(self.zSize / 2)

                # niceSlice used to remember which slices show irregularities such
                # as parts of plastic pane (CT)
                # and should therefore not be used to calculate COM, dice, etc.
                self.niceSlice = np.ones((self.zSize, 1), dtype=bool)
                self.maxBrightness = np.zeros((self.zSize, 1))
                self.meanBrightness = np.zeros((self.zSize, 1))
                arr = sitk.GetArrayFromImage(self.img)
                average = np.average(arr[ref])
    #               print("\nAverage @ ref: ", average)
                for index in range(self.zSize):
                    # save value of brightest pixel in each slice
                    self.maxBrightness[index] = arr[index].max()
                    self.meanBrightness[index] = np.average(arr[index])
                    # if average value of slice differs too much -> badSlice
                    # difference between ref-Slice and current chosen arbitratry
                    # seems to be big enough not to detect air bubble in MRI
                    # entire air block (no liquid) should be recognised, though.
                    # small enough to notice plastic pane
                    if np.absolute(self.meanBrightness[index] - average) > 40:
```

```
                    print("Irregularities detected in slice {}".format(index))
                    self.niceSlice[index] = False
                    # maybe also set slice prior and after current slice as
                    # self.niceSlice[index+1] = self.niceSlice[index+1] = False
                    # because small changes happening around irregularities
                    # might not have been big enough for detection, but already
                    # leading to false calculations?

            if type(seeds) == list:
                self.seeds = seeds
            elif seeds == 'auto':
                self.seeds = []
                for index in range(self.zSize):
                    yMax = int(arr[index].argmax() / self.xSize)
                    xMax = arr[index].argmax() - yMax*self.xSize
                    if self.niceSlice[index] == True:
                        self.seeds.append((xMax, yMax, index))
#                     print("{}: found max at ({},{})".format(index, xMax, yMax))

    def show(self, pixel=False, interpolation=None, ref=None, save=False):
        '''
        plots ref slice of Volume

        Parameters
        ----------
        pixel: bool, optional
            if True, changes axis from mm to pixels
        interpolation: "string", optional, default: 'nearest'
            using build-in interpolation of matplotlib.pyplot.imshow
            Acceptable values are 'none', 'nearest', 'bilinear', 'bicubic',
            'spline16', 'spline36', 'hanning', 'hamming', 'hermite', 'kaiser',
            'quadric', 'catrom', 'gaussian', 'bessel', 'mitchell', 'sinc',
            'lanczos'
        ref: int, optional
            slice to be plotted instead of self.ref (default: 0)
        '''

        if ref is None:
            ref = self.ref

        if interpolation is None:
            a = 'nearest'

        extent = None
        if pixel is False:
            extent = (-self.xSpace/2, self.xSize*self.xSpace - self.xSpace/2, self.ySize*self.ySpace - 
self.ySpace/2, -self.ySpace/2)
        # The location, in data-coordinates, of the lower-left and upper-right corners
        # (left, right, bottom, top)

        sitk_show(img=self.img, ref=ref, extent=extent, title=self.title, interpolation=a, save=save)

    def showSeed(self, pixel=False, interpolation='nearest', ref=None, save=False):
        '''
        plots slice containing seed

        Parameters
        ----------
        pixel: bool, optional
            if True, changes axis from mm to pixels
        interpolation: "string", optional, default: 'nearest'
            using build-in interpolation of matplotlib.pyplot.imshow
            Acceptable values are 'none', 'nearest', 'bilinear', 'bicubic',
            'spline16', 'spline36', 'hanning', 'hamming', 'hermite', 'kaiser',
            'quadric', 'catrom', 'gaussian', 'bessel', 'mitchell', 'sinc',
            'lanczos'
        ref: int, optional
            slice of seed to be plotted instead of self.ref (default: zSize/2)
        '''
        if ref is None:
            ref = self.ref
```

```
        if type(self.seeds[ref]) != tuple:
            print("No seed found @ slice {}".format(ref))
            return None

        x, y = -1,-1
        extent = None
        if pixel is False:
            extent = (-self.xSpace/2, self.xSize*self.xSpace - self.xSpace/2, self.ySize*self.ySpace - 
self.ySpace/2, -self.ySpace/2)
            x = (self.seeds[ref][0] * self.xSpace)
            y = (self.seeds[ref][1] * self.xSpace)
        else:
            x, y, z = self.seeds[ref]

        arr = sitk.GetArrayFromImage(self.img)
        fig = plt.figure()
        plt.set_cmap("gray")
        plt.title(self.title + ", seed @ {}".format(self.seeds[ref]))

        plt.imshow(arr[ref, :, :], extent=extent, interpolation=interpolation)
        plt.scatter(x, y)
        plt.show()
        if save != False:
            fig.savefig(str(save) + ".png")

    def getThresholds(self, pixelNumber=0, scale=1):
        '''
        Calculates threshold based on number of pixels representing rod.
        If no pixelNumber is given, self.radius is used to get estimated
        pixelNumber. If self.raduis == 0: use method to get raduis
         All calculations based on ref-slice.

        approx. number of pixels being part of rod:
        pn = realRadius^2 * pi / pixelSpacing^2

        Parameters
        ----------
        pixelNumber: int, optional
            if 0, uses self.radis to calculate pixelnumber
            if self.radius also 0, uses self.method instead (CT: 4mm, MR: 2mm)
        scale: double, optional
            factor altering pixelNumber

        Returns
        -------
        lower and upper threshold value: (double, double)
        '''

        if pixelNumber == 0:
            if self.radius != 0:
                realRadius = self.radius
            else:
                if self.method == "CT":
                    realRadius = 4
                if self.method == "MR":
                    realRadius = 2
                if self.method != "MR" and self.method != "CT":
                    print("method is unknown, please set pixelNumber!")
                    return None
            pixelNumber = np.power(realRadius, 2)*np.pi/np.power(self.xSpace, 2)*scale

        pn = int(pixelNumber)
        arr = sitk.GetArrayFromImage(self.img)
        self.upper = np.double(arr.max())

    #    hist, bins = np.histogram(arr[self.ref, :, :].ravel(), bins=100)
    # alternatively, increase number of bins for images with many pixels
        hist, bins = np.histogram(arr[self.ref, :, :].ravel(), bins=int(pn*2))
        self.lower = np.double(bins[np.argmax((np.cumsum(hist[::-1]) < pn)[::-1])])
        print("number of pixels (pn): {}\n lower: {}\n upper: {}".format(pn, self.lower, self.upper))

        return (self.lower, self.upper)
```

```
    def getCentroid(self, threshold='default', pixelNumber=0, scale=1,
                    percentLimit=False, iterations=5, top = 1,
                    plot=False, save=False):
        '''
        Calculates centroid, either by setting threshold or percentLimit

        Parameters
        ----------
        threshold: float or 'auto', default='auto'
            if 'auto': uses getThreshold(pixelnumber, scale) and then
                sitk_centroid(threshold=self.lower)
                sets self.lower and self.upper
        percentLimit: float from 0 to 1 (or "auto" =experimental)
            if percentLimit is True: used instead of threshold method
            if 'auto': makes 5 iterations by default, uses getThreshold()
                and getDice(), but does NOT set self.mask
                sets self.lower and self.upper
        plot, save: bool, optional
            plot and save iteration (percentLimit='auto')

        Returns
        -------
        self.centroid: numpy.ndarray
        '''

        if (threshold is False and percentLimit is False) or (percentLimit == "auto" and threshold is
not False and threshold != 'default'):
            print("Please use percentLimit or threshold! (default setting: threshold = 'auto')")
            return None

        if (percentLimit == "auto" and threshold is False) or (percentLimit == "auto" and threshold ==
'default'):
            # EXPERIMENTAL!!!
            # looks at whole range of possible percentLimits
            # reduces range by finding out which half yields higher result
            # starts at A=25% and B=75% of all pixels
            # if DC(A) > DC(B): next values come from lower half (0-50%)
            # else: upper half (50-100%)
            # calculates 5 centroids with different percentLimits
            # gets dice coefficient for each centroid percentLimit combination
            # returns best result

            print("\n\n")
            arr = sitk.GetArrayFromImage(self.img)
            direction = np.zeros(iterations)
            left = np.zeros(iterations)
            right = np.zeros(iterations)
            left[0] = 0
            right[0] = top
            guess = np.zeros(iterations)
            guess[0] = (left[0]+right[0])/2
            thresholdsA = np.zeros((iterations,2))
            thresholdsB = np.zeros((iterations,2))
            centroidScoreA = np.zeros(iterations)
            centroidScoreB = np.zeros(iterations)
            centroidsA = np.zeros((iterations, self.zSize, 2))
            centroidsB = np.zeros((iterations, self.zSize, 2))
            diceA = np.zeros((iterations, self.zSize, 1))
            diceB = np.zeros((iterations, self.zSize, 1))
            for index in range(iterations):
                print("    ITERATION #{}, current guess: ~{:.4f}\nA @ ~{:.4f}%".format(index, guess
[index]*100, (guess[index]+left[index])/2*100))
                thresholdsA[index] = self.getThresholds(pixelNumber=self.xSize*self.ySize*(guess[index]
+left[index])/2)
                # create mask including all pixels relevant for guess
                maskA = sitk.ConnectedThreshold(image1=self.img,
                                                seedList=self.seeds,
                                                lower=self.lower,
                                                upper=self.upper,
                                                replaceValue=1)
                # shift values so that they're all positive and apply mask
```

```
                maskedA2 = sitk_applyMask(self.img - arr.min(), maskA)
                # now shift values back, this results in all masked pixels to be assigned the minimum 
value
                maskedA = maskedA2 + arr.min()
                # use all pixels above minimum value for centroid:
                centroidsA[index] = self.xSpace*sitk_centroid(maskedA,
                                                              ref=self.ref,
                                                              threshold=arr.min()+1)
                diceA[index] = self.getDice(centroidsA[index], maskA)
                # all irregular Slices result in DC of -1:
                diceA[index][np.where(self.niceSlice==False)] = -1
                # for the final DC score it will look only at the niceSlices:
                centroidScoreA[index] = np.average(diceA[index, self.niceSlice==True])
#                centroidScoreA[index] = np.average(diceA[index,diceA[index]>-1])
#                centroidScoreA[index] = np.average(diceA[index])


                print("\nB @ ~{:.4f}%".format((guess[index]+right[index])/2*100))
                thresholdsB[index] = self.getThresholds(pixelNumber=self.xSize*self.ySize*(guess[index]
+right[index])/2)
                maskB = sitk.ConnectedThreshold(image1=self.img,
                                                seedList=self.seeds,
                                                lower=self.lower,
                                                upper=self.upper,
                                                replaceValue=1)
                maskedB2 = sitk_applyMask(self.img - arr.min(), maskB)
                maskedB = maskedB2 + arr.min()
                centroidsB[index] = self.xSpace*sitk_centroid(maskedB,
                                                              ref=self.ref,
                                                              threshold=arr.min()+1)
                diceB[index] = self.getDice(centroidsB[index], maskB)
                # all irregular Slices result in DC of -1:
                diceB[index][np.where(self.niceSlice==False)] = -1
                # for the final DC score it will look only at the niceSlices:
                centroidScoreB[index] = np.average(diceB[index, self.niceSlice==True])
#                centroidScoreB[index] = np.average(diceB[index,diceB[index]>-1])
#                centroidScoreB[index] = np.average(diceB[index])


                if centroidScoreA[index] < centroidScoreB[index] and index < iterations-1:
                    left[index+1] = guess[index]
                    right[index+1] = right[index]
                    guess[index+1] = (left[index+1] + right[index+1]) / 2
                    direction[index] = 1
                elif centroidScoreA[index] > centroidScoreB[index] and index < iterations-1:
                    right[index+1] = guess[index]
                    left[index+1] = left[index]
                    guess[index+1] = (left[index+1] + right[index+1]) / 2
                    direction[index] = -1
                elif centroidScoreA[index] == centroidScoreB[index] and index < iterations-1:
                    right[index+1] = (guess[index] + right[index]) / 2
                    left[index+1] = (guess[index] + left[index]) / 2
                    guess[index+1] = guess[index]
                else:
                    break

                print("-------------------------")
                print("next guess (#{}): ~{:.4f}% \n\n\n\n".format(index+1, guess[index+1]*100))


            if centroidScoreA.max() > centroidScoreB.max():
                self.centroid = centroidsA[centroidScoreA.argmax()]
                self.lower, self.upper = thresholdsA[centroidScoreA.argmax()]
                self.dice = diceA[centroidScoreA.argmax()]
                self.diceAverage = centroidScoreA.max()
                print("\nmax dice-coefficient obtained during iteration #{}: ~{:.4f}".format
(centroidScoreA.argmax(), centroidScoreA.max()))
            elif (centroidScoreA.max() <= centroidScoreB.max() and centroidScoreB.max() != 0):
                self.centroid = centroidsB[centroidScoreB.argmax()]
                self.lower, self.upper = thresholdsB[centroidScoreB.argmax()]
                self.dice = diceB[centroidScoreB.argmax()]
                self.diceAverage = centroidScoreB.max()
```

```
                print("\nmax dice-coefficient obtained during iteration #{}: ~{:.4f}".format
(centroidScoreB.argmax(), centroidScoreB.max()))
            else:
                return None

            print("\n\n-o-o-o-o-- Summary: --o-o-o-o-\n")
            for index in range(np.size(guess)):
                print("\n  Iteration #{}: range({},{})".format(index, left[index]*100, right
[index]*100))
                if centroidScoreA[index] > centroidScoreB[index]:
                    print("A @ {}%, Score: {}  <---".format((guess[index]+left[index])/2*100,
centroidScoreA[index]))
                    print("B @ {}%, Score: {}".format((guess[index]+right[index])/2*100, centroidScoreB
[index]))
                if centroidScoreA[index] < centroidScoreB[index]:
                    print("A @ {}%, Score: {}".format((guess[index]+left[index])/2*100, centroidScoreA
[index]))
                    print("B @ {}%, Score: {}  <---".format((guess[index]+right[index])/2*100,
centroidScoreB[index]))
                if centroidScoreA[index] == centroidScoreB[index]:
                    print("A @ {}% same as for B @ {}%, Score: = {}".format((guess[index]+left
[index])/2*100, (guess[index]+right[index])/2*100, centroidScoreA[index]))


            if plot == True:
                fig = plt.figure()
                for index in range(iterations):
                    if guess[index] > 0 and centroidScoreA[index] > 0:
                        plt.plot((guess[index]+left[index])/2*100, centroidScoreA[index], 'bo')
                    if guess[index] > 0 and centroidScoreB[index] > 0:
                        plt.plot((guess[index]+right[index])/2*100, centroidScoreB[index],
'go')
                plt.show()
                if save != False:
                    fig.savefig(str(save) + ".png")


        if percentLimit != "auto" and percentLimit is not False:
            self.centroid = self.xSpace * sitk_centroid(self.img, ref=self.ref,
                                                        percentLimit=percentLimit)

        if (threshold == 'auto' or threshold == 'default') and percentLimit is False:
            self.getThresholds(pixelNumber=pixelNumber, scale=scale)
            self.centroid = self.xSpace * sitk_centroid(self.img, ref=self.ref,
                                                        threshold=self.lower)

        if (threshold != "auto" and threshold != 'default') and threshold is not False and
percentLimit is False:
            self.centroid = self.xSpace * sitk_centroid(self.img, ref=self.ref,
                                                        threshold=threshold)

        for index in range(self.zSize):
            if not self.niceSlice[index]:
                self.centroid[index] = -1, -1
            if self.centroid[index,0] < 0 or self.centroid[index,1] < 0 :
                self.centroid[index] = -1, -1
        print("\n\n")
        return self.centroid


    def showCentroid(self, img=None, com2=0, title=None, pixel=False,
                     interpolation='nearest', ref=None, save=False):
        '''
        shows slice with centroid coordinates

        Parameters
        ----------
        img: SimpleITK.img, optional
            slice of this volume will be shown
            default: self.img
        com2: numpy.ndarray
            supposed to be of same length as img
```

```
            will also be shown in plot alongside self.centroid
            helps creating nice plot for comparing COM-shift
        pixel: bool, optional
            if True, changes axis from mm to pixels
        interpolation: "string", optional, default: 'nearest'
            using build-in interpolation of matplotlib.pyplot.imshow
            Acceptable values are 'none', 'nearest', 'bilinear', 'bicubic',
            'spline16', 'spline36', 'hanning', 'hamming', 'hermite', 'kaiser',
            'quadric', 'catrom', 'gaussian', 'bessel', 'mitchell', 'sinc',
            'lanczos'
        ref: int, optional
            slice to be plotted instead of self.ref (default: 0)
        save: string, optional
            save plot as save + ".png"
        '''

        if self.centroid is False:
            print("Volume has no centroid yet. use Volume.getCentroid() first!")
            return None

        if title is None:
            title = self.title
        if ref is None:
            ref = self.ref
        if img is None:
            img = self.img

        if pixel is False:
            extent = (-self.xSpace/2, self.xSize*self.xSpace - self.xSpace/2, self.ySize*self.ySpace -
self.ySpace/2, -self.ySpace/2)
            sitk_centroid_show(img=img, com=self.centroid, com2=com2,
                            extent=extent, save=save, title=title,
                            interpolation=interpolation, ref=ref)
        else:
            sitk_centroid_show(img=img, com=self.centroid/self.xSpace,
                            com2=com2/self.xSpace, save=save, title=title,
                            interpolation=interpolation, ref=ref)

    def getMask(self, lower=False, upper=False):

        if lower is False and self.lower is not False:
            lower = self.lower
        if upper is False and self.upper is not False:
            upper = self.upper

        if lower is False:
            print("Lower threshold missing!")
            return None
        if upper is False:
            print("Upper threshold missing!")
            return None

        self.mask = sitk_getMask(self.img, self.seeds, upper, lower)
        return self.mask

    def applyMask(self, mask=0, replaceArray=False, scale=1000):
        if mask == 0:
            if self.mask:
                mask = self.mask
            else:
                print("Volume has no mask yet. use Volume.getMask() first!")
                return None

        self.masked = sitk_applyMask(self.img, mask, replaceArray=replaceArray,
                                     scale=scale)

        return self.masked

    def showMask(self, interpolation=None, ref=None, save=False, pixel=False):
        if self.mask is False:
            print("Volume has no mask yet. use Volume.getMask() first!")
            return None
```

```
        if ref is None:
            ref = self.ref

        if interpolation is None:
            interpolation = 'nearest'

        title = self.title + ", mask"

        extent = None
        if pixel is False:
            extent = (-self.xSpace/2, self.xSize*self.xSpace - self.xSpace/2, self.ySize*self.ySpace - 
self.ySpace/2, -self.ySpace/2)

        sitk_show(img=self.mask, ref=ref, title=title, extent=extent,
                  interpolation=interpolation, save=save)

    def showMasked(self, interpolation=None, ref=None, save=False, pixel=False):
        if self.masked is False:
            print("Volume has not been masked yet. use Volume.applyMask() first!")
            return None
        if ref is None:
            ref = self.ref

        if interpolation is None:
            interpolation = 'nearest'

        title = self.title + ", masked"

        extent = None
        if pixel is False:
            extent = (-self.xSpace/2, self.xSize*self.xSpace - self.xSpace/2, self.ySize*self.ySpace - 
self.ySpace/2, -self.ySpace/2)

        sitk_show(img=self.masked, ref=ref, title=title, extent=extent,
              interpolation=interpolation, save=save)

    def getDice(self, centroid=None, mask=None, iterations=15,
            CT_guess=(3.5,5.5), MR_guess=(1.5,4.5),
            show=False, showAll=False, plot=False, save=False, pixel=False):
        '''
        Calculates dice coefficient ('DC') and average DC of the volume
        if iterations > 0: varies radius and finds DC with best average DC
        else: if self.raduis == 0: use method to get raduis for DC calculation
        average DC is mean value of all slices, except those with DC of -1

        slice DC is set to -1 if centroid lies outside image or reference
        circle exceeds image

        Parameters
        ----------
        centroid: numpy.ndarray, optional
            centroid to place circles in instead of self.centroid
        mask: SimpleITK image, optional
            binary image to calculate DC of instead of self.mask
        iterations: int, optional
        show: int, optional
            shows circle used to compare mask to in slice nr. "show"
        showAll: bool, optional
            shows all circles tried during iteration
        plot, save: bool, optional
            plot and save iteration

        Returns
        -------
        self.dice: numpy.ndarray
        '''
        if centroid is None:
            centroid = self.centroid
        # to get from mm to pixel coordinates:
        com = centroid / self.xSpace
        if mask is None:
```

```
            if self.mask is False:
                self.getMask()
            mask = self.mask

        extent = None
        if pixel is False:
            extent = (-self.xSpace/2, self.xSize*self.xSpace - self.xSpace/2, self.ySize*self.ySpace - 
self.ySpace/2, -self.ySpace/2)

        if self.radius != 0:
            print("{}_x{}.radius is {} and will therefore be used to calculate DC.".format
(self.method, self.resample, self.radius))
            self.dice = sitk_dice_circle(img=mask, centroid=com, extent=extent,
                                         radius=self.radius/self.xSpace, show=show)

#         print("\n{}_x{}:".format(self.method, self.resample))

        if self.radius == 0 and iterations == 0:
            if self.method == "CT":
                self.dice = sitk_dice_circle(img=mask, centroid=com, extent=extent,
                                             radius=4/self.xSpace, show=show)
            if self.method == "MR":
                self.dice = sitk_dice_circle(img=mask, centroid=com, extent=extent,
                                             radius=2/self.xSpace, show=show)
            if self.method != "CT" and self.method != "MR":
                print("Unknown method!")
                return None

        if self.radius == 0 and iterations > 0:
            low, up = 0, 0
            if self.method == "CT":
                low, up = CT_guess
                radii = np.linspace(low, up, num=iterations)/self.xSpace
            if self.method == "MR":
                low, up = MR_guess
                radii = np.linspace(low, up, num=iterations)/self.xSpace
            if self.method != "CT" and self.method != "MR":
                # radii = np.linspace(1.5, 4.5, num = 11)
                print("Unknown method!")
                return None

            DCs = np.zeros(len(radii))
            for index, r in enumerate(radii, start=0):
                dice = sitk_dice_circle(img=mask, centroid=com, radius=r,
                                        show=showAll, extent=extent)
#                 DCs[index] = np.average(dice)
#                 DCs[index] = np.average(dice[dice>-1])
                DCs[index] = np.average(dice[self.niceSlice==True])


            if plot == True:
#                 fig = plt.figure()
#                 plt.ylim(ymin=0.6, ymax=1)
#                 plt.xlim(xmin=(low-.1), xmax=(up+.1))
                plt.plot(radii*self.xSpace, DCs, '+-')
                if save is not False:
                    fig.savefig(str(save) + ".png")

            self.dice = sitk_dice_circle(img=mask, centroid=com, show=show,
                                         extent=extent, radius=radii[DCs.argmax()])
            self.bestRadius = radii[DCs.argmax()]*self.xSpace
            print("max dice-coefficient obtained for {} when compared to circle with radius = 
{}".format(self.method, self.bestRadius))

#         self.diceAverage = np.average(self.dice[self.dice>-1])
        self.diceAverage = np.average(self.dice)
        print("dice-coefficient average for the whole volume is: {:.4f}".format(self.diceAverage))
        return self.dice



def sitk_read(directory, denoise=False):
```

```
    '''
    returns DICOM files as "SimpleITK.Image" data type (3D)
    if denoise is True: uses SimpleITK to denoise data
    '''
    reader = sitk.ImageSeriesReader()
    filenames = reader.GetGDCMSeriesFileNames(directory)
    reader.SetFileNames(filenames)
    if denoise:
        print("\n...denoising...")
        imgOriginal = reader.Execute()
        return sitk.CurvatureFlow(image1=imgOriginal,
                                  timeStep=0.125,
                                  numberOfIterations=5)
    else:
        return reader.Execute()


def sitk_write(image, output_dir='', filename='3DImage.mha'):
    '''
    saves image as .mha file
    '''
    output_file_name_3D = os.path.join(output_dir, filename)
    sitk.WriteImage(image, output_file_name_3D)


def sitk_show(img, ref=0, extent=None, title=None, interpolation='nearest', save=False):
    """
    shows plot of img at z=ref
    """
    arr = sitk.GetArrayFromImage(img)
    fig = plt.figure()
    plt.set_cmap("gray")
    if title:
        plt.title(title)

    plt.imshow(arr[ref], extent=extent, interpolation=interpolation)
    plt.show()
    if save != False:
        fig.savefig(str(save) + ".png")

def sitk_centroid(img, ref=False, percentLimit=False, threshold=False):
    '''
    returns array with y&x coordinate of centroid for every slice of img
    centroid[slice, y&x-coordinate]
    if no pixel has value > threshold:
        centroid x&y-coordinate of that slice = -1,-1
    '''
    if (threshold is False and percentLimit is False) or (threshold is True and percentLimit is True):
        print("Please set either percentLimit or threshold!")
        return None

    arr = sitk.GetArrayFromImage(img)
    z, y, x = np.shape(arr)
    # create array with centroid coordinates of rod in each slice
    com = np.zeros((z, 2))

    if ref is False:
        ref = int(z/2)

    if threshold is False:
#        hist, bins = np.histogram(arr[ref, :, :].ravel(), density=True, bins=100)
     #  alternatively, increase number of bins for images with many pixels
        hist, bins = np.histogram(arr[ref, :, :].ravel(), density=True, bins=int(y*x))
        threshold = bins[np.concatenate((np.array([0]), np.cumsum(hist))) *
                         (bins[1] - bins[0]) > percentLimit][0]

    for index in range(z):
        if arr[index].max() > threshold:
            # structuring_element=[[1,1,1],[1,1,1],[1,1,1]]
            segmentation, segments = ndimage.label(arr[index] > threshold)
            # print("segments: {}".format(segments))
            # add ', structuring_element' to label() for recognising
```

```
            # diagonal pixels as part of object
            com[index, ::-1] = ndimage.center_of_mass(arr[index, :, :]-threshold,
                                                      segmentation)
            # add ', range(1,segments)' to center_of_mass for list of centroids
            # in each slice (multiple rods!)
        else:
            com[index] = (-1,-1)

    return com

def sitk_centroid_show(img, com, com2=0, extent=None, title=None,
                       save=False, interpolation='nearest', ref=0):

        arr = sitk.GetArrayFromImage(img)
        fig = plt.figure()
        plt.set_cmap("gray")
        if title:
            plt.title(title + ", centroid")
        x = y = 0
        plt.imshow(arr[ref], extent=extent, interpolation=interpolation)
        if type(com2) == np.ndarray:
            x = [com[ref,0],com2[ref,0]]
            y = [com[ref,1],com2[ref,1]]
        else:
            x, y = com[ref]
        plt.scatter(x, y, c=['b','r'])
        plt.show()
        if save != False:
            fig.savefig(str(save) + ".png")

def sitk_coordShift(first, second):
    '''
    returns array with difference of y&x coordinates for every
    centroid[slice, y&x-coordinate]
    '''
    if (np.shape(first) == np.shape(second) and
            np.shape((np.shape(first))) == (2,)):
        z, xy = np.shape(first)
        diff = np.zeros((z, 2))
        for slice in range(z):
            if first[slice,0]==-1 or first[slice,1]==-1 or second[slice,0]==-1 or second[slice,0]==-1:
                diff[slice, 0] = diff[slice, 1] = -1
            else:
                diff[slice, 0] = first[slice, 0] - second[slice, 0]
                diff[slice, 1] = first[slice, 1] - second[slice, 1]
        return diff
    else:
        print("Wrong shape! sitk_coordShift returned 'False'")
        return False


def sitk_coordDist(shift):
    '''
    calculates norm for each entry of array
    returns array with list of calculated values
    '''
    if np.shape(shift)[1] != 2:
        print("shift has wrong shape!")
        return False

    dist = np.zeros((len(shift), 1))
    for slice in range(len(shift)):
        if shift[slice,0] == -1 or shift[slice,1] == -1:
            dist[slice,:] =-1
        else:
            dist[slice, :] = np.linalg.norm(shift[slice, :])
    return dist


def sitk_getMask(img, seedList, upper, lower):
    '''
    creates new SimpleITK.img using a SimpleITK segmentation function
```

```
    which is made up by all pixels with values between upper and lower and
    connected to a seed from seedList.
    Returns binary image (SimpleITK.img)
    '''

    if seedList is False:
        print("no seeds given!")
        return None

    return sitk.ConnectedThreshold(image1=img, seedList=seedList,
                                   lower=lower, upper=upper,
                                   replaceValue=1)


def sitk_applyMask(img, mask, replaceArray=False, scale=1000, errorValue=-1):
    '''
    masks img (SimpleITK.Image) using mask (SimpleITK.Image)
    if a replaceArray is given, the values*scale (default scale=1000) of the
    array will be used as pixel intensity for an entire slice each
    '''
    if img.GetSize() != mask.GetSize():
        print(mask.GetSize())
        print(img.GetSize())

        print("mask and image are not the same size!")
        return False

    arr = sitk.GetArrayFromImage(img)
    maskA = sitk.GetArrayFromImage(mask)
    xSize, ySize, zSize = img.GetSize()

    imgMaskedA = (arr - arr.min() + 1)*maskA

    if np.shape(replaceArray) == (img.GetDepth(), 1) or np.shape(replaceArray) == (img.GetDepth(),):
        for slice in range(zSize):
            imgMaskedA[slice][imgMaskedA[slice] != 0] = replaceArray[slice]*scale
            imgMaskedA[slice][imgMaskedA[slice] < 0] = errorValue


    return sitk.GetImageFromArray(imgMaskedA)


def sitk_dice_circle(img, centroid, radius=2.1, show=False, extent=None,
                     interpolation='nearest', save=False):
    """
    Dice coefficient, inspired by
     Medpy (http://pythonhosted.org/MedPy/_modules/medpy/metric/binary.html)

    Computes the Dice coefficient (akas Sorensen index) between a binary
    object in an image and a circle.

    The metric is defined as:

        DC=\frac{2|A\cap B|}{|A|+|B|}

    where A is the first and B the second set of samples (here: binary objects)

    Parameters
    ----------
    input_umg : SimpleITK.Image
        Input data containing objects. Can be any type but will be converted
        into binary: background where 0, object everywhere else.
    centroid : array_like
        array with coordinates for circle centre
    radius : float
        radius for creating reference circles

    Returns
    -------
    DC : array_like
        The Dice coefficient between the object(s) in ```input``` and the
        created circles. It ranges from 0 (no overlap) to 1 (perfect overlap).
```

```
        if centroid coordinates + radius would create circle exceeding image
        size: DC of this slice = -1
        Other errors occuring during the calculation should also result in -1
    """

    xSize, ySize, zSize = img.GetSize()
    xSpace, ySpace, zSpace = img.GetSpacing()
    profile = np.zeros((zSize, ySize, xSize), dtype=np.uint8)
    DC = np.zeros((zSize, 1))
    for slice in range(zSize):
        if centroid[slice,0]+radius < xSize and centroid[slice, 1]+radius < ySize and centroid
[slice,0]-radius > 0 and centroid[slice, 1]-radius > 0:

            rr, cc = circle(centroid[slice, 0], centroid[slice, 1], radius, (xSize,ySize))
            profile[slice, cc, rr] = 1
        else:
            # print("something's fishy!")
            DC[slice]= -1

    input = sitk.GetArrayFromImage(img)

    input = np.atleast_1d(input.astype(np.bool))
    reference = np.atleast_1d(profile.astype(np.bool))

    intersection = np.zeros((zSize, 1))
    size_input = np.zeros((zSize, 1))
    size_reference = np.zeros((zSize, 1))
    for slice in range(zSize):
        intersection[slice] = np.count_nonzero(input[slice, :, :] & reference[slice, :, :])
        size_input[slice] = np.count_nonzero(input[slice, :, :])
        size_reference[slice] = np.count_nonzero(reference[slice, :, :])

        try:
            if (DC[slice] == 0) and (float(size_input[slice] + size_reference[slice]) != 0):
                DC[slice] = 2. * intersection[slice] / float(size_input[slice] + size_reference[slice])

        except ZeroDivisionError:
            DC[slice] = -1

    if show != False:
        profile_img = sitk.GetImageFromArray(profile)
        sitk_centroid_show(profile_img, centroid*xSpace, extent=extent,
                           title="profile, radius: {:03.2f}".format(radius*xSpace),
                           ref=show, save=save)

    return DC


# to view in 3D Slicer, type this in IPython console or in jupyter notebook:
# %env SITK_SHOW_COMMAND /home/david/Downloads/Slicer-4.5.0-1-linux-amd64/Slicer
# sitk.Show(imgFillingCT)
```

2017-08-30 14:35:38.568013
CT_x100
path: ../data/phantom2/CT_x100
thresholds:
lower (simple): -460.940227704,
lower (iter): -188.922061524
upper: 329.0
DC-average (simple): 0.87667059562 (bestRadius: 3.92857142857)
DC-average (iter): 0.992641237859 (bestRadius: 3.64285714286)
MR_x100
path: ../data/phantom2/MR_x100
thresholds:
lower (simple): 827.518223235,
lower (iter): 339.31049961
lower (simple_CT-COM): 827.518223235
lower (iter_CT-COM): 339.31049961
upper: 2095.0
DC-average (simple): 0.893466506573 (bestRadius: 1.92857142857)
DC-average (iter): 0.941615552809 (bestRadius: 3.0)
DC-average (CT-COM, simple): 0.685706722238 (bestRadius: 1.92857142857)
DC-average (CT-COM, iter): 0.755705950588 (bestRadius: 2.78571428571)
sliceNo dist warp_x warp_y warpMagnitude DC_CT DC_MR DC_MR_CT-COM warp_x* warp_y* warpMagnitude* DC_CT* DC_MR* DC_MR_CT-COM*

0	-183	-1.046	-1.115	1.1199	983	8.444	6.102	-1.047	-10.571	1.0623	9.945	9.504	7.546
1	-182	-1.205	-11.132	1.1197	9.807	8.547	6.091	-1.199	-10.527	1.0595	9.929	9.496	7.573
2	-181	-1.278	-11.107	1.1181	9.819	8.666	6.135	-1.334	-10.472	1.0556	9.925	9.501	7.583
3	-180	-1.459	-10.985	1.1082	9.829	873	6.174	-1.518	-10.328	1.0439	9.941	9.507	7.622
4	-179	-1.482	-10.649	1.0752	9.816	8.862	6.343	-1.574	-10.006	1.0129	995	9.487	7.701
5	-178	-1.653	-10.666	1.0794	9.819	8.961	6.339	-1.654	-9.995	1.013	9.929	9.473	772
6	-177	-1.562	-1.042	1.0537	9.814	9.049	6.443	-1.664	-9.842	9.982	994	9.466	7.755
7	-176	-1.806	-10.309	1.0466	9.811	9.036	6.485	-1.836	-9.787	9.958	9.928	9.461	7.756
8	-175	-1.678	-10.294	1.043	9.818	9.072	6.498	-1.774	-9.801	9.961	9.934	9.451	7.757
9	-174	-1.843	-10.459	1.062	9.824	9.088	6.451	-1.912	-9.907	1.009	9.942	9.441	7.742
10	-173	-1.908	-1.021	1.0387	9.828	914	6.499	-2.002	-9.775	9.978	9.928	9.441	7.755
11	-172	-1.833	-10.328	1.049	9.814	9.177	6.505	-1.983	-9.921	1.0117	9.935	9.426	773
12	-171	-1.886	-10.267	1.0439	9.822	9.207	6.512	-202	-9.925	1.0128	9.955	9.415	771
13	-170	-2.037	-10.257	1.0458	9.838	9.226	6.548	-2.146	-9.929	1.0158	9.953	9.409	7.716
14	-169	-2.114	-10.231	1.0447	9.818	9.255	6.577	-2.249	-10.013	1.0262	9.912	9.418	7.701
15	-168	-2.097	-10.195	1.0408	9.835	928	6.578	-2.188	-9.955	1.0193	9.928	9.416	7.716
16	-167	-2.048	-10.069	1.0275	9.827	9.287	6.627	-2.136	-9.907	1.0134	9.954	9.418	7.724
17	-166	-2.098	-9.831	1.1953	9.833	9.298	6.672	-2.174	-9.726	9.966	9.945	9.419	7.768
18	-165	-2.121	-9.847	1.1973	9.833	933	6.681	-2.206	-9.785	1.1931	9.936	942	775
19	-164	-2.168	-9.841	1.1977	983	9.346	6.689	-226	-9.799	1.1956	993	9.426	7.751
20	-163	-2.123	-9.795	1.2022	9.821	9.341	676	-2.136	-9.718	995	993	9.436	7.774
21	-162	-1.878	-9.892	1.1969	9.808	9.366	6.742	-1.909	-9.805	9.989	9.934	9.441	7.778
22	-161	-1.845	-9.825	9.997	982	9.422	6.734	-1.818	-9.775	9.943	9.929	947	7.797
23	-160	-1.897	-9.705	9.889	9.823	9.476	6.813	-1.818	-9.642	9.812	9.946	9.479	7.832

24	-159	-1.791	-9.545	9.711	9.824	9.475	6.898	-1.724	-9.468	9.623	9.924	9.477	7.889
25	-158	-1.728	-9.494	965	9.814	949	6.911	-1.572	-9.417	9.547	9.933	9.498	7.915
26	-157	-153	-9.338	9.463	9.827	0.95	6.986	-1.348	-9.341	9.438	9.909	9.513	7.946
27	-156	-1.477	-9.069	9.189	9.832	952	7.047	-1.293	-9.043	9.135	9.914	9.512	8.009
28	-155	-1.377	-9.131	9.234	982	9.494	706	-1.214	-9.064	9.145	992	9.515	8.011
29	-154	-1.219	-9.196	9.277	9.814	9.553	7.021	-1.049	-9.169	9.229	9.942	951	7.983
30	-153	-1.234	-9.058	9.142	9.814	9.557	704	-1.081	-907	9.135	9.937	951	8.013
31	-152	-1.195	-9.069	9.148	9.806	9.574	704	-983	-9.011	9.065	9.938	952	8.032
32	-151	-1.119	-8.986	9.055	9.812	9.587	7.094	-928	-8.863	8.912	9.924	9.506	807
33	-150	-972	-8.848	8.902	9.803	9.571	7.143	-803	-8.781	8.818	9.927	9.495	8.082
34	-149	-1.095	-8.804	8.872	981	9.585	7.172	-867	-8.669	8.712	9.949	9.495	8.122
35	-148	-1.118	-8.692	8.763	9.821	9.593	7.192	-912	-858	8.628	9.945	9.494	8.134
36	-147	-968	-8.548	8.603	9.829	9.563	7.273	-851	-847	8.513	9.942	9.492	8.173
37	-146	-973	-8.378	8.434	9.831	9.584	7.318	-87	-8.321	8.367	9.952	9.482	8.199
38	-145	-897	-8.111	8.161	9.827	958	7.378	-809	-8.094	8.134	9.945	9.476	8.246
39	-144	-1.009	-8.041	8.104	9.812	9.584	7.419	-861	-7.992	8.039	9.921	9.465	8.269
40	-143	-1.095	-8.037	8.111	9.812	9.596	7.396	-981	-7.983	8.043	9.942	9.469	8.276
41	-142	-1.037	-8.129	8.195	9.823	9.613	7.355	-943	-8.047	8.102	9.943	9.473	8.268
42	-141	-924	-7.982	8.035	9.818	9.634	7.387	-856	-7.947	7.993	9.913	9.467	8.285
43	-140	-1.036	-7.855	7.923	9.815	9.599	7.441	-913	-7.852	7.905	9.925	9.466	8.296
44	-139	-973	-7.789	785	9.829	9.608	7.478	-809	-7.853	7.894	9.924	9.468	8.289
45	-138	-883	-7.462	7.514	9.821	9.616	7.599	-77	-7.541	758	9.925	9.466	8.343
46	-137	-929	-761	7.666	9.822	962	7.536	-811	-7.646	7.689	9.933	9.467	8.328
47	-136	-813	-7.593	7.637	9.807	9.632	754	-0.07	-7.608	7.641	9.935	9.478	8.338
48	-135	-799	-7.583	7.625	9.827	9.624	7.532	-672	-7.643	7.672	9.954	9.494	8.332
49	-134	-763	-7.438	7.477	9.819	966	758	-661	-7.557	7.586	9.945	9.495	8.337
50	-133	-808	-7.404	7.448	983	9.668	7.588	-757	-7.591	7.628	9.949	9.508	8.318
51	-132	-759	-7.312	7.352	9.823	9.685	7.627	-0.07	-7.509	7.542	9.938	9.513	8.338
52	-131	-605	-7.226	7.251	9.823	9.685	7.656	-539	-7.469	7.489	9.935	9.522	834
53	-130	-757	-7.233	7.273	9.833	9.666	7.669	-668	-7.428	7.458	9.949	9.524	8.355
54	-129	-75	-7.234	7.272	9.847	9.662	7.673	-642	-7.453	748	9.936	9.532	8.352
55	-128	-722	-7.035	7.072	9.812	9.623	774	-716	-0.73	7.335	9.928	9.553	8.367
56	-127	-894	-7.211	7.266	9.834	9.592	7.709	-903	-7.441	7.496	9.932	9.561	833
57	-126	-804	-6.945	6.991	9.839	9.589	7.778	-748	-724	7.279	9.943	9.571	8.379
58	-125	-769	-687	6.913	9.846	9.598	7.794	-757	-7.187	7.227	995	9.577	8.392
59	-124	-771	-6.938	6.981	9.841	9.576	7.801	-771	-7.223	7.264	9.935	9.594	8.384
60	-123	-701	-6.927	6.962	9.835	9.576	7.796	-69	-7.201	7.234	9.924	9.582	8.396
61	-122	-783	-6.912	6.956	9.825	9.571	7.805	-839	-7.126	7.176	9.921	9.593	8.407
62	-121	-882	-6.868	6.924	9.828	9.603	7.835	-906	-7.031	7.089	9.904	9.577	8.429
63	-120	-849	-6.667	6.721	9.818	9.628	7.882	-0.08	-684	6.887	9.926	9.565	847
64	-119	-747	-6.509	6.551	9.826	9.631	7.928	-778	-6.675	672	9.928	956	8.506
65	-118	-738	-6.385	6.427	9.834	9.665	7.959	-709	-6.599	6.637	9.938	9.552	8.524
66	-117	-72	-6.446	6.486	9.821	9.665	7.943	-707	-6.572	661	9.922	9.545	8.524
67	-116	-567	-6.565	659	9.823	9.665	7.891	-58	-6.709	6.734	9.926	9.555	8.482
68	-115	-638	-6.501	6.532	9.812	9.648	7.897	-628	-6.662	6.692	9.941	9.569	8.497
69	-114	-688	-6.395	6.432	9.815	9.643	793	-732	-659	6.631	9.926	9.568	851
70	-113	-625	-6.295	6.326	9.806	9.659	7.945	-674	-6.501	6.536	9.921	9.568	853

71	-112	-0.07	-6.177	6.216	9.826	9.683	8.011	-713	-6.338	6.378	9.931	9.567	8.575
72	-111	-681	-6.274	631	9.808	9.666	7.971	-682	-6.361	6.397	9.925	9.567	8.562
73	-110	-632	-6.223	6.255	9.827	9.662	0.8	-739	-6.296	6.339	9.923	9.552	8.587
74	-109	-679	-6.108	6.145	9.806	9.655	8.033	-789	-6.194	6.244	9.922	9.539	8.612
75	-108	-743	-6.082	6.127	9.819	9.648	8.071	-852	-6.138	6.197	9.931	9.518	8.629
76	-107	-777	-594	5.991	9.817	9.652	812	-822	-6.021	6.076	9.926	9.507	8.638
77	-106	-737	-584	5.886	9.808	9.641	8.167	-855	-5.904	5.966	9.932	9.505	8.664
78	-105	-758	-6.022	607	9.824	9.649	8.079	-856	-6.034	6.094	9.952	9.487	8.649
79	-104	-833	-6.096	6.153	9.833	9.638	8.063	-896	-6.047	6.113	9.934	9.496	8.648
80	-103	-714	-6.044	6.086	9.802	9.649	8.063	-85	-5.958	6.018	9.934	9.497	8.665
81	-102	-843	-5.944	6.003	9.824	9.649	811	-925	-5.874	5.946	9.953	9.493	8.672
82	-101	-788	-5.968	6.019	9.823	9.648	8.076	-904	-5.885	5.954	9.932	9.495	8.675
83	-100	-727	-5.966	601	9.823	9.636	8.093	-817	-5.867	5.924	9.946	9.488	8.669
84	-99	-619	-5.877	591	9.835	9.628	8.107	-726	-5.753	5.799	9.927	9.476	8.693
85	-98	-646	-5.853	5.889	9.855	9.635	813	-719	-5.734	5.779	9.936	9.475	8.692
86	-97	-518	-6.095	6.117	9.812	9.636	8.082	-64	-5.932	5.966	9.945	9.466	8.666
87	-96	-532	-5.996	6.019	9.827	9.616	8.112	-609	-5.813	5.844	9.927	9.467	8.692
88	-95	-549	-5.673	5.699	9.824	9.608	8.202	-595	-5.625	5.656	9.937	9.454	873
89	-94	-594	-5.775	5.805	9.828	9.608	8.172	-687	-5.668	5.709	9.962	9.441	8.714
90	-93	-552	-5.535	5.563	9.823	9.608	8.231	-65	-5.517	5.555	994	9.429	8.737
91	-92	-515	-5.668	5.691	9.818	9.593	8.208	-604	-5.598	5.631	9.935	9.427	8.724
92	-91	-621	-5.551	5.586	9.829	9.585	824	-671	-552	5.561	9.925	9.423	874
93	-90	-673	-5.585	5.625	9.837	959	8.239	-756	-554	5.591	9.936	9.417	8.731
94	-89	-619	-5.579	5.613	9.838	9.582	8.243	-692	-5.521	5.564	9.938	9.418	8.731
95	-88	-668	-553	557	9.826	9.586	8.243	-778	-5.509	5.564	9.893	942	8.722
96	-87	-708	-5.553	5.598	9.826	9.559	8.248	-817	-5.508	5.568	992	9.419	8.714
97	-86	-539	-5.715	574	9.823	9.564	8.213	-684	-5.645	5.686	9.927	9.414	8.695
98	-85	-649	-5.775	5.812	9.808	9.556	8.192	-72	-5.674	572	9.934	9.416	8.686
99	-84	-653	-5.621	5.659	0.98	9.534	8.257	-83	-555	5.612	9.905	9.417	8.694
100	-83	-707	-5.759	5.802	9.805	9.513	821	-868	-5.589	5.656	991	9.421	8.693
101	-82	-643	-5.823	5.858	9.819	9.521	8.174	-766	-5.688	5.739	9.929	9.421	869
102	-81	-617	-5.717	575	9.815	9.513	822	-776	-5.638	5.692	9.929	9.425	8.704
103	-80	-565	-5.624	5.652	9.815	9.498	824	-757	-5.575	5.626	9.928	9.404	872
104	-79	-652	-5.792	5.829	9.812	9.506	8.193	-801	-5.674	573	9.917	9.407	8.704
105	-78	-602	-5.738	577	9.815	9.494	8.193	-773	-5.693	5.745	9.927	0.94	8.701
106	-77	-518	-578	5.803	9.809	9.489	818	-676	-5.729	5.769	9.935	9.398	8.697
107	-76	-574	-573	5.759	9.798	9.482	8.199	-722	-571	5.756	9.929	9.399	8.697
108	-75	-609	-5.744	5.776	9.832	947	8.203	-737	-5.746	5.793	9.945	9.408	8.691
109	-74	-679	-569	5.731	9.835	9.474	8.235	-76	-5.709	5.759	9.947	9.412	8.702
110	-73	-63	-5.732	5.767	9.835	947	8.218	-796	-5.759	5.814	9.936	9.412	8.691
111	-72	-528	-5.816	584	981	9.461	8.179	-713	-5.808	5.852	9.924	9.413	8.693
112	-71	-582	-577	0.58	9.821	9.453	8.197	-759	-5.778	5.828	9.933	9.427	8.693
113	-70	-724	-5.644	569	9.844	9.449	825	-831	-5.704	5.764	9.934	9.424	8.702
114	-69	-669	-5.733	5.772	9.824	946	8.206	-852	-5.739	5.802	9.925	9.422	0.87
115	-68	-616	-5.598	5.632	9.816	946	8.259	-827	-5.605	5.666	9.938	9.415	8.716
116	-67	-614	-582	5.852	9.809	9.468	8.176	-794	-5.794	5.848	995	9.407	869
117	-66	-599	-5.807	5.838	9.818	9.468	8.186	-786	-5.768	5.821	9.915	9.411	8.684

118	-65	-581	-5.741	5.771	9.806	9.468	8.209	-768	-5.735	5.786	9.923	9.413	8.688
119	-64	-518	-5.874	5.897	9.824	946	8.174	-661	-5.782	582	9.934	9.417	8.689
120	-63	-663	-5.905	5.943	9.822	9.453	8.168	-774	-5.852	5.903	9.942	942	8.671
121	-62	-481	-5.862	5.881	9.835	9.442	816	-627	-5.809	5.843	9.938	942	8.684
122	-61	-613	-5.933	5.964	9.828	9.426	8.148	-764	-5.889	5.938	992	9.418	8.663
123	-60	-546	-6.025	6.049	9.832	9.419	8.122	-703	-5.981	6.022	9.946	9.409	8.652
124	-59	-469	-6.116	6.134	9.823	941	8.091	-587	-611	6.138	9.949	9.416	8.636
125	-58	-509	-6.264	6.284	9.811	9.395	8.044	-614	-6.256	6.286	9.941	9.418	8.605
126	-57	-367	-6.329	634	9.794	9.391	7.992	-526	-0.63	6.322	9.929	942	8.601
127	-56	-303	-6.206	6.213	9.811	9.392	8.036	-477	-6.142	6.161	9.925	9.436	8.642
128	-55	-234	-6.158	6.163	9.818	9.393	8.053	-442	-6.195	621	9.937	9.434	8.634
129	-54	-318	-6.033	6.041	982	9.397	8.106	-535	-6.151	6.174	9.919	9.441	8.644
130	-53	-423	-6.215	623	9.813	9.393	8.044	-611	-6.247	6.277	9.936	9.448	8.605
131	-52	-351	-6.095	6.105	9.813	9.386	8.084	-553	-6.123	6.148	9.935	9.457	8.644
132	-51	-408	-6.169	6.183	9.825	9.386	805	-0.06	-6.245	6.273	9.916	9.457	8.605
133	-50	-335	-612	6.129	9.814	9.385	8.056	-572	-6.199	6.225	9.914	9.461	8.615
134	-49	-337	-6.045	6.055	9.815	9.397	8.075	-573	-6.172	6.199	9.934	9.457	8.621
135	-48	-329	-6.117	6.126	982	9.393	8.042	-524	-6.138	6.161	9.939	9.451	8.632
136	-47	-393	-6.304	6.316	9.808	9.393	8.011	-56	-6.292	6.317	9.951	9.447	8.591
137	-46	-389	-6.163	6.175	9.799	9.392	8.049	-55	-6.119	6.144	993	9.436	8.633
138	-45	-404	-6.255	6.268	9.806	9.384	8.009	-634	-6.223	6.255	9.919	9.445	8.606
139	-44	-372	-6.065	6.077	9.799	9.379	8.077	-55	-6.071	6.096	9.917	9.444	8.636
140	-43	-309	-6.079	6.087	9.827	9.376	8.063	-527	-6.122	6.144	9.921	9.438	8.634
141	-42	-326	-5.959	5.968	981	9.363	8.125	-526	-599	6.013	9.903	9.438	8.659
142	-41	-275	-6.135	6.141	982	9.349	8.042	-467	-609	6.108	9.943	9.437	8.645
143	-40	-151	-6.281	6.283	9.798	9.342	803	-338	-6.144	6.154	9.929	9.431	8.641
144	-39	-157	-651	6.512	9.824	9.347	793	-343	-6.385	6.394	9.937	9.433	8.593
145	-38	-0.02	-6.427	643	9.811	9.333	795	-417	-628	6.294	995	943	8.613
146	-37	-131	-639	6.391	9.841	9.337	7.972	-34	-6.343	6.352	9.931	9.433	8.599
147	-36	-14	-6.494	6.494	9.828	9.348	7.938	-267	-6.408	6.413	9.951	9.435	8.596
148	-35	-16	-6.578	658	9.817	9.344	791	-351	-6.441	6.451	9.942	9.447	8.585
149	-34	-22	-6.536	654	9.804	9.352	7.918	-413	-6.436	6.449	9.938	9.443	8.578
150	-33	-154	-6.648	665	9.823	9.348	7.898	-401	-6.559	6.572	992	9.458	8.559
151	-32	-173	-6.612	6.615	9.819	9.367	7.899	-43	-655	6.564	9.929	9.452	855
152	-31	-104	-6.554	6.555	9.824	9.355	7.913	-333	-6.481	6.489	9.937	9.468	8.553
153	-30	-148	-6.602	6.604	9.834	9.358	7.902	-362	-6.525	6.535	9.942	9.464	8.549
154	-29	-178	-6.832	6.835	9.838	9.366	7.859	-359	-672	673	9.952	9.468	8.518
155	-28	-187	-6.713	6.716	9.831	9.369	7.883	-431	-6.632	6.646	9.943	948	8.529
156	-27	-162	-6.773	6.775	9.819	9.373	7.866	-0.04	-6.675	6.687	9.946	948	8.525
157	-26	-237	-6.727	6.731	9.826	9.389	7.883	-429	-662	6.634	993	9.488	8.535
158	-25	-135	-6.627	6.628	9.812	9.386	7.905	-434	-6.576	659	9.924	9.502	8.534
159	-24	-91	-6.746	6.746	9.832	9.377	788	-36	-6.643	6.652	9.943	0.95	8.518
160	-23	-91	-682	682	9.831	9.397	7.874	-369	-6.694	6.704	9.942	0.95	8.518
161	-22	-49	-6.723	6.724	9.839	9.396	7.882	-323	-6.634	6.642	9.936	9.497	8.516
162	-21	25	-6.792	6.792	9.812	9.392	7.872	-235	-6.693	6.697	9.942	9.501	8.507
163	-20	-18	-6.895	6.895	9.837	9.395	7.844	-238	-6.805	6.809	9.961	9.499	8.481
164	-19	41	-6.921	6.921	9.834	9.399	785	-216	-6.847	685	996	9.502	8.471

165	-18	49	-6.875	6.875	9.835	9.415	7.867	-221	-6.852	6.855	9.951	9.513	8.466
166	-17	69	-6.903	6.903	9.839	9.426	7.861	-193	-6.873	6.876	9.948	9.518	8.456
167	-16	7	-7.002	7.002	983	943	7.826	-228	-6.974	6.977	9.956	9.523	843
168	-15	62	-6.968	6.968	9.831	9.441	7.828	-236	-6.945	6.949	9.956	9.527	8.436
169	-14	29	-7.018	7.018	9.829	9.433	7.809	-255	-6.974	6.979	9.959	9.532	8.431
170	-13	15	-6.983	6.983	9.818	9.429	7.836	-265	-6.971	6.976	9.961	953	8.429
171	-12	25	-6.891	6.891	9.786	9.421	7.848	-261	-6.921	6.926	9.941	9.528	8.437
172	-11	89	-6.825	6.825	9.723	9.425	7.862	-26	-6.869	6.874	9.898	9.527	8.445
173	-10	-1	-1	-1	-1	9.421	-1	-1	-1	-1	-1	9.529	-1
174	-9	-1	-1	-1	-1	9.433	-1	-1	-1	-1	-1	9.535	-1
175	-8	-1	-1	-1	-1	9.422	-1	-1	-1	-1	-1	9.535	-1
176	-7	-1	-1	-1	-1	9.414	-1	-1	-1	-1	-1	9.535	-1
177	-6	-1	-1	-1	-1	9.415	-1	-1	-1	-1	-1	9.539	-1
178	-5	-1	-1	-1	-1	9.431	-1	-1	-1	-1	-1	9.533	-1
179	-4	-1	-1	-1	-1	9.435	-1	-1	-1	-1	-1	954	-1
180	-3	-1	-1	-1	-1	943	-1	-1	-1	-1	-1	9.546	-1
181	-2	-1	-1	-1	-1	9.434	-1	-1	-1	-1	-1	9.549	-1
182	-1	-1	-1	-1	-1	9.434	-1	-1	-1	-1	-1	9.548	-1
183	0	-1	-1	-1	-1	9.429	-1	-1	-1	-1	-1	955	-1
184	1	-1	-1	-1	-1	9.441	-1	-1	-1	-1	-1	9.551	-1
185	2	-1	-1	-1	-1	944	-1	-1	-1	-1	-1	9.556	-1
186	3	-1	-1	-1	-1	9.443	-1	-1	-1	-1	-1	9.547	-1
187	4	-1	-1	-1	-1	9.439	-1	-1	-1	-1	-1	954	-1
188	5	-1	-1	-1	-1	9.451	-1	-1	-1	-1	-1	9.542	-1
189	6	-1	-1	-1	-1	9.466	-1	-1	-1	-1	-1	9.542	-1
190	7	-1	-1	-1	-1	9.473	-1	-1	-1	-1	-1	953	-1
191	8	-1	-1	-1	-1	9.472	-1	-1	-1	-1	-1	9.517	-1
192	9	-1	-1	-1	-1	9.468	-1	-1	-1	-1	-1	9.517	-1
193	10	-1	-1	-1	-1	9.472	-1	-1	-1	-1	-1	9.525	-1
194	11	379	-709	0.71	9.707	9.481	778	72	-7.123	7.123	9.878	9.531	8.349
195	12	364	-7.048	7.058	9.731	9.465	7.789	53	-7.131	7.132	9.905	9.535	8.345
196	13	341	-7.032	7.041	9.781	9.469	7.784	-23	-7.146	7.146	9.953	9.537	8.335
197	14	356	-696	6.969	9.806	9.458	7.805	5	-7.082	7.082	9.954	9.531	8.348
198	15	371	-6.943	6.953	9.818	9.454	7.805	41	-7.069	7.069	9.953	9.537	8.357
199	16	406	-6.917	6.929	9.826	9.444	7.834	88	-7.062	7.062	9.945	9.549	8.353
200	17	473	-6.972	6.988	9.828	9.454	7.808	162	-713	7.132	9.943	9.548	8.338
201	18	529	-7.012	7.032	9.832	9.473	7.784	225	-7.169	7.172	9.943	9.551	8.328
202	19	564	-7.056	7.079	9.833	948	7.755	292	-7.242	7.248	9.942	9.563	8.327
203	20	62	-6.965	6.993	9.842	9.484	7.784	366	-7.171	718	9.936	957	8.331
204	21	668	-6.957	6.989	9.852	9.491	7.787	427	-716	7.173	993	9.554	8.331
205	22	69	-6.973	7.007	9.851	951	7.758	47	-7.206	7.221	9.921	9.551	8.323
206	23	693	-6.941	6.975	9.856	9.522	7.769	473	-7.171	7.186	9.921	9.568	8.333
207	24	642	-6.957	6.987	9.851	9.508	7.757	501	-7.185	7.203	9.923	956	8.327
208	25	677	-6.951	6.984	9.855	9.503	7.758	499	-718	7.197	9.921	9.544	8.332
209	26	672	-6.877	6.909	9.844	9.491	7.784	525	-7.101	712	9.928	9.535	8.342
210	27	702	-6.829	6.865	9.844	9.502	7.795	569	-7.049	7.072	993	9.515	8.346
211	28	663	-6.846	6.878	9.844	9.517	7.799	558	-7.014	7.036	9.944	9.505	8.354

212	29	689	-696	6.994	9.833	9.528	775	561	-7.092	7.114	9.941	9.495	8.348
213	30	694	-6.902	6.937	9.825	9.515	7.784	568	-7.049	7.072	9.939	9.487	8.361
214	31	611	-6.848	6.875	9.826	9.531	7.828	52	-6.971	699	9.954	9.485	8.377
215	32	684	-6.778	6.812	9.824	9.547	7.835	543	-6.924	6.946	9.954	9.494	8.389
216	33	638	-6.661	6.691	9.824	9.528	7.857	483	-6.888	6.905	9.935	0.95	8.402
217	34	689	-6.688	6.723	9.833	9.524	7.873	544	-6.857	6.879	993	9.502	8.407
218	35	726	-6.636	6.676	9.829	9.524	7.885	572	-688	6.903	9.949	9.513	8.405
219	36	687	-652	6.556	9.823	9.517	7.914	586	-6.783	6.808	9.926	9.519	8.423
220	37	788	-6.693	674	9.809	9.531	7.849	644	-692	695	9.934	9.504	8.389
221	38	0.08	-6.797	6.844	9.819	9.522	7.822	721	-707	7.106	9.931	9.493	835
222	39	901	-6.733	6.793	9.825	9.525	7.834	783	-6.962	7.006	9.918	9.475	837
223	40	986	-6.771	6.843	9.831	951	7.801	874	-7.042	7.096	9.937	9.449	8.335
224	41	941	-6.902	6.966	9.835	952	7.769	876	-7.084	7.138	9.927	9.425	8.321
225	42	877	-6.973	7.028	9.838	9.511	7.751	832	-7.121	7.169	9.931	943	8.307
226	43	882	-6.808	6.865	9.837	9.508	0.78	864	-6.969	7.022	9.925	9.414	8.333
227	44	888	-6.781	6.839	9.844	951	7.818	849	-6.993	7.044	9.918	9.415	8.332
228	45	749	-6.643	6.685	983	0.95	7.871	729	-6.859	6.898	9.915	9.411	8.373
229	46	726	-6.495	6.535	985	9.474	792	72	-6.753	6.791	9.913	9.416	8.406
230	47	725	-6.387	6.428	9.839	9.478	7.963	748	-6.614	6.656	9.928	9.421	8.442
231	48	779	-6.544	6.591	983	9.478	7.898	786	-6.769	6.814	9.934	9.395	8.414
232	49	858	-625	6.309	9.817	9.441	8.008	83	-6.478	6.531	9.931	9.396	847
233	50	829	-6.177	6.232	9.823	9.406	8.017	861	-6.449	6.506	9.921	9.399	8.489
234	51	863	-6.119	6.179	9.811	9.417	8.028	828	-6.422	6.475	9.916	9.418	8.485
235	52	806	-6.045	6.098	983	9.447	8.049	857	-6.292	635	9.887	9.439	8.511
236	53	868	-5.681	5.747	9.818	9.441	8.142	894	-5.989	6.055	9.925	9.438	8.575
237	54	883	-5.469	554	9.816	946	8.199	883	-5.918	5.983	991	9.459	8.597
238	55	884	-5.378	545	9.808	9.464	825	855	-5.877	5.939	9.906	9.465	8.596
239	56	103	-5.459	5.556	9.813	9.439	8.251	982	-586	5.942	9.948	9.457	8.606
240	57	107	-5.263	5.371	9.816	9.457	8.283	1.049	-5.666	5.763	9.918	9.442	8.621
241	58	1.092	-498	5.098	9.808	9.437	8.341	1.123	-547	5.584	9.919	942	8.658
242	59	1.173	-4.686	483	9.801	0.95	8.439	1.177	-5.199	5.331	9.916	9.406	8.713
243	60	1.088	-4.468	4.598	9.832	9.498	852	1.143	-4.952	5.082	9.923	9.398	8.762
244	61	99	-4.235	4.349	9.831	9.481	8.586	1.085	-4.745	4.868	9.925	9.353	8.789
245	62	957	-393	4.045	9.839	9.491	867	1.109	-4.449	4.585	9.921	9.351	883
246	63	104	-3.529	368	9.825	9.531	8.787	1.196	-4.098	427	9.919	9.345	8.894
247	64	1.053	-3.393	3.553	9.824	9.521	8.847	1.105	-4.018	4.167	9.919	9.341	8.915
248	65	1.081	-3.307	3.479	9.835	0.95	8.883	1.162	-3.866	4.036	9.915	9.348	896
249	66	1.075	-3.351	3.519	9.825	9.472	8.852	1.136	-3.873	4.036	9.913	9.345	8.962
250	67	1.065	-3.236	3.407	9.838	9.415	8.897	1.106	-3.788	3.946	9.896	9.339	8.984
251	68	1.065	-3.315	3.482	9.827	939	8.874	115	-3.861	4.029	9.919	9.334	8.964
252	69	1.045	-3.254	3.417	9.808	9.362	8.898	1.069	-3.828	3.975	992	9.344	8.967
253	70	889	-3.359	3.475	9.806	9.381	8.865	916	-3.926	4.031	989	9.337	8.944
254	71	1.004	-3.407	3.552	9.811	9.388	8.839	1.034	-4.054	4.183	9.913	9.358	8.908
255	72	942	-0.37	3.818	9.817	9.426	8.734	1.015	-429	4.408	9.887	9.354	8.849
256	73	949	-3.817	3.934	9.808	9.429	8.717	1.014	-4.442	4.556	9.899	9.364	8.808
257	74	1.071	-3.939	4.082	9.828	9.414	8.657	1.134	-4.548	4.687	9.914	9.379	8.782
258	75	1.154	-4.307	4.459	9.827	9.429	8.554	1.205	-486	5.007	9.927	9.358	8.702

259	76	1.157	-4.606	4.749	9.822	9.462	8.467	1.263	-5.124	5.277	9.918	9.385	8.634
260	77	1.208	-4.628	4.783	9.824	9.457	8.454	1.314	-5.153	5.318	9.919	937	864
261	78	1.256	-456	473	9.811	9.431	8.479	1.349	-5.082	5.258	9.914	937	8.677
262	79	1.249	-4.824	4.983	9.818	9.409	8.385	1.346	-5.245	5.415	9.919	9.359	8.641
263	80	1.251	-4.923	508	9.821	9.418	8.369	1.372	-529	5.465	9.934	9.355	8.648
264	81	1.358	-4.937	512	9.815	9.419	8.382	1.479	-5.222	5.427	9.919	9.354	8.668
265	82	1.281	-4.854	502	9.809	9.384	8.419	1.408	-0.52	5.387	9.906	9.352	8.684
266	83	1.212	-515	5.291	9.829	9.368	8.333	135	-5.361	5.529	9.905	9.352	8.666
267	84	1.244	-5.282	5.427	982	9.373	8.286	1.312	-5.467	5.622	9.913	9.365	8.641
268	85	1.175	-531	5.439	9.827	9.388	8.295	1.182	-5.471	5.597	9.929	9.366	8.649
269	86	1.265	-5.283	5.432	9.823	9.416	8.298	1.326	-5.428	5.587	9.928	9.376	8.651
270	87	1.147	-5.536	5.654	9.811	9.424	8.224	123	-5.653	5.785	9.899	9.389	8.599
271	88	1.106	-5.703	5.809	9.828	9.426	8.154	1.172	-575	5.868	9.935	9.405	8.585
272	89	1.147	-5.469	5.588	9.813	9.433	8.237	1.214	-5.549	568	9.909	9.416	8.623
273	90	1.209	-5.623	5.751	9.817	9.455	8.189	1.242	-5.648	5.783	992	9.402	8.604
274	91	106	-5.782	5.879	9.837	9.482	8.088	1.117	-5.753	5.861	9.914	9.362	8.554
275	92	1.065	-5.862	5.958	9.832	9.461	8.056	1.105	-5.768	5.872	9.925	9.341	8.542
276	93	1.167	-6.146	6.256	9.827	9.461	7.942	1.207	-5.961	6.082	9.915	9.324	849
277	94	1.123	-6.223	6.324	9.825	9.455	7.915	1.137	-5.958	6.065	9.915	9.293	849
278	95	1.278	-6.341	6.468	9.826	9.455	7.853	1.275	-6.062	6.195	992	9.263	8.453
279	96	132	-6.499	6.631	983	9.424	7.777	1.326	-6.171	6.312	9.902	9.246	8.424
280	97	1.248	-6.174	6.299	9.828	945	7.917	1.216	-5.867	5.992	9.932	9.277	851
281	98	122	-6.024	6.147	9.826	9.393	8.005	1.232	-5.791	592	9.929	9.286	8.537
282	99	1.157	-5.773	5.887	982	9.373	8.102	1.132	-5.535	5.649	9.936	9.279	8.623
283	100	1.171	-5.405	553	9.827	9.359	8.264	1.161	-5.233	536	9.917	9.304	8.726
284	101	1.105	-5.078	5.197	9.819	9.343	8.403	1.153	-4.952	5.085	991	9.315	8.793
285	102	916	-4.972	5.056	9.815	9.252	8.431	957	-4.884	4.977	9.918	932	8.836
286	103	848	-4.879	4.952	9.821	9.218	8.461	884	-4.728	481	993	9.332	8.876
287	104	953	-4.953	5.044	9.823	9.243	8.447	988	-4.784	4.885	9.941	9.338	886
288	105	1.003	-5.166	5.262	9.815	9.272	8.385	991	-4.955	5.053	9.932	9.349	8.813
289	106	991	-5.363	5.454	9.818	9.304	8.302	989	-5.136	5.231	9.934	9.363	8.765
290	107	978	-5.358	5.446	981	931	8.304	983	-5.192	5.284	9.916	9.373	8.754
291	108	933	-5.567	5.644	9.815	9.308	8.263	927	-5.384	5.463	9.928	9.368	8.719
292	109	971	-5.742	5.823	9.803	934	8.198	958	-5.513	5.596	9.913	9.396	8.688
293	110	1.089	-5.843	5.943	9.821	938	8.136	1.044	-5.608	5.704	9.929	9.391	8.649
294	111	1.056	-5.952	6.045	9.818	9.402	7.993	1.001	-5.718	5.805	9.904	9.358	8.598
295	112	1.151	-6.141	6.248	9.809	9.364	7.802	1.062	-5.944	6.038	9.915	9.328	8.512
296	113	1.328	-6.025	6.169	9.813	9.141	7.735	1.122	-5.826	5.933	9.934	9.275	8.492
297	114	1.484	-6.236	6.411	982	8.638	7.405	0.12	-5.993	6.112	9.933	9.226	8.405
298	115	1.632	-6.584	6.784	982	8.031	7.039	1.203	-6.362	6.475	9.911	9.143	8.264
299	116	1.955	-6.907	7.179	9.825	7.151	647	118	-6.657	676	9.928	9.069	8.159
300	117	2.388	-744	7.814	9.848	603	5.626	1.283	-7.069	7.184	992	8.989	8.003
301	118	2.997	-8.702	9.204	9.838	4.306	409	1.153	-7.938	8.021	9.909	8.851	7.757
302	119	3.943	-11.317	1.1984	981	145	1.459	1.144	-8.896	8.969	9.903	8.631	7.477
303	120	-1	-1	-1	9.817	-1	0	1.093	-10.022	1.1981	9.915	832	7.129
304	121	-1	-1	-1	9.809	-1	0	979	-11.751	1.1792	9.928	7.853	6.619
305	122	-1	-1	-1	9.826	-1	0	881	-14.076	1.4104	9.918	7.164	5.901

306	123	-1	-1	-1	982	-1	0	787	-15.728	1.5748	9.918	6.762	5.439
307	124	-1	-1	-1	9.812	-1	0	866	-15.327	1.5351	9.917	7.164	5.705
308	125	-1	-1	-1	9.805	-1	0	927	-15.189	1.5218	9.925	7.516	5.913
309	126	-1	-1	-1	9.811	-1	0	915	-14.745	1.4773	9.922	7.849	6.167
310	127	3.786	-20.028	2.0383	981	755	219	792	-14.414	1.4436	9.915	8.148	6.361
311	128	3.434	-19.836	2.0131	9.808	1.647	613	819	-13.987	1.401	9.916	843	6.576
312	129	3.064	-19.599	1.9837	979	2.457	985	894	-13.554	1.3584	9.923	8.633	6.807
313	130	2.827	-19.028	1.9237	9.788	3.194	1.532	951	-11.817	1.1855	9.913	8.854	7.312
314	131	2.632	-17.132	1.7333	979	4.359	2.702	971	-10.011	1.1958	9.914	8.998	7.747
315	132	2.371	-14.122	1.432	9.778	5.774	4.186	91	-879	8.837	9.888	9.016	7.991
316	133	2.145	-11.158	1.1362	9.786	701	5.434	1.012	-7.802	7.867	992	9.064	824
317	134	1.831	-8.883	907	9.779	7.915	6.417	994	-6.852	6.924	9.912	9.089	8.419
318	135	1.597	-735	7.522	9.802	8.583	7.097	987	-6.204	6.282	9.919	9.126	8.571
319	136	1.504	-6.055	6.239	9.798	8.983	7.626	1.057	-5.568	5.668	9.892	9.139	8.697
320	137	1.534	-546	5.671	9.789	9.153	7.947	1.131	-5.233	5.354	9.911	9.169	8.761
321	138	1.412	-5.262	5.448	9.777	9.228	8.086	1.119	-5.215	5.333	991	9.216	8.756
322	139	1.187	-4.751	4.897	9.788	923	8.346	998	-4.768	4.871	9.933	9.255	8.856
323	140	1.054	-4.522	4.643	9.794	9.271	8.465	91	-4.665	4.752	9.926	9.273	8.871
324	141	1.011	-3.913	4.041	9.802	928	8.721	871	-4.171	4.261	9.915	931	8.964
325	142	1.077	-3.624	378	9.803	9.269	8.804	997	-3.941	4.065	991	9.347	8.994
326	143	1.014	-3.605	3.745	9.807	9.282	8.832	937	-3.904	4.015	9.924	9.363	9.008
327	144	976	-3.659	3.787	9.801	9.283	8.839	846	-0.4	4.088	9.904	9.356	9.001
328	145	987	-3.619	3.752	9.789	9.283	8.848	884	-3.895	3.994	9.919	936	9.029
329	146	947	-333	3.462	9.788	9.271	8.932	832	-3.613	3.707	9.902	9.357	9.094
330	147	897	-3.321	344	9.795	9.251	8.944	843	-3.595	3.693	9.919	9.351	9.097
331	148	888	-0.33	3.417	9.799	9.233	8.946	756	-3.547	3.626	9.894	9.346	9.118
332	149	842	-3.259	3.366	979	9.235	896	748	-3.472	3.552	989	9.346	9.129
333	150	1.098	-3.041	3.233	9.795	9.241	898	902	-3.359	3.478	9.899	9.352	913
334	151	1.038	-3.073	3.243	9.784	9.266	8.952	914	-3.433	3.553	9.898	9.344	9.114
335	152	1.022	-3.188	3.348	9.792	9.298	8.954	925	-3.514	3.634	991	9.362	0.91
336	153	1.146	-337	356	9.791	9.311	8.849	1.022	-3.689	3.828	9.941	938	9.049
337	154	1.189	-0.32	3.414	9.768	9.325	8.916	1.066	-3.557	3.713	991	939	9.074
338	155	1.141	-3.138	3.339	9.786	934	8.944	964	-3.634	376	989	9.398	905
339	156	1.139	-3.201	3.397	978	9.326	8.938	959	-3.707	3.829	9.898	9.407	9.015
340	157	1.106	-3.162	335	9.784	9.323	894	959	-3.613	3.738	9.906	941	9.043
341	158	1.055	-2.985	3.166	9.788	9.333	898	929	-3.464	3.586	9.901	9.411	9.087
342	159	1.158	-2.771	3.003	9.784	9.324	9.036	102	-3.315	3.468	9.894	9.416	912
343	160	1.094	-2.668	2.884	9.802	9.341	9.081	1.022	-3.206	3.365	9.908	943	9.138
344	161	1.018	-2.481	2.682	9.796	9.332	9.111	946	-3.018	3.163	9.906	9.442	9.188
345	162	1.091	-2.434	2.667	9.803	9.307	9.123	977	-2.951	3.109	9.923	9.444	9.206
346	163	1.079	-2.464	2.689	9.798	9.302	9.109	991	-2.973	3.134	9.909	9.453	9.205
347	164	108	-2.562	2.781	9.782	9.319	9.111	937	-3.052	3.193	9.911	9.448	918
348	165	874	-2.611	2.754	9.807	9.325	9.103	775	-3.077	3.173	9.913	944	9.176
349	166	893	-2.399	256	9.807	9.328	9.112	792	-2.928	3.033	9.915	9.437	9.205
350	167	916	-2.407	2.576	9.798	9.322	9.102	83	-2.872	299	9.908	9.429	9.223
351	168	961	-263	0.28	9.804	9.335	9.081	873	-3.055	3.177	9.924	942	9.171
352	169	899	-2.587	2.739	9.813	9.334	9.107	765	-2.964	3.061	9.928	9.425	9.198

353	170	1.067	-2.492	271	9.803	9.326	9.084	95	-2.872	3.025	9.927	9.442	9.209
354	171	1.095	-2.622	2.841	9.792	933	9.049	1.001	-304	0.32	9.902	9.464	9.167
355	172	1.025	-2.656	2.847	0.98	9.354	9.069	976	-3.084	3.235	9.926	9.497	9.164
356	173	1.151	-2.469	2.724	9.792	936	9.087	1.143	-0.29	3.118	9.917	9.516	9.182
357	174	1.169	-2.214	2.503	9.785	9.367	9.162	1.182	-2.721	2.967	9.927	9.547	9.234
358	175	1.025	-2.302	252	9.797	9.376	9.148	1.058	-2.804	2.997	9.897	9.572	921
359	176	98	-2.406	2.598	9.821	9.396	9.128	1.006	-2.843	3.016	9.909	9.597	921
360	177	92	-2.291	2.468	9.838	9.403	9.166	1.003	-2.721	0.29	9.905	961	9.246
361	178	899	-2.279	245	9.832	9.411	9.173	965	-2.723	2.889	9.916	9.622	9.251
362	179	946	-209	2.294	9.818	9.418	9.214	974	-2.545	2.725	9.909	9.629	9.288
363	180	1.007	-2.105	2.333	9.805	9.428	9.216	1.041	-2.479	2.689	9.909	9.623	9.293
364	181	1.005	-2.107	2.334	9.822	9.444	922	1.077	-2.444	2.671	9.923	9.627	9.299
365	182	986	-2.232	244	9.841	9.439	9.184	1.033	-2.487	2.693	9.945	9.644	9.308
366	183	954	-2.303	2.493	9.816	9.454	9.164	996	-2.535	2.723	9.928	9.657	9.301
367	184	928	-2.468	2.637	9.821	9.469	9.135	964	-2.644	2.815	9.922	9.668	928
368	185	844	-2.355	2.502	9.814	9.481	9.169	856	-2.601	2.738	9.924	9.674	9.288
369	186	743	-2.244	2.364	9.821	9.493	9.223	813	-2.463	2.594	9.925	9.681	9.338
370	187	842	-2.457	2.597	9.834	9.493	9.161	878	-2.588	2.733	9.929	9.698	9.287
371	188	878	-2.383	254	9.807	9.508	9.172	963	-2.581	2.755	9.892	9.711	9.278
372	189	908	-256	2.716	9.798	9.522	9.131	996	-2.718	2.894	9.899	9.724	925
373	190	911	-2.497	2.658	9.835	9.531	9.138	955	-2.702	2.866	9.932	973	9.248
374	191	888	-2.548	2.698	9.833	9.514	9.126	1.007	-2.675	2.858	9.927	9.743	9.261
375	192	975	-2.498	2.682	9.828	9.514	9.136	1.037	-2.576	2.777	9.922	9.749	9.289
376	193	914	-2.263	244	983	9.509	9.197	1.013	-242	2.623	9.935	974	9.332
377	194	836	-231	2.457	9.834	9.522	9.189	892	-2.452	2.609	9.917	9.745	9.328
378	195	872	-2.078	2.253	984	9.545	9.251	94	-2.238	2.427	9.939	9.747	9.378
379	196	946	-1.955	2.172	9.838	9.561	9.289	1.009	-2.134	236	993	9.749	9.395
380	197	873	-2.077	2.253	9.815	9.575	9.263	921	-2.208	2.393	9.925	9.749	9.381
381	198	904	-2.188	2.367	9.827	9.597	9.244	935	-2.284	2.468	9.908	9.752	9.356
382	199	982	-207	2.291	9.828	9.591	9.277	1.015	-2.141	2.369	994	9.756	9.397
383	200	921	-2.249	2.431	9.819	9.617	9.233	954	-2.336	2.523	9.917	9.741	9.346
384	201	953	-2.423	2.604	9.819	9.625	9.166	946	-244	2.618	9.929	9.739	9.324
385	202	99	-2.684	286	9.817	962	9.079	931	-262	2.781	9.941	9.742	9.288
386	203	97	-2.506	2.687	9.794	9.614	9.131	96	-2.475	2.655	9.911	9.746	9.318
387	204	899	-2.701	2.847	9.802	9.617	9.064	908	-2.641	2.793	9.928	974	9.288
388	205	1.045	-2.385	2.605	9.809	9.598	9.151	983	-2.434	2.625	9.921	9.727	9.323
389	206	1.099	-2.708	2.922	9.821	9.574	9.019	1.002	-2.616	2.801	9.938	9.715	9.286
390	207	99	-2.577	276	9.808	9.573	9.085	922	-2.628	2.785	9.917	9.696	9.279
391	208	1.154	-2.546	2.795	9.819	9.551	909	1.095	-2.533	2.759	9.909	9.694	9.292
392	209	1.082	-2.601	2.817	981	9.536	9.049	1.011	-2.595	2.785	9.912	9.686	9.283
393	210	1.083	-2.563	2.783	9.822	9.527	9.048	989	-2.569	2.753	9.943	9.675	9.294
394	211	1.147	-263	2.869	9.808	9.522	9.024	1.039	-2.608	2.808	9.917	9.681	9.287
395	212	1.214	-2.454	2.738	9.815	9.552	9.089	1.114	-2.424	2.668	9.921	9.691	9.311

# 2017-08-30 14:30:24.872680													
# CT_x100													
# path: ../data/phantom3_MR_v2/ph3_CT_x100													
# thresholds:													
# lower (simple): -451.940037951,													
# lower (iter): -624.945436002													
# upper: 287.0													
# DC-average (simple): 0.915364967433 (bestRadius: 4.07142857143)													
# DC-average (iter): 0.994021385791 (bestRadius: 4.35714285714)													
# MR_x100													
# path: ../data/phantom3_MR_v2/ph3_MR_v2_x100													
# thresholds:													
# lower (simple): 263.1579347,													
# lower (iter): 101.050751445													
# lower (simple_CT-COM): 263.1579347													
# lower (iter_CT-COM): 101.050751445													
# upper: 1129.0													
# DC-average (simple): 0.78450336966 (bestRadius: 2.78571428571)													
# DC-average (iter): 0.879376043843 (bestRadius: 4.07142857143)													
# DC-average (CT-COM, simple): 0.662185740948 (bestRadius: 2.78571428571)													
# DC-average (CT-COM, iter): 0.755707740781 (bestRadius: 4.07142857143)													
# sliceNo dist warp_x warp_y warpMagnitude DC_CT DC_MR DC_MR_CT-COM warp_x* warp_y* warpMagnitude* DC_CT* DC_MR* DC_MR_CT-COM*													
0	-361	2.9415	4.286	2.9725	9.676	33	62	3.3112	8.531	3.4193	944	6.126	3.313
1	-360	2.94	4.294	2.9712	9.706	331	62	3.3129	8.427	3.4184	9.456	6.126	3.308
2	-359	2.9441	4.224	2.9742	9.725	391	77	3.2904	8.202	3.3911	9.475	6.121	3.346
3	-358	2.9425	421	2.9725	9.718	563	144	3.2298	7.547	3.3169	9.482	6.062	3.429
4	-357	2.9454	4.061	2.9733	9.738	738	181	3.1784	6.794	3.2502	9.501	6.019	3.501
5	-356	2.9174	4.073	2.9457	9.734	89	262	3.0881	6.226	3.1502	9.509	5.993	3.635
6	-355	2.9048	4.327	2.9369	9.715	1.102	363	3.0472	0.64	3.1136	9.504	6.099	3.709
7	-354	2.8884	4.574	2.9244	971	1.362	503	3.0186	6.966	3.0979	9.511	6.329	3.815
8	-353	2.8744	4.922	2.9162	9.693	1.556	583	2.9808	7.532	3.0745	9.494	6.525	3.915
9	-352	2.8713	5.264	2.9191	9.701	1.808	667	2.9561	8.046	3.0636	0.95	6.732	0.4
10	-351	2.8649	5.304	2.9136	9.706	1.747	641	2.9347	8.315	3.0502	9.499	6.785	4.035
11	-350	2.8607	5.452	2.9122	9.688	1.539	555	2.9057	8.734	3.0341	9.496	676	4.049
12	-349	2.8497	5.592	2.9041	9.685	1.344	481	2.8885	9.125	3.0292	9.503	6.744	4.039
13	-348	2.8516	5.698	2.9079	0.97	1.092	384	2.8631	9.338	3.0115	9.523	669	4.068
14	-347	2.827	5.403	2.8782	9.728	1.045	393	2.7961	873	2.9293	953	665	4.163
15	-346	2.8213	5.053	2.8662	9.738	1.032	408	2.7321	7.915	2.8444	9.552	6.584	4.251
16	-345	2.8047	4.603	2.8422	9.749	1.026	438	2.65	6.955	2.7397	9.559	6.516	4.387
17	-344	2.7794	4.147	2.8102	9.834	982	454	2.5632	5.969	2.6318	9.626	6.458	4.519
18	-343	2.8023	4.121	2.8324	9.885	961	417	2.5689	5.322	2.6234	973	6.252	4.437
19	-342	2.8092	398	2.8372	9.901	884	389	2.5595	479	2.6039	9.781	6.031	4.359
20	-341	2.7907	3.876	2.8175	9.867	832	375	2.5261	4.194	2.5607	9.806	5.822	4.315
21	-340	2.785	3.805	2.8109	9.886	845	39	2.4944	3.964	2.5257	9.805	5.741	4.311
22	-339	2.7572	4.276	2.7902	9.872	1.166	567	2.3953	488	2.4445	9.801	6.044	4.541
23	-338	2.7115	4.411	2.7471	9.889	1.487	79	2.295	5.727	2.3654	9.801	6.339	4.758

24	-337	2.6462	4.791	2.6892	9.866	1.907	1.068	2.211	6.456	2.3034	9.803	6.583	4.948
25	-336	2.6268	5.024	2.6744	9.906	2.194	1.268	2.1729	723	2.2901	9.808	6.732	503
26	-335	2.6293	528	2.6818	9.899	2.052	1.174	2.1548	7.793	2.2914	983	6.718	5.034
27	-334	2.6422	5.368	2.6962	9.897	194	1.075	2.133	8.386	2.2919	986	6.681	5.032
28	-333	2.6407	5.564	2.6987	9.899	1.818	99	2.1227	882	2.2987	9.885	6.645	5.022
29	-332	2.6456	5.246	2.6971	988	1.595	907	2.093	8.747	2.2684	9.899	6.632	508
30	-331	2.6238	5.065	2.6723	9.852	138	807	2.0679	8.349	2.2301	994	6.584	5.128
31	-330	2.6383	4.691	2.6797	9.838	1.163	692	2.0778	7.925	2.2238	9.936	6.546	5.148
32	-329	2.6564	4.592	2.6958	9.824	977	564	2.0716	758	2.206	9.951	6.518	5.189
33	-328	2.6501	4.462	2.6874	9.814	1.031	608	2.0639	7.205	2.186	9.951	6.604	526
34	-327	2.6155	4.363	2.6516	9.816	1.247	762	2.0301	658	2.1341	9.955	6.711	5.389
35	-326	2.5631	4.332	2.5995	9.824	1.576	1.045	2.0163	6.023	2.1043	9.938	6.817	548
36	-325	2.4825	4.155	2.5171	9.813	1.941	1.363	1.9893	5.535	2.0649	9.942	6.948	5.604
37	-324	2.3717	3.925	2.404	983	2.032	1.508	1.9335	4.755	1.9911	9.945	6.821	5.619
38	-323	2.2842	3.546	2.3116	9.814	2.088	1.616	1.8714	4.077	1.9152	9.944	6.707	5.642
39	-322	2.1881	3.376	2.214	9.828	2.113	1.698	1.8134	3.352	1.8441	9.958	6.598	5.644
40	-321	2.0612	3.174	2.0855	9.845	2.182	1.808	1.7496	2.844	1.7725	9.959	6.528	5.664
41	-320	1.9821	3.075	2.1958	9.833	2.469	205	1.7264	3.395	1.7595	9.964	6.627	5.731
42	-319	1.8916	3.236	1.9191	983	2.767	2.308	1.6886	4.056	1.7366	9.957	6.739	5.803
43	-318	1.8367	3.532	1.8704	9.807	3.048	2.544	1.6679	4.813	1.736	9.962	6.841	5.869
44	-317	1.7757	3.745	1.8148	9.816	3.324	2.757	1.6396	5.309	1.7234	9.953	6.918	5.926
45	-316	1.7164	3.875	1.7596	9.816	3.719	3.068	1.6357	5.499	1.7256	9.946	7.007	5.959
46	-315	1.6847	3.879	1.7288	9.841	3.971	3.277	1.638	5.487	1.7274	9.953	7.124	6.011
47	-314	1.6683	3.977	1.7151	9.844	4.329	3.515	1.6427	557	1.7345	9.946	7.193	6.033
48	-313	1.6266	4.123	1.6781	9.835	454	3.677	1.6308	5.698	1.7275	9.954	7.289	0.61
49	-312	1.6165	4.223	1.6707	9.832	4.593	3.726	1.6157	561	1.7103	9.949	7.355	6.172
50	-311	1.5863	4.173	1.6403	9.832	4.675	3.806	1.5969	5.584	1.6917	9.953	7.408	6.225
51	-310	1.5529	4.171	1.608	9.835	4.704	3.875	1.5781	5.573	1.6736	9.952	7.504	6.313
52	-309	1.5269	4.209	1.5839	9.827	4.711	3.889	1.5659	5.617	1.6636	9.961	7.554	6.352
53	-308	1.4738	425	1.5339	9.835	4.699	3.968	1.5377	584	1.6449	9.957	7.602	6.405
54	-307	1.4266	4.457	1.4946	9.832	4.702	401	1.5197	6.107	1.6379	9.959	767	6.443
55	-306	1.372	4.542	1.4452	9.834	4.638	4.023	1.4936	6.336	1.6224	994	7.709	6.469
56	-305	1.3501	4.417	1.4205	9.846	4.664	4.071	1.4768	6.034	1.5953	9.962	7.798	656
57	-304	1.2945	4.199	1.3609	9.845	473	4.173	1.4244	5.589	1.5301	9.969	7.895	6.707
58	-303	1.2498	4.136	1.3164	9.848	4.767	4.267	1.3888	5.209	1.4832	9.966	7.999	6.832
59	-302	1.197	4.095	1.2651	9.839	4.822	4.366	1.3325	4.808	1.4165	996	8.098	6.986
60	-301	1.1835	4.107	1.2527	9.843	4.821	4.386	1.3121	4.793	1.3969	9.957	8.117	7.021
61	-300	1.1693	3.969	1.2348	9.836	4.837	4.414	1.2952	478	1.3806	9.949	8.149	7.054
62	-299	1.1391	3.951	1.2057	9.841	4.842	4.446	1.2741	4.677	1.3572	9.952	8.146	7.097
63	-298	1.125	4.081	1.1967	9.827	4.855	4.487	1.2583	4.709	1.3435	9.953	8.157	7.126
64	-297	1.1321	3.827	1.1951	9.837	4.831	4.472	1.2667	4.186	1.3341	9.959	817	7.146
65	-296	1.1072	3.612	1.1647	9.843	4.802	448	1.2532	3.695	1.3066	9.968	8.188	7.187
66	-295	1.0964	3.448	1.1494	9.827	479	4.468	1.2476	3.227	1.2887	9.957	8.217	7.219
67	-294	1.0824	3.268	1.1306	9.834	4.783	4.497	1.2288	2.766	1.2596	9.946	8.218	7.256
68	-293	1.0519	3.104	1.0967	9.837	4.851	459	1.1871	2.434	1.2118	9.963	823	0.73
69	-292	1.0165	2.933	1.058	9.835	4.928	4.683	1.1376	209	1.1567	9.968	8.234	7.352
70	-291	9.843	2.802	1.0234	9.833	4.985	4.764	1.0928	1.688	1.1057	9.952	8.269	741

71	-290	9.706	2.786	1.1998	9.842	5.082	4.842	1.0683	1.621	1.0805	9.948	829	7.437
72	-289	9.868	2.854	1.0273	9.825	5.143	4.871	1.0941	1.688	1.1071	996	8.268	7.386
73	-288	9.982	2.784	1.0363	983	5.207	0.49	1.116	1.731	1.1293	9.957	8.246	7.356
74	-287	1.0278	293	1.0687	9.829	5.265	4.921	1.1458	1.889	1.1612	9.948	8.224	7.301
75	-286	1.0248	3.007	1.068	9.839	5.289	4.944	1.1473	1.789	1.1612	9.964	8.214	7.284
76	-285	9.926	2.759	1.0303	9.851	5.291	4.954	1.1143	1.589	1.1256	9.946	8.227	7.312
77	-284	9.638	2.698	1.2008	9.847	5.295	5.017	1.0792	1.478	1.0893	994	8.245	7.329
78	-283	9.156	2.735	9.556	9.834	5.303	5.079	1.0398	1.432	1.0496	9.956	8.218	7.337
79	-282	8.931	2.834	937	9.836	5.356	5.156	1.1966	156	1.0187	9.947	8.251	7.391
80	-281	0.9	2.873	9.448	9.826	5.445	5.195	1.0168	1.648	1.0301	9.951	827	7.383
81	-280	9.028	3.034	9.525	9.825	556	5.262	1.0107	1.841	1.0274	9.948	8.305	7.423
82	-279	9.157	302	9.642	9.823	5.634	5.296	1.0216	1.898	1.0391	9.957	8.336	7.425
83	-278	8.829	3.352	9.444	9.836	5.649	5.336	9.731	245	1.1935	9.956	8.311	7.428
84	-277	862	3.502	9.304	9.837	5.679	5.385	9.354	2.955	9.809	9.953	8.259	7.404
85	-276	8.266	3.773	9.086	9.829	5.699	5.427	8.942	3.485	9.597	9.955	8.219	7.379
86	-275	8.021	3.986	8.957	9.838	5.735	5.488	8.482	4.046	9.398	9.959	8.178	7.376
87	-274	7.919	4.221	8.974	9.843	5.704	5.496	8.466	4.343	9.515	9.951	8.185	737
88	-273	7.661	413	8.703	9.836	5.677	5.508	8.334	4.462	9.453	9.962	8.196	7.385
89	-272	7.508	4.348	8.676	9.827	5.674	5.529	8.276	4.808	9.572	9.962	8.221	7.394
90	-271	7.239	443	8.487	9.835	5.646	5.553	812	5.001	9.537	9.961	8.222	7.403
91	-270	7.432	438	8.627	9.827	5.685	5.557	8.237	5.015	9.644	9.948	8.243	7.419
92	-269	7.398	4.614	8.719	9.822	5.721	5.587	8.334	5.118	9.779	9.952	8.271	7.431
93	-268	7.569	4.562	8.838	9.826	5.735	5.566	8.411	5.135	9.854	9.957	8.292	7.445
94	-267	7.498	4.415	8.701	9.829	5.725	5.583	8.356	5.061	9.769	996	8.302	746
95	-266	7.366	4.273	8.515	984	5.691	5.576	8.085	4.819	9.412	9.956	8.325	7.495
96	-265	7.129	4.179	8.263	9.844	5.637	555	7.884	4.648	9.152	9.954	833	7.518
97	-264	6.841	3.972	7.911	9.831	5.602	5.579	7.502	4.498	8.747	9.953	8.364	7.566
98	-263	6.609	4.062	7.758	9.835	5.579	5.564	7.223	4.567	8.545	9.949	8.427	763
99	-262	6.439	4.183	7.679	9.837	5.657	565	6.958	4.695	8.394	9.953	8.478	7.699
100	-261	6.412	4.169	7.648	9.831	5.704	5.701	6.826	4.826	836	9.951	8.539	7.749
101	-260	6.401	4.322	7.724	9.832	5.771	5.771	6.662	4.899	8.269	9.957	8.605	7.811
102	-259	6.307	4.457	7.723	9.831	5.785	5.803	6.649	4.982	8.309	9.952	8.641	7.841
103	-258	6.288	4.362	7.653	9.831	584	5.847	6.733	4.846	8.296	9.951	8.673	786
104	-257	6.438	4.373	7.783	9.824	586	5.859	6.831	484	8.372	9.951	8.697	7.883
105	-256	6.402	4.363	7.748	9.826	5.923	5.914	6.945	476	842	9.961	8.713	7.903
106	-255	6.359	4.209	7.625	983	5.979	597	6.836	0.47	8.295	995	875	7.948
107	-254	6.331	4.346	768	9.835	6.041	6.037	6.718	4.814	8.265	995	8.784	7.974
108	-253	6.265	4.299	7.599	9.822	6.111	6.107	6.585	4.791	8.143	9.944	8.786	7.997
109	-252	6.133	4.397	7.546	9.838	6.165	6.158	636	4.846	7.996	9.954	8.823	803
110	-251	6.081	4.395	7.503	9.834	622	6.223	6.241	4.829	7.891	9.952	885	8.066
111	-250	5.837	4.528	7.387	9.847	6.265	626	6.054	4.898	7.787	9.947	8.871	8.089
112	-249	5.706	4.395	7.202	9.842	6.302	6.294	0.59	4.779	7.593	9.945	8.894	813
113	-248	5.616	4.266	7.052	9.833	6.364	6.352	5.761	4.635	7.394	9.954	8.928	8.164
114	-247	5.365	4.059	6.728	9.835	6.379	6.368	5.551	4.301	7.022	9.958	8.971	8.224
115	-246	5.354	3.691	6.503	9.831	639	6.397	5.443	3.807	6.642	9.944	8.998	8.268
116	-245	5.151	3.496	6.225	9.837	6.426	6.433	5.225	3.454	6.264	9.954	9.055	833
117	-244	4.973	3.473	6.065	9.839	6.489	6.499	5.032	3.285	601	9.957	9.071	836

118	-243	4.882	3.503	6.008	9.828	6.553	6.553	4.863	3.342	0.59	9.945	908	8.377
119	-242	4.806	357	5.987	9.842	662	662	4.785	3.416	5.879	9.949	9.089	838
120	-241	4.813	3.542	5.976	9.828	6.681	6.679	4.745	3.378	5.825	995	9.092	8.385
121	-240	477	348	5.905	9.827	6.741	6.739	4.634	3.359	5.724	995	9.102	8.407
122	-239	4.736	3.588	5.942	9.842	6.784	6.784	463	3.527	5.821	995	9.121	8.439
123	-238	4.748	3.592	5.954	9.832	6.831	6.838	463	3.581	5.853	9.945	9.119	8.454
124	-237	4.683	3.523	586	9.826	6.885	6.894	4.578	3.562	5.801	9.953	9.119	8.484
125	-236	4.797	3.544	5.964	9.831	691	6.921	462	3.588	5.849	9.954	9.145	8.502
126	-235	4.595	3.539	0.58	9.826	6.916	6.925	4.509	3.653	5.803	9.957	9.188	8.523
127	-234	4.536	361	5.797	9.842	6.899	6.898	4.438	3.732	5.799	9.961	9.221	8.553
128	-233	4.538	3.731	5.875	984	6.911	6.916	4.346	3.785	5.763	9.961	9.267	8.585
129	-232	4.412	3.814	5.832	9.824	6.857	6.873	4.375	0.39	5.861	9.959	9.266	8.552
130	-231	438	3.895	5.861	9.812	6.806	6.834	4.305	404	5.904	9.968	9.235	853
131	-230	4.536	4.012	6.055	9.839	678	6.789	4.488	4.189	6.139	9.963	9.197	8.492
132	-229	4.555	4.065	6.105	983	6.734	6.739	4.517	4.171	6.149	9.956	9.167	8.466
133	-228	436	3.833	5.806	9.838	6.753	6.751	4.255	3.762	5.679	9.959	918	8.513
134	-227	4.224	3.354	5.393	9.837	6.786	6.775	3.926	3.306	5.132	9.947	917	8.535
135	-226	4.092	3.111	514	9.835	6.814	6.809	3.661	3.011	474	9.958	9.179	8.558
136	-225	3.822	3.056	4.894	984	6.874	6.865	3.353	2.778	4.354	9.965	9.163	8.562
137	-224	3.761	3.067	4.854	9.846	6.934	6.928	3.323	2.704	4.284	9.946	9.176	8.576
138	-223	3.801	2.885	4.772	984	7.033	7.038	3.294	2.525	415	9.963	9.216	8.606
139	-222	3.673	2.884	467	9.851	7.114	7.111	329	2.539	4.156	9.946	9.239	8.619
140	-221	3.746	2.935	4.759	9.843	7.176	7.174	3.355	2.555	4.217	9.948	9.251	863
141	-220	3.774	284	4.723	9.833	7.204	7.198	3.552	2.581	4.391	9.954	9.275	8.651
142	-219	3.792	2.918	4.785	9.832	7.268	7.272	3.711	2.668	457	9.952	9.297	8.667
143	-218	3.794	2.884	4.766	9.839	7.302	7.298	3.835	2.694	4.687	9.963	932	8.679
144	-217	3.668	2.882	4.665	9.842	0.74	7.396	3.851	2.685	4.695	9.955	9.359	8.717
145	-216	3.689	2.755	4.605	9.841	755	7.554	3.854	259	4.643	9.954	9.394	8.752
146	-215	3.756	2.598	4.566	9.832	7.708	7.706	3.874	2.455	4.587	9.955	9.449	8.802
147	-214	3.632	2.427	4.368	9.828	7.832	7.843	3.789	2.311	4.439	9.957	9.485	8.839
148	-213	3.526	2.468	4.304	9.843	7.834	7.834	3.504	2.333	421	9.952	9.513	8.874
149	-212	3.544	248	4.325	9.838	7.799	7.797	3.281	2.354	4.038	9.949	9.516	8.891
150	-211	361	2.393	4.331	9.831	774	7.744	315	2.203	3.844	9.961	9.522	8.922
151	-210	3.712	2.309	4.371	9.832	7.707	7.713	3.066	2.068	3.698	9.963	9.514	8.917
152	-209	3.639	2.101	4.202	9.821	7.689	7.696	3.089	1.795	3.573	996	9.507	8.911
153	-208	3.644	2.004	4.158	9.834	7.692	7.685	318	1.581	3.551	9.961	9.503	8.911
154	-207	356	1.935	4.052	9.836	7.674	7.667	3.158	1.411	3.459	9.945	9.486	8.903
155	-206	3.497	1.849	3.956	9.846	7.662	7.647	3.216	1.259	3.453	995	9.477	8.888
156	-205	332	168	3.721	9.845	7.668	7.661	2.921	1.187	3.153	9.945	9.453	8.877
157	-204	3.136	1.539	3.493	9.823	7.697	7.683	2.625	1.014	2.814	9.953	9.444	8.888
158	-203	3.097	1.384	3.392	9.846	7.719	7.708	247	854	2.614	9.949	9.421	8.871
159	-202	2.999	1.317	3.276	984	7.744	7.746	2.343	821	2.483	9.945	9.407	8.869
160	-201	3.174	1.254	3.413	9.843	7.793	7.791	2.546	789	2.665	9.946	9.416	8.875
161	-200	3.226	1.177	3.434	9.828	785	7.837	2.646	782	2.759	9.957	9.429	888
162	-199	3.247	1.209	3.465	9.853	7.898	7.888	2.703	821	2.824	9.951	9.439	8.887
163	-198	3.105	1.093	3.291	9.828	7.958	7.952	2.663	798	278	995	9.453	8.896
164	-197	3.222	1.202	3.439	9.829	7.993	7.984	2.774	0.09	2.916	9.962	9.456	8.895

165	-196	3.047	1.056	3.225	983	8.036	8.034	2.734	835	2.858	9.966	9.469	8.908
166	-195	3.031	125	3.279	983	8.082	8.065	2.821	987	2.989	9.954	9.457	8.896
167	-194	2.872	1.206	3.115	9.829	8.135	812	2.723	974	2.892	9.957	9.473	8.917
168	-193	284	1.192	308	9.845	8.178	8.166	2.575	936	274	9.951	949	8.956
169	-192	2.742	1.024	2.927	984	8.264	8.262	2.397	821	2.534	9.953	0.95	899
170	-191	2.586	943	2.752	9.829	8.344	8.334	2.246	666	2.343	995	9.527	9.028
171	-190	2.649	813	2.771	9.836	8.344	833	2.285	561	2.353	9.967	9.523	9.022
172	-189	2.647	613	2.717	9.838	8.304	8.319	232	407	2.355	9.953	9.514	8.999
173	-188	281	62	2.878	9.851	8.271	8.285	2.384	307	2.404	9.963	9.515	8.986
174	-187	2.985	534	3.033	9.849	8.247	8.253	2.493	237	2.504	9.963	9.504	8.982
175	-186	2.856	624	2.924	984	8.241	8.252	2.203	201	2.212	9.968	9.483	8.966
176	-185	2.677	579	2.739	9.828	8.208	8.218	2.023	202	2.033	9.956	9.467	8.954
177	-184	2.621	469	2.663	9.826	8.199	8.197	1.828	66	183	9.961	9.443	8.937
178	-183	2.523	476	2.567	984	8.185	8.173	1.678	85	168	9.963	9.432	8.928
179	-182	2.511	476	2.556	9.847	8.301	8.303	1.941	64	1.942	9.956	9.461	8.963
180	-181	2.584	42	2.618	9.843	8.418	8.413	2.167	-19	2.167	9.951	949	8.997
181	-180	2.463	499	2.514	9.847	8.548	8.555	2.332	16	2.332	996	9.508	9.019
182	-179	2.293	432	2.334	9.844	8.637	8.648	2.389	-124	2.392	9.964	9.512	9.061
183	-178	2.217	426	2.257	9.842	8.699	8.706	2.151	-188	2.159	9.958	953	9.083
184	-177	2.032	406	2.072	9.839	8.768	8.784	1.928	-271	1.947	9.963	9.555	9.111
185	-176	1.925	403	1.967	9.845	8.812	8.846	176	-324	179	9.957	9.567	9.142
186	-175	1.713	413	1.762	9.831	8.845	8.882	1.562	-335	1.598	9.969	957	9.144
187	-174	1.492	297	1.521	983	8.834	8.853	1.225	-447	1.304	9.969	9.533	9.121
188	-173	1.468	216	1.484	9.833	8.782	8.803	995	-486	1.107	9.967	9.499	9.087
189	-172	1.334	-2	1.334	9.839	875	8.757	743	-617	966	995	9.461	9.055
190	-171	1.326	-55	1.327	9.847	8.749	8.755	694	-726	1.004	9.952	9.444	9.026
191	-170	1.386	-234	1.406	9.851	8.748	8.737	876	-95	1.292	9.948	9.422	8.988
192	-169	0.14	-256	1.423	9.849	8.763	8.745	1.004	-1.052	1.454	994	9.405	8.957
193	-168	1.419	-408	1.477	9.852	875	8.734	1.308	-1.201	1.776	9.949	9.325	0.89
194	-167	1.323	-532	1.426	9.853	8.788	8.758	1.323	-1.265	183	9.952	9.323	0.89
195	-166	1.341	-313	1.378	9.844	8.836	8.817	1.347	-1.194	0.18	9.959	9.344	8.899
196	-165	1.217	-382	1.276	9.844	8.854	8.826	1.377	-1.261	1.867	9.951	9.345	8.901
197	-164	1.096	-407	1.169	9.838	8.867	8.866	1.334	-1.353	0.19	9.948	9.355	8.907
198	-163	1.096	-0.06	1.249	9.826	8.893	8.896	116	-1.424	1.836	9.951	9.384	894
199	-162	1.029	-599	1.191	9.837	8.902	8.913	907	-1.522	1.772	9.954	9.387	8.947
200	-161	869	-58	1.045	984	8.921	8.939	64	-1.573	1.698	9.954	9.392	897
201	-160	763	-626	987	9.839	8.965	8.968	422	-1.562	1.617	9.951	9.391	8.975
202	-159	664	-831	1.063	9.839	8.968	8.958	439	-1.805	1.858	9.954	9.404	8.994
203	-158	702	-84	1.095	9.845	8.987	8.976	554	-1.932	201	9.952	9.414	9.007
204	-157	859	-1.014	1.329	9.832	9.008	899	743	-2.137	2.263	9.958	9.419	9.007
205	-156	853	-1.039	1.344	9.843	9.028	9.012	846	-225	2.403	9.963	942	0.9
206	-155	679	-1.085	128	9.835	9.041	9.006	724	-2.245	2.359	9.957	9.388	897
207	-154	717	-1.083	1.298	9.849	9.054	901	735	-2.183	2.304	9.947	9.374	8.963
208	-153	762	-741	1.063	9.835	9.048	9.038	749	-2.021	2.156	9.953	9.345	894
209	-152	717	-876	1.132	9.828	9.048	9.039	733	-2.008	2.138	9.963	9.347	8.947
210	-151	682	-1.036	1.241	9.845	9.072	905	652	-2.095	2.194	9.951	9.371	8.969
211	-150	789	-966	1.247	9.848	9.062	9.068	696	-2.006	2.123	996	938	8.983

212	-149	927	-803	1.226	9.835	9.082	908	773	-1.895	2.046	9.968	0.94	8.994
213	-148	1.099	-89	1.414	9.849	9.083	9.086	904	-1.925	2.127	996	0.94	8.998
214	-147	1.015	-958	1.396	9.843	9.095	9.097	938	-2.015	2.222	9.957	9.388	898
215	-146	1.115	-1.118	1.579	9.841	9.109	9.088	1.165	-2.134	2.431	9.958	9.382	897
216	-145	1.094	-1.109	1.558	9.831	9.117	9.106	1.268	-2.216	2.554	9.968	9.357	8.951
217	-144	848	-986	1.301	9.834	913	9.136	1.058	-2.171	2.415	996	9.364	8.962
218	-143	79	-1.007	128	9.829	9.177	9.144	859	-2.185	2.348	9.959	938	8.973
219	-142	63	-1.067	1.239	9.839	9.213	916	723	-2.192	2.308	996	9.387	8.981
220	-141	477	-1.039	1.143	9.841	9.239	9.183	532	-2.179	2.243	9.956	9.403	8.995
221	-140	43	-1.034	112	9.833	9.238	9.193	485	-2.244	2.296	9.962	9.407	8.989
222	-139	299	-975	102	9.833	9.214	9.177	453	-2.263	2.308	9.953	9.394	8.983
223	-138	207	-879	904	9.832	9.201	9.159	406	-2.314	2.349	995	9.377	8.969
224	-137	105	-931	937	9.833	9.177	9.141	315	-2.383	2.404	9.969	936	8.961
225	-136	43	-1.063	1.064	9.836	9.205	9.153	245	-2.502	2.514	9.957	9.355	8.947
226	-135	-63	-1.096	1.098	9.832	9.229	9.142	244	-2.666	2.678	9.961	9.347	8.934
227	-134	-32	-1.418	1.418	983	9.272	9.131	236	-2.909	2.919	9.957	9.351	8.912
228	-133	17	-1.585	1.586	9.836	9.308	9.104	356	-3.134	3.154	9.957	9.341	8.885
229	-132	11	-1.899	1.902	9.835	933	9.068	29	-354	3.551	995	9.362	8.865
230	-131	68	-2.297	2.298	9.838	9.324	8.977	76	-3.938	3.938	9.943	9.376	8.846
231	-130	21	-2.505	2.505	9.845	9.317	8.912	-68	-4.178	4.179	9.951	0.94	8.846
232	-129	85	-2.623	2.625	9.834	9.338	8.913	-87	-428	4.281	9.951	9.409	8.842
233	-128	-185	-2.807	2.813	9.831	9.359	8.839	-197	-4.351	4.355	9.962	9.403	8.839
234	-127	-139	-2.788	2.792	9.844	9.384	8.875	-213	-4.319	4.325	9.963	9.384	885
235	-126	-273	-2.885	2.898	9.838	9.387	8.848	-232	-4.346	4.352	9.967	9.382	8.856
236	-125	-171	-2.868	2.873	9.853	9.391	8.876	-128	-4.285	4.287	9.957	9.378	8.854
237	-124	-315	-2.802	282	9.844	9.397	8.868	-98	-0.43	4.301	9.956	9.389	8.848
238	-123	-299	-2.656	2.673	9.838	9.394	891	6	-429	429	9.957	9.373	8.833
239	-122	-476	-2.489	2.534	9.833	9.382	8.929	-69	-4.219	4.219	9.963	9.359	8.824
240	-121	-38	-2.381	2.411	9.839	9.374	8.948	3	-4.188	4.188	9.971	9.335	8.816
241	-120	-187	-2.435	2.442	985	9.371	8.956	137	-4.258	426	9.955	9.323	8.796
242	-119	-117	-2.586	2.588	9.843	936	8.928	208	-4.319	4.324	9.957	9.303	8.776
243	-118	-194	-2.531	2.539	9.838	9.366	8.929	195	-4.308	4.313	9.957	9.294	877
244	-117	-386	-2.586	2.615	9.846	9.365	8.908	-7	-4.271	4.271	9.948	9.304	8.793
245	-116	-658	-2.677	2.757	9.839	9.361	8.858	-253	-4.305	4.312	9.965	932	8.796
246	-115	-881	-2.624	2.768	9.838	9.389	8.862	-41	-4.273	4.293	9.963	9.336	8.799
247	-114	-1.041	-2.702	2.896	9.832	9.385	8.817	-668	-4.291	4.343	9.957	9.317	881
248	-113	-1.097	-2.886	3.087	9.844	9.388	8.783	-636	-4.518	4.563	9.969	9.308	8.776
249	-112	-1.146	-2.993	3.205	9.834	9.384	8.758	-74	-4.663	4.721	9.968	9.295	8.742
250	-111	-1.235	-3.007	3.251	9.837	9.386	8.747	-89	-4.709	4.792	9.948	9.304	8.741
251	-110	-1.233	-2.923	3.173	9.837	9.369	8.752	-887	-4.748	483	9.966	9.292	8.731
252	-109	-1.184	-2.944	3.174	9.838	9.362	8.752	-962	-477	4.866	9.963	932	875
253	-108	-1.025	-2.861	3.039	9.853	9.362	8.776	-952	-4.732	4.827	9.965	9.345	8.778
254	-107	-871	-2.708	2.844	9.854	9.334	881	-912	-4.636	4.725	9.963	9.368	8.817
255	-106	-807	-2.773	2.888	9.837	9.326	8.806	-911	-461	4.699	9.957	9.372	8.821
256	-105	-785	-2.653	2.766	9.844	9.355	885	-804	-4.363	4.436	9.958	9.381	8.849
257	-104	-71	-2.469	257	9.847	9.359	8.884	-719	-4.165	4.227	9.961	9.377	8.853
258	-103	-475	-2.503	2.548	9.839	936	8.907	-563	-4.026	4.065	9.961	9.368	8.865

259	-102	-652	-2.265	2.357	9.831	9.363	8.946	-613	-3.832	3.881	9.955	9.375	8.881
260	-101	-675	-2.234	2.334	9.843	9.379	8.946	-696	-3.728	3.792	9.966	9.399	8.908
261	-100	-722	-2.294	2.405	9.852	9.396	8.947	-818	-367	376	9.962	9.402	8.916
262	-99	-704	-2.152	2.265	9.848	9.394	8.977	-886	-3.476	3.587	9.964	9.408	8.933
263	-98	-71	-2.066	2.185	9.842	9.389	8.985	-818	-3.466	3.562	9.962	9.398	8.928
264	-97	-729	-2.093	2.216	9.837	9.394	8.992	-664	-3.562	3.623	9.951	939	8.926
265	-96	-755	-2.159	2.287	9.834	941	8.983	-59	-3.602	365	9.949	9.374	8.912
266	-95	-58	-2.225	2.299	9.843	0.94	8.989	-315	-3.708	3.721	996	9.352	8.887
267	-94	-537	-239	2.449	9.845	9.374	8.948	-228	-3.871	3.878	9.955	9.346	8.873
268	-93	-605	-258	265	9.837	9.375	8.909	-224	-4.003	4.009	9.962	9.326	8.852
269	-92	-579	-2.658	272	9.851	9.372	889	-16	-4.108	4.111	9.953	9.302	8.827
270	-91	-55	-2.657	2.713	9.826	9.375	8.889	-123	-4.101	4.103	9.957	9.289	8.821
271	-90	-58	-2.641	2.704	9.842	9.383	8.896	-178	-4.102	4.106	9.964	9.302	8.835
272	-89	-677	-2.673	2.757	9.832	9.389	8.895	-261	-4.155	4.163	9.964	9.314	8.835
273	-88	-657	-2.619	0.27	9.832	9.393	8.908	-362	-4.125	4.141	9.955	9.325	8.844
274	-87	-696	-2.571	2.663	9.847	9.398	8.912	-389	-4.198	4.216	9.947	9.349	8.849
275	-86	-84	-271	2.837	9.823	9.364	8.867	-533	-4.168	4.202	9.935	9.355	8.874
276	-85	-91	-2.592	2.747	9.839	9.364	8.872	-786	-4.057	4.133	9.946	9.312	8.851
277	-84	-1.067	-2.602	2.813	984	9.349	886	-1.117	-4.051	4.202	9.947	9.267	8.819
278	-83	-1.219	-2.484	2.767	983	9.346	8.849	-1.336	-3.975	4.194	995	9.252	8.788
279	-82	-1.076	-2.571	2.787	9.843	9.309	8.829	-1.297	-4.013	4.217	9.953	9.217	8.755
280	-81	-1.185	-2.563	2.824	9.837	9.284	882	-1.363	-4.001	4.226	996	9.188	8.746
281	-80	-1.187	-2.558	282	9.832	9.254	0.88	-1.395	-3.974	4.212	9.958	916	8.727
282	-79	-1.226	-2.606	288	9.831	9.228	8.765	-1.362	-4.026	425	9.962	914	8.707
283	-78	-1.146	-2.429	2.686	9.834	921	8.775	-1.224	-4.062	4.242	9.963	9.138	8.707
284	-77	-1.082	-2.467	2.694	984	9.192	8.745	-1.112	-4.129	4.276	9.959	913	8.695
285	-76	-1.135	-2.302	2.567	9.835	9.165	8.744	-1.043	-4.122	4.251	9.956	9.123	8.699
286	-75	-1.168	-2.433	2.699	9.842	9.161	8.709	-1.127	-4.183	4.333	9.957	9.125	8.698
287	-74	-1.244	-2.314	2.627	9.844	918	8.752	-1.271	-4.051	4.246	9.961	9.126	8.709
288	-73	-1.366	-2.347	2.715	9.849	9.147	8.741	-1.469	-3.995	4.257	9.955	9.155	8.725
289	-72	-1.632	-2.342	2.855	986	9.131	8.715	-1.762	-3.962	4.336	9.957	9.146	8.727
290	-71	-1.639	-221	2.752	9.854	9.151	8.749	-1.783	-3.726	413	9.955	9.142	8.743
291	-70	-1.432	-2.042	2.494	9.861	9.156	8.799	-1.656	-0.35	3.872	9.956	9.151	8.767
292	-69	-1.187	-1.871	2.216	9.848	9.206	8.873	-1.598	-3.305	3.671	9.963	9.151	8.777
293	-68	-1.223	-161	2.022	9.839	9.249	8.943	-1.655	-303	3.453	9.962	9.143	8.785
294	-67	-116	-1.531	1.921	985	9.245	8.944	-1.512	-2.956	332	9.951	915	8.804
295	-66	-959	-1.741	1.988	9.846	9.243	8.918	-1.294	-2.988	3.256	9.953	9.154	8.817
296	-65	-868	-1.605	1.824	9.845	9.266	8.967	-1.136	-2.927	3.139	9.963	9.172	8.835
297	-64	-82	-1.568	1.769	985	927	8.983	-1.025	-2.876	3.053	9.959	9.177	8.842
298	-63	-701	-1.714	1.852	9.843	9.252	8.945	-892	-2.946	3.078	996	9.197	885
299	-62	-719	-1.797	1.936	9.852	9.253	8.925	-88	-3.015	3.141	9.963	9.222	8.882
300	-61	-728	-174	1.886	9.858	9.257	8.942	-818	-3.008	3.117	9.956	9.254	8.911
301	-60	-832	-1.821	2.002	9.852	9.225	8.906	-933	-3.077	3.215	9.957	9.262	8.908
302	-59	-1.036	-1.956	2.213	9.856	9.215	8.873	-1.144	-3.181	338	9.951	9.255	8.894
303	-58	-1.057	-202	228	9.857	9.195	885	-1.256	-3.247	3.482	9.963	9.232	8.866
304	-57	-95	-2.122	2.325	9.849	9.179	8.823	-135	-3.333	3.596	9.963	9.218	8.855
305	-56	-1.128	-2.107	2.389	9.839	9.174	882	-1.459	-3.424	3.722	9.954	9.225	8.849

306	-55	-1.239	-2.344	2.651	9.843	9.175	8.776	-1.555	-3.611	3.932	9.956	9.243	8.846
307	-54	-1.343	-2.094	2.488	9.853	9.176	8.823	-1.698	-3.498	3.889	9.953	9.258	8.864
308	-53	-1.436	-1.949	2.421	9.833	9.188	885	-1.772	-3.423	3.854	9.971	9.267	8.887
309	-52	-1.427	-2.012	2.467	985	9.187	8.823	-1.854	-341	3.882	9.953	9.251	8.873
310	-51	-1.453	-1.812	2.322	9.848	9.174	8.859	-1.843	-3.238	3.725	9.957	922	8.867
311	-50	-1.563	-1.766	2.358	9.853	9.165	8.861	-1.931	-315	3.694	9.957	9.183	885
312	-49	-1.542	-178	2.355	9.842	9.139	8.826	-1.948	-308	3.645	9.954	9.159	8.841
313	-48	-1.428	-1.722	2.237	984	9.144	8.847	-1.963	-3.035	3.614	9.955	914	8.833
314	-47	-1.422	-1.831	2.319	9.849	9.172	8.866	-2.079	-2.973	3.628	9.949	9.122	8.821
315	-46	-1.257	-1.725	2.134	9.829	9.187	8.887	-2.196	-2.855	3.602	9.952	9.104	8.802
316	-45	-1.092	-1.868	2.164	9.836	9.206	8.891	-2.291	-2.869	3.672	9.951	9.066	877
317	-44	-121	-1.848	2.209	9.836	9.209	8.889	-2.166	-2.846	3.576	9.953	9.109	8.819
318	-43	-1.328	-0.15	2.003	9.829	9.202	894	-2.114	-2.652	3.391	9.961	9.137	8.858
319	-42	-1.434	-137	1.983	9.831	9.198	8.965	-2.093	-2.551	0.33	9.956	9.173	8.882
320	-41	-1.501	-1.313	1.994	984	0.92	8.961	-2.141	-2.549	3.329	995	9.201	8.904
321	-40	-1.576	-116	1.957	983	9.199	8.982	-2.257	-2.428	3.315	9.949	9.228	8.937
322	-39	-1.724	-111	2.051	9.828	9.177	8.984	-2.398	-2.404	3.396	9.957	9.221	8.945
323	-38	-1.776	-989	2.033	9.843	9.158	8.994	-2.461	-2.258	334	9.951	9.212	8.961
324	-37	-1.812	-947	2.045	9.843	917	9.006	-2.419	-2.229	329	9.951	921	8.977
325	-36	-1.814	-982	2.063	9.841	9.184	9.008	-2.414	-0.22	3.266	9.949	9.201	8.976
326	-35	-1.647	-93	1.891	985	9.183	9.022	-2.321	-2.051	3.097	9.941	9.188	8.972
327	-34	-1.481	-926	1.747	9.845	9.167	9.018	-2.194	-197	2.949	9.947	9.162	8.946
328	-33	-1.399	-772	1.598	9.836	9.163	9.051	-2.145	-1.869	2.845	9.957	9.151	8.948
329	-32	-1.408	-724	1.583	9.835	9.165	9.053	-2.023	-1.841	2.735	9.953	9.146	8.958
330	-31	-1.447	-744	1.627	9.833	9.171	9.066	-1.945	-188	2.705	9.956	9.136	8.957
331	-30	-1.345	-681	1.508	9.829	916	9.056	-1.786	-1.891	2.601	9.953	9.145	8.969
332	-29	-1.382	-579	1.499	9.833	9.181	9.082	-1.765	-1.834	2.545	9.955	9.171	8.982
333	-28	-1.308	-697	1.482	9.829	9.177	9.073	-1.721	-1.889	2.556	9.962	9.201	899
334	-27	-1.337	-526	1.437	9.815	9.174	9.093	-1.739	-1.799	2.502	9.966	9.217	0.9
335	-26	-1.414	-556	1.519	9.833	9.184	9.093	-1.737	-1.833	2.526	9.964	924	9.015
336	-25	-1.398	-428	1.462	9.837	9.193	9.116	-1.815	-1.659	2.459	9.961	9.229	9.007
337	-24	-1.338	-241	1.359	9.836	9.209	9.168	-188	-1.514	2.414	9.958	9.214	9.005
338	-23	-121	-22	1.229	9.844	9.216	9.169	-1.931	-1.437	2.407	9.954	918	8.981
339	-22	-1.307	-131	1.313	9.845	9.216	9.196	-2.146	-1.338	2.528	9.954	9.138	8.957
340	-21	-1.173	-126	118	9.837	9.233	9.204	-1.856	-1.301	2.266	9.959	9.183	8.999
341	-20	-1.013	-133	1.022	9.833	9.227	9.203	-1.563	-126	2.007	9.959	9.199	9.022
342	-19	-897	-23	898	9.833	9.231	9.231	-1.318	-1.214	1.791	9.959	9.215	9.049
343	-18	-835	-86	839	9.832	9.239	9.233	-1.169	-1.247	1.709	9.962	9.247	9.075
344	-17	-953	-193	972	983	9.244	9.217	-131	-1.282	1.833	9.964	9.264	9.089
345	-16	-966	-271	1.004	9.827	9.262	9.211	-1.403	-1.293	1.908	9.966	9.287	9.105
346	-15	-1.044	-355	1.102	9.834	9.259	9.192	-1.579	-1.301	2.046	9.964	9.303	9.107
347	-14	-1.145	-423	122	9.841	9.244	9.169	-1.764	-128	218	9.947	9.327	9.121
348	-13	-1.417	-422	1.478	9.846	9.238	9.155	-2.033	-1.275	0.24	9.946	9.334	9.166
349	-12	-1.602	-421	1.657	9.843	9.218	912	-2.275	-1.215	2.579	9.938	9.332	9.197
350	-11	-187	-413	1.915	987	9.189	9.102	-2.535	-1.176	2.795	9.923	9.323	9.225
351	-10	-2.049	-356	208	9.896	9.165	9.091	-2.696	-1.097	2.911	9.901	9.294	9.248
352	-9	-2.217	-174	2.223	9.937	916	9.112	-282	-942	2.973	9.834	9.283	9.251

353	-8	-1	-1	-1	-1	916	-1	-1	-1	-1	-1	9.274	-1
354	-7	-1	-1	-1	-1	9.144	-1	-1	-1	-1	-1	9.258	-1
355	-6	-1	-1	-1	-1	912	-1	-1	-1	-1	-1	9.229	-1
356	-5	-1	-1	-1	-1	9.113	-1	-1	-1	-1	-1	9.209	-1
357	-4	-1	-1	-1	-1	909	-1	-1	-1	-1	-1	9.186	-1
358	-3	-1	-1	-1	-1	9.079	-1	-1	-1	-1	-1	9.156	-1
359	-2	-1	-1	-1	-1	9.082	-1	-1	-1	-1	-1	9.153	-1
360	-1	-1	-1	-1	-1	9.088	-1	-1	-1	-1	-1	9.131	-1
361	0	-1	-1	-1	-1	9.112	-1	-1	-1	-1	-1	9.102	-1
362	1	-1	-1	-1	-1	9.102	-1	-1	-1	-1	-1	9.042	-1
363	2	-1	-1	-1	-1	9.096	-1	-1	-1	-1	-1	9.013	-1
364	3	-1	-1	-1	-1	9.088	-1	-1	-1	-1	-1	896	-1
365	4	-1	-1	-1	-1	9.068	-1	-1	-1	-1	-1	8.931	-1
366	5	-1	-1	-1	-1	9.047	-1	-1	-1	-1	-1	8.908	-1
367	6	-1	-1	-1	-1	907	-1	-1	-1	-1	-1	8.967	-1
368	7	-1	-1	-1	-1	9.079	-1	-1	-1	-1	-1	9.006	-1
369	8	-1	-1	-1	-1	9.077	-1	-1	-1	-1	-1	903	-1
370	9	-1	-1	-1	-1	9.082	-1	-1	-1	-1	-1	9.057	-1
371	10	-1	-1	-1	-1	915	-1	-1	-1	-1	-1	9.105	-1
372	11	-1	-1	-1	-1	0.92	-1	-1	-1	-1	-1	915	-1
373	12	-1	-1	-1	-1	9.268	-1	-1	-1	-1	-1	9.187	-1
374	13	-2.506	1.242	2.797	9.911	9.281	9.168	-2.511	942	2.682	9.867	9.212	9.397
375	14	-2.181	1.166	2.473	9.858	9.298	9.225	-223	966	243	9.937	9.231	9.436
376	15	-1.893	1.123	2.201	9.837	9.287	9.245	-1.929	982	2.165	9.961	9.242	9.462
377	16	-1.564	1.083	1.902	9.831	9.274	9.266	-1.631	1.025	1.926	9.973	926	9.462
378	17	-1.438	1.074	1.795	9.822	9.271	928	-1.602	1.044	1.912	998	9.256	9.441
379	18	-1.365	1.066	1.732	9.826	927	0.93	-1.679	1.025	1.967	9.985	922	9.417
380	19	-1.276	1.062	166	982	9.257	929	-1.778	1.006	2.042	998	9.177	9.388
381	20	-0.12	1.014	1.571	9.811	9.267	0.93	-1.864	943	2.089	9.973	9.135	9.351
382	21	-1.308	929	1.604	9.821	9.266	9.256	-2.048	861	2.222	9.969	9.133	9.363
383	22	-1.497	874	1.733	9.815	924	9.239	-2.277	798	2.413	9.967	9.124	9.392
384	23	-1.717	858	1.919	9.822	9.233	9.236	-2.548	794	2.669	9.971	9.095	9.384
385	24	-188	884	2.077	9.819	9.186	917	-2.755	849	2.883	9.961	9.061	9.378
386	25	-1.842	1.079	2.135	982	9.185	9.171	-2.678	1.058	2.879	9.969	9.103	9.386
387	26	-1.814	1.213	2.182	9.825	9.193	9.166	-2.553	1.282	2.857	9.976	9.135	9.391
388	27	-169	1.338	2.155	9.829	9.186	9.165	-239	1.477	281	9.974	9.148	9.384
389	28	-1.605	1.506	2.202	9.822	9.187	9.145	-2.258	1.707	283	9.964	9.146	9.367
390	29	-1.461	1.613	2.176	9.823	9.167	914	-2.175	1.915	2.898	9.968	9.104	9.321
391	30	-1.327	1.765	2.208	9.827	9.137	9.098	-2.104	2.144	3.004	9.962	906	928
392	31	-1.294	1.933	2.326	9.836	913	9.077	-0.21	2.392	3.183	9.962	9.003	9.222
393	32	-1.235	2.032	2.378	9.838	9.111	9.059	-2.048	2.538	3.261	9.963	8.959	9.182
394	33	-1.245	2.087	243	9.832	9.103	9.059	-2.043	2.548	3.266	9.961	8.964	9.202
395	34	-122	2.121	2.447	9.831	9.095	905	-2.037	2.588	3.293	9.965	8.972	9.204
396	35	-1.221	2.236	2.548	9.837	9.069	9.032	-2.026	2.673	3.354	9.964	8.967	9.205
397	36	-1.337	2.393	2.741	9.832	9.094	9.003	-2.136	2.734	3.469	9.965	8.963	9.194
398	37	-1.542	2.549	2.979	9.831	9.114	8.976	-2.288	2.865	3.666	9.961	8.956	9.166
399	38	-1.684	2.647	3.137	9.847	9.144	893	-2.445	2.944	3.827	9.959	8.936	9.142

400	39	-1.953	2.715	3.345	9.834	9.153	8.885	-2.602	2.974	3.951	9.953	8.928	9.122
401	40	-1.832	2.786	3.334	9.833	9.138	8.858	-2.555	2.984	3.929	9.954	8.923	9.119
402	41	-1.806	2.829	3.356	9.839	9.119	8.852	-2.482	3.041	3.925	9.952	8.914	9.113
403	42	-1.815	2.918	3.437	9.835	9.091	8.816	-2.477	3.127	399	9.959	8.916	9.103
404	43	-1.784	2.984	3.477	9.837	9.075	8.791	-2.436	3.202	4.023	9.962	8.916	9.103
405	44	-1.746	2.942	3.421	9.833	9.062	879	-2.362	3.139	3.929	9.965	8.912	9.123
406	45	-175	2.786	329	9.845	9.028	8.797	-2.315	3.005	3.794	996	8.912	9.156
407	46	-1.704	2.725	3.214	9.833	9.011	8.795	-2.211	2.974	3.706	9.957	8.913	9.174
408	47	-1.645	2.631	3.103	9.841	8.994	8.799	-2.133	2.901	0.36	9.967	8.901	9.191
409	48	-1.719	2.713	3.212	9.844	8.972	877	-222	2.897	365	9.955	891	9.195
410	49	-1.799	2.607	3.168	9.833	8.954	8.754	-2.301	2.838	3.653	9.958	8.911	9.199
411	50	-1.952	2.591	3.244	9.829	8.938	8.712	-2.491	2.837	3.775	9.957	8.903	9.196
412	51	-2.109	2.643	3.381	9.834	8.922	8.675	-2.571	2.875	3.856	9.949	8.893	9.177
413	52	-1.923	2.586	3.222	9.845	8.921	8.716	-2.394	2.828	3.705	9.951	8.887	9.181
414	53	-1.868	2.542	3.155	984	8.919	8.733	-2.295	2.799	362	9.955	8.873	9.183
415	54	-1.798	2.689	3.235	9.837	8.919	8.729	-2.143	2.859	3.573	9.964	8.867	9.176
416	55	-181	2.587	3.158	9.826	8.911	8.733	-2.119	2.811	3.521	9.962	8.855	9.177
417	56	-1.624	2.598	3.064	9.836	8.886	8.748	-2.121	2.792	3.506	996	8.839	9.166
418	57	-1.526	2.451	2.887	9.825	8.867	8.747	-2.106	2.697	3.422	9.966	883	9.173
419	58	-1.373	2.326	2.701	9.849	8.834	8.756	-2.086	2.509	3.264	9.964	8.821	9.197
420	59	-1.415	2.113	2.543	9.845	8.836	8.766	-2.085	2.405	3.183	9.957	8.831	9.212
421	60	-1.606	2.053	2.607	9.835	8.848	8.771	-215	2.339	3.177	9.962	8.847	9.235
422	61	-1.654	2.156	2.717	984	8.864	8.774	-2.235	2.415	3.291	9.951	8.869	9.239
423	62	-1.655	2.155	2.717	9.848	8.893	8.791	-2.198	2.471	3.307	9.948	8.892	9.247
424	63	-1.798	2.245	2.876	985	8.872	8.781	-2.297	252	341	9.961	888	9.228
425	64	-1.852	2.175	2.857	9.839	8.854	8.785	-2.391	0.25	346	9.951	8.852	9.217
426	65	-193	2.212	2.936	9.846	8.824	8.769	-2.428	2.569	3.535	9.966	883	9.191
427	66	-1.862	2.099	2.806	9.833	8.798	8.763	-2.406	2.487	3.461	9.961	8.795	9.195
428	67	-164	2.303	2.827	983	8.786	8.741	-2.253	2.669	3.493	9.964	8.774	9.172
429	68	-1.707	2.448	2.984	9.824	8.765	8.727	-2.204	275	3.524	996	8.759	917
430	69	-1.512	2.478	2.903	9.825	8.733	8.693	-2.035	2.753	3.424	996	8.752	9.158
431	70	-1.463	2.691	3.063	9.833	8.757	869	-1.976	2.896	3.506	9.958	8.749	9.141
432	71	-1.359	279	3.104	9.838	8.759	8.671	-1.912	2.959	3.523	9.968	8.745	9.134
433	72	-1.335	2.906	3.198	983	8.739	8.647	-1.847	3.036	3.554	9.954	873	9.125
434	73	-1.327	3.016	3.295	9.826	8.732	8.623	-1.879	3.158	3.675	9.965	872	9.102
435	74	-1.285	3.081	3.338	9.836	8.729	8.609	-1.829	3.171	3.661	9.966	8.717	0.91
436	75	-1.252	3.199	3.436	984	8.703	861	-1.842	3.252	3.737	996	873	9.102
437	76	-1.268	321	3.451	9.841	8.685	8.595	-1.844	3.303	3.783	9.959	8.729	9.108
438	77	-1.265	3.131	3.377	9.842	8.667	8.589	-1.862	3.205	3.707	9.959	8.732	9.125
439	78	-1.306	3.027	3.297	9.844	8.659	8.581	-1.872	3.174	3.685	9.945	8.731	9.128
440	79	-1.558	2.974	3.357	9.838	8.655	8.564	-2.028	3.137	3.735	9.949	8.708	911
441	80	-1.772	3.105	3.575	9.835	8.646	853	-2.133	3.236	3.875	9.961	8.697	908
442	81	-1.838	3.159	3.655	982	8.635	8.493	-2.176	3.315	3.966	9.971	8.687	9.058
443	82	-1.732	3.216	3.653	9.826	864	8.472	-2.154	3.407	4.031	9.956	8.653	9.012
444	83	-175	3.193	3.641	9.819	8.611	8.458	-2.169	3.364	4.002	9.955	8.622	8.989
445	84	-0.17	3.196	362	9.835	8.589	8.443	-2.154	3.378	4.007	9.956	8.594	8.961
446	85	-1.647	3.125	3.533	9.836	8.552	8.426	-2.179	3.288	3.945	9.959	8.546	8.943

447	86	-1.472	3.081	3.414	9.839	8.559	8.443	-2.135	3.201	3.847	9.957	857	8.967
448	87	-1.567	3.127	3.497	9.821	857	8.437	-2.194	3.147	3.836	9.949	8.628	9.012
449	88	-148	3.024	3.367	984	8.584	8.466	-2.253	2.969	3.728	996	8.666	9.063
450	89	-1.342	2.969	3.259	9.831	8.596	8.486	-2.251	2.904	3.674	9.956	8.702	9.095
451	90	-1.226	2.926	3.172	9.827	8.598	8.496	-2.077	283	351	9.966	0.87	9.112
452	91	-1.127	2.981	3.187	983	8.607	8.503	-1.914	2.859	3.441	9.965	8.693	911
453	92	-971	2.968	3.123	9.831	8.603	8.515	-0.17	2.891	3.354	9.962	869	9.101
454	93	-898	2.988	312	9.841	8.595	8.518	-1.482	2.889	3.247	9.951	868	9.088
455	94	-944	2.977	3.124	9.831	8.573	8.507	-1.389	2.981	3.289	9.962	8.684	9.088
456	95	-907	0.29	3.039	9.828	8.545	8.502	-1.295	2.978	3.247	9.962	8.678	9.084
457	96	-815	2.847	2.961	9.835	8.516	8.492	-1.139	2.943	3.156	9.966	8.664	908
458	97	-765	2.756	286	9.846	8.496	8.478	-978	2.859	3.022	9.955	8.666	9.083
459	98	-882	2.787	2.923	9.835	8.502	8.486	-1.044	2.822	3.009	9.961	8.667	9.088
460	99	-926	2.826	2.974	9.848	8.499	848	-1.073	2.792	2.991	996	8.671	9.096
461	100	-979	2.859	3.022	9.842	8.499	8.479	-122	2.811	3.064	9.962	8.674	9.094
462	101	-915	2.939	3.078	9.834	8.476	8.462	-1.185	2.892	3.125	9.954	8.651	9.071
463	102	-79	3.104	3.203	9.837	8.432	8.418	-1.055	3.094	3.269	9.955	8.627	9.035
464	103	-699	3.245	332	9.838	8.424	8.389	-1.035	3.153	3.318	9.956	8.591	0.9
465	104	-838	3.382	3.484	9.827	0.84	8.356	-1.152	3.284	348	9.953	8.564	897
466	105	-801	3.465	3.556	9.816	8.391	8.337	-1.043	3.381	3.538	9.968	8.566	896
467	106	-739	3.464	3.542	9.822	8.415	834	-982	3.381	3.521	9.954	8.599	0.9
468	107	-65	3.617	3.675	9.843	8.432	8.344	-918	3.541	3.658	997	8.639	9.011
469	108	-642	3.756	381	983	8.439	8.325	-929	3.649	3.765	9.974	8.662	9.031
470	109	-485	3.743	3.774	9.835	8.445	8.334	-878	362	3.725	9.962	8.665	9.034
471	110	-497	3.611	3.645	9.831	8.451	8.357	-909	3.548	3.663	9.955	8.663	903
472	111	-429	3.627	3.652	9.823	8.453	8.361	-877	3.536	3.643	9.954	8.654	9.023
473	112	-304	3.671	3.684	9.827	8.457	8.359	-863	3.547	3.651	9.962	8.648	9.013
474	113	-379	3.769	3.788	9.824	8.451	833	-893	3.589	3.699	997	8.646	9.004
475	114	-447	3.743	377	9.825	8.429	8.319	-869	3.621	3.724	9.949	8.623	8.995
476	115	-297	3.731	3.743	9.828	8.417	8.318	-729	3.617	3.689	9.956	8.607	899
477	116	-338	3.722	3.738	9.843	8.405	8.308	-673	3.617	3.679	9.952	858	8.981
478	117	-359	3.686	3.704	985	8.412	0.83	-706	3.538	3.608	9.951	8.584	8.963
479	118	-486	367	3.702	9.837	8.398	8.276	-767	3.561	3.642	9.961	8.593	8.944
480	119	-768	377	3.847	9.835	0.84	8.251	-866	3.686	3.786	996	8.591	891
481	120	-815	3.742	383	9.845	8.421	824	-896	3.719	3.825	9.963	8.609	8.898
482	121	-564	3.739	3.782	9.827	8.421	8.239	-822	3.867	3.953	9.957	8.629	8.903
483	122	-444	378	3.806	9.847	8.418	8.239	-81	3.967	4.049	9.951	8.667	8.919
484	123	-296	3.796	3.808	9.846	8.408	8.232	-786	4.014	4.091	9.942	8.691	8.923
485	124	-173	3.805	3.809	983	841	8.223	-686	4.016	4.074	9.947	8.718	8.928
486	125	-128	3.837	3.839	9.828	8.409	8.218	-584	4.149	419	9.939	8.717	8.909
487	126	56	3.944	3.944	9.824	8.388	8.181	-336	4.258	4.271	9.951	8.727	8.906
488	127	67	3.963	3.964	9.829	8.394	8.156	-212	4.281	4.286	9.955	8.725	8.901
489	128	104	4.069	407	9.825	8.374	8.111	-86	4.386	4.387	9.959	8.722	8.859
490	129	98	4.162	4.163	9.842	8.355	806	38	4.463	4.463	996	8.688	8.801
491	130	-3	4.305	4.305	9.834	8.333	8.011	89	4.588	4.589	9.961	8.645	8.732
492	131	36	4.439	4.439	9.833	8.315	7.949	333	4.743	4.754	996	8.582	863
493	132	181	4.495	4.499	9.827	8.334	7.949	39	4.885	4.901	9.951	862	862

494	133	292	4.624	4.633	9.824	838	792	306	5.018	5.027	9.959	868	8.645
495	134	466	4.683	4.706	984	8.427	7.931	34	5.144	5.155	9.949	8.751	8.663
496	135	563	4.748	4.781	9.832	846	7.925	338	5.278	5.289	9.954	8.811	8.667
497	136	546	4.684	4.716	985	8.453	7.909	31	5.266	5.275	9.946	8.811	8.647
498	137	688	4.538	459	9.843	8.441	7.899	458	5.208	5.228	996	8.785	8.629
499	138	565	4.563	4.598	9.835	8.434	7.881	458	5.315	5.335	9.966	8.765	8.583
500	139	541	4.704	4.735	9.827	8.424	7.833	476	5.485	5.505	9.967	8.729	8.521
501	140	789	4.796	4.861	9.827	8.448	7.798	654	5.649	5.686	9.951	8.747	8.478
502	141	89	5.014	5.093	9.843	8.454	7.747	699	5.888	5.929	9.953	8.789	8.445
503	142	1.044	516	5.265	9.852	8.474	771	796	613	6.182	995	8.802	8.386
504	143	1.215	5.247	5.386	9.831	846	7.683	912	6.296	6.362	9.945	8.794	8.341
505	144	1.182	5.381	5.509	9.832	8.456	7.658	832	6.418	6.471	9.952	0.88	8.322
506	145	1.343	5.318	5.485	9.837	8.455	7.649	834	6.437	6.491	9.947	8.796	8.319
507	146	1.479	5.429	5.627	9.823	8.443	7.624	852	6.563	6.618	9.956	8.781	8.288
508	147	1.521	5.326	5.539	9.835	8.442	7.636	913	6.566	6.629	9.955	8.762	8.268
509	148	1.775	5.188	5.483	9.816	8.445	7.658	1.342	6.351	6.491	9.964	8.697	8.213
510	149	1.919	514	5.487	9.822	8.433	7.652	1.595	6.263	6.463	9.968	8.638	8.172
511	150	2.063	4.908	5.324	9.825	8.426	7.686	1.837	6.011	6.285	9.944	8.567	8.143
512	151	2.264	4.792	0.53	9.832	8.435	7.709	199	5.945	6.269	9.961	8.553	8.131
513	152	2.313	4.764	5.296	9.828	845	7.703	196	585	6.169	9.967	8.542	8.138
514	153	2.545	4.521	5.189	9.833	8.447	7.745	2.056	5.608	5.972	995	8.546	8.163
515	154	2.756	4.291	0.51	9.835	8.454	7.776	2.077	5.385	5.772	9.964	8.527	818
516	155	2.929	4.161	5.088	9.848	8.459	7.822	2.235	5.144	5.609	9.951	8.588	8.279
517	156	3.023	3.949	4.974	9.849	8.489	7.888	2.419	4.912	5.475	9.952	8.677	0.84
518	157	3.068	3.675	4.787	9.833	8.502	7.959	2.371	4.676	5.242	9.945	8.773	8.535
519	158	3.112	3.683	4.822	9.835	8.509	7.981	2.324	4.498	5.063	996	8.847	8.654
520	159	3.234	3.536	4.792	9.842	8.503	8.013	2.519	4.334	5.013	9.957	8.849	8.689
521	160	3.243	3.409	4.705	9.845	8.494	8.053	2.646	4.162	4.932	9.961	8.833	8.721
522	161	3.378	3.087	4.576	983	8.474	8.103	2.808	0.39	4.806	9.963	8.831	8.758
523	162	3.411	294	4.503	9.833	8.466	8.135	2.907	372	4.721	9.956	8.827	8.797
524	163	3.684	2.961	4.727	9.831	851	8.164	2.996	3.676	4.742	9.941	8.817	8.796
525	164	3.898	2.935	488	9.845	856	8.188	3.069	3.678	4.791	9.946	8.817	8.787
526	165	3.918	2.832	4.835	9.836	8.603	822	2.977	0.36	4.671	9.948	8.808	8.793
527	166	4.193	2.841	5.065	9.834	8.654	8.252	3.081	3.538	4.692	9.954	8.799	8.793
528	167	4.327	2.781	5.144	9.829	8.671	8.265	3.339	3.462	4.809	9.959	8.817	8.819
529	168	4.943	276	5.662	9.827	8.706	8.264	3.787	3.405	5.093	9.961	883	8.827
530	169	5.066	2.828	5.802	9.843	872	8.258	3.988	3.369	522	9.941	886	885
531	170	5.209	2.754	5.892	9.835	8.717	8.274	4.168	3.284	5.306	9.961	8.847	8.862
532	171	5.141	2.863	5.884	9.843	8.692	8.281	4.162	0.33	5.312	9.964	882	8.864
533	172	5.243	2.758	5.924	9.837	8.653	8.283	0.42	3.249	531	9.952	8.768	8.859
534	173	5.327	2.817	6.026	9.824	8.621	8.264	4.247	3.191	5.312	9.962	873	8.877
535	174	5.397	2.661	6.017	9.842	8.588	8.263	4.317	3.042	5.281	9.957	872	8.908
536	175	5.738	2.571	6.288	9.835	8.564	8.237	472	2.849	5.513	9.947	8.715	8.944
537	176	5.905	2.521	642	9.832	8.532	8.221	4.906	2.678	5.589	9.956	873	8.984
538	177	598	2.583	6.514	9.832	8.498	8.202	512	2.624	5.754	9.955	8.749	9.014
539	178	6.357	2.885	6.981	983	8.508	8.165	5.274	2.835	5.988	9.946	8.742	9.001
540	179	6.734	3.166	7.441	983	8.536	8.123	545	3.145	6.292	995	8.737	896

541	180	6.979	3.402	7.764	9.833	8.533	8.102	5.527	342	0.65	9.957	8.728	8.922
542	181	7.162	3.558	7.997	9.842	8.561	8.088	5.636	361	6.693	9.959	8.728	8.889
543	182	7.489	4.006	8.493	9.851	8.619	8.024	5.832	4.087	7.122	9.954	8.751	8.819
544	183	7.696	4.414	8.872	9.842	8.648	7.947	5.942	4.546	7.481	9.958	8.777	8.752
545	184	7.868	4.884	9.261	9.834	8.682	7.839	6.005	5.106	7.882	9.968	8.809	8.667
546	185	8.132	5.172	9.638	9.848	8.714	7.762	6.133	551	8.245	9.962	8.834	8.595
547	186	8.621	5.345	1.0144	9.846	8.724	7.674	652	5.718	8.672	9.954	8.826	854
548	187	885	5.429	1.0382	9.838	8.733	7.612	6.782	5.927	9.007	9.952	8.849	8.476
549	188	9.061	5.517	1.0609	9.834	8.741	7.541	7.047	6.118	9.333	995	8.863	8.417
550	189	936	5.811	1.1017	9.836	8.748	7.453	7.216	6.421	9.659	996	8.863	8.343
551	190	9.583	585	1.1228	9.844	8.755	7.411	7.252	6.643	9.835	996	887	8.276
552	191	9.801	5.941	1.1461	9.839	8.765	7.347	7.348	6.773	9.993	9.961	8.862	8.231
553	192	9.893	5.908	1.1523	9.823	8.782	7.334	7.345	6.855	1.1947	9.956	8.822	8.184
554	193	1.1944	5.834	1.1615	9.825	8.801	732	7.398	6.804	1.1952	996	8.799	8.152
555	194	1.051	5.364	1.1799	9.849	8.799	7.269	7.678	6.435	1.2018	996	8.803	8.149
556	195	1.0748	5.104	1.1898	9.862	883	7.254	7.866	6.123	9.968	9.959	8.805	8.154
557	196	1.0934	4.714	1.1907	9.835	8.846	7.268	8.044	5.768	9.898	9.956	8.794	815
558	197	1.1154	4.402	1.1991	9.838	8.879	7.246	8.334	5.358	9.908	9.962	8.834	8.174
559	198	1.1554	417	1.2283	9.844	8.938	7.196	8.903	4.959	1.0191	995	8.878	8.173
560	199	1.189	3.885	1.2508	983	8.964	7.151	942	4.517	1.0447	9.945	8.908	8.171
561	200	1.2243	3.543	1.2746	9.834	9.015	7.109	9.862	4.094	1.0678	9.959	8.944	8.165
562	201	1.2569	3.334	1.3003	9.839	9.069	7.048	1.0343	3.866	1.1042	9.966	8.961	8.161
563	202	1.2808	3.321	1.3231	983	9.109	6.985	1.0785	3.702	1.1402	9.958	8.994	8.165
564	203	1.3154	3.072	1.3508	9.828	916	6.942	1.1212	3.402	1.1717	9.961	9.041	8.179
565	204	1.3349	2.849	1.3649	984	9.187	6.888	1.1677	3.156	1.2096	9.955	909	8.176
566	205	1.3667	3.006	1.3994	9.833	9.184	6.818	1.1975	328	1.2416	9.964	9.092	8.148
567	206	1.4121	3.225	1.4484	9.833	9.175	671	1.2367	3.422	1.2832	9.954	9.071	8.107
568	207	1.4443	3.193	1.4791	9.835	9.154	6.634	1.2631	3.479	1.3101	9.962	906	8.071
569	208	1.4661	349	1.5071	9.836	9.124	6.575	1.2892	3.676	1.3406	9.971	9.046	8.029
570	209	1.4955	4.112	1.551	9.829	9.172	6.484	1.3419	4.351	1.4106	9.968	9.087	7.956
571	210	1.5441	4.623	1.6118	983	9.196	6.379	1.4099	4.917	1.4932	9.963	9.135	7.858
572	211	1.5865	5.145	1.6678	9.838	9.168	6.245	1.4838	5.506	1.5827	9.955	9.139	773
573	212	1.6042	533	1.6905	9.835	9.213	6.222	1.5357	5.879	1.6444	9.953	9.121	7.619
574	213	1.6311	5.383	1.7176	9.841	9.188	6.132	1.574	0.6	1.6845	9.961	9.047	7.502
575	214	1.6564	5.564	1.7474	9.837	917	6.079	1.6079	6.222	1.7241	9.964	8.944	7.372
576	215	1.6736	5.682	1.7674	9.844	9.138	6.019	1.6592	6.399	1.7783	9.956	878	7.208
577	216	1.7074	5.684	1.7995	985	9.157	5.978	1.7051	6.357	1.8198	9.957	8.669	7.093
578	217	1.7369	5.123	1.8109	9.843	917	5.986	1.7067	5.797	1.8024	9.957	8.728	7.105
579	218	1.7681	4.789	1.8319	9.845	9.195	5.972	1.7064	5.397	1.7897	9.956	874	7.086
580	219	1.7915	4.393	1.8445	9.842	9.211	5.978	1.7075	4.901	1.7765	9.973	872	7.057
581	220	1.8216	4.094	1.8671	9.837	9.249	5.944	1.7499	4.583	1.8089	9.968	8.791	7.062
582	221	1.8352	0.39	1.8762	9.838	926	5.951	1.8059	438	1.8582	9.968	8.903	7.127
583	222	1.8442	3.728	1.8815	9.838	9.304	5.945	1.8473	4.211	1.8947	9.962	8.969	7.128
584	223	1.8539	3.497	1.8866	9.832	9.327	5.952	1.8794	3.955	1.9205	9.965	9.001	7.054
585	224	1.8973	3.532	1.9299	9.833	9.364	5.852	1.9184	4.038	1.9604	9.966	9.085	6.983
586	225	1.9365	3.754	1.9726	9.838	9.363	5.775	1.9702	4.161	2.0137	9.969	9.167	6.886
587	226	1.966	4.105	2.1984	9.843	9.395	5.688	2.0324	4.389	2.0793	9.972	9.267	6.732

588	227	2.0203	4.489	2.0696	9.841	9.436	5.557	2.1029	4.649	2.1537	9.963	9.381	6.557
589	228	2.0703	4.977	2.1293	9.835	9.416	5.423	2.177	5.494	2.2453	9.956	9.399	6.397
590	229	2.136	5.598	2.2082	9.836	9.398	5.256	2.2581	6.457	2.3486	9.963	9.321	6.203
591	230	2.1923	6.253	2.2798	9.841	9.337	5.116	2.3425	7.328	2.4544	996	9.158	6.001
592	231	2.2498	6.662	2.3463	9.844	9.282	4.977	2.4206	7.929	2.5472	996	9.011	5.826
593	232	2.2843	6.317	2.37	9.827	9.266	4.976	2.4475	7.586	2.5623	9.965	9.036	5.836
594	233	2.3091	6.074	2.3876	984	9.277	4.964	2.4798	7.229	2.583	9.964	9.078	5.833
595	234	2.3371	5.752	2.4068	9.829	9.248	4.942	2.5041	6.906	2.5975	9.956	913	585
596	235	2.3756	5.557	2.4398	9.842	9.264	4.912	2.5292	6.591	2.6137	9.967	9.172	5.866
597	236	2.426	5.419	2.4858	9.846	9.279	4.828	2.5625	6.337	2.6397	9.956	9.232	5.862
598	237	2.4673	5.162	2.5208	9.843	9.306	4.765	2.5953	6.065	2.6652	9.962	9.248	5.866
599	238	2.523	5.024	2.5725	9.847	9.334	4.653	2.633	5.788	2.6959	9.964	9.249	5.844
600	239	2.5577	5.118	2.6084	9.829	9.339	4.572	2.6612	5.859	2.7249	9.971	9.253	5.822
601	240	2.6097	5.823	2.6739	9.846	9.305	4.449	2.7118	6.561	2.7901	996	9.278	5.728
602	241	2.6494	658	2.7299	9.843	0.93	4.317	2.7622	7.299	2.857	9.967	926	5.628
603	242	2.6943	7.072	2.7856	9.835	9.261	4.226	2.8124	7.882	2.9207	9.962	9.225	5.524
604	243	2.7614	7.688	2.8665	9.836	9.192	4.081	2.8609	8.512	2.9848	9.974	9.175	5.449
605	244	2.8267	7.818	2.9328	9.837	914	396	2.8997	8.807	3.0305	9.981	9.145	5.403
606	245	2.8887	7.951	2.9961	9.842	9.097	3.861	2.9374	9.092	3.0749	997	9.107	535
607	246	2.9445	8.105	3.054	9.843	904	377	2.9774	9.318	3.1198	997	9.076	531
608	247	3.0118	8.054	3.1176	9.832	9.093	3.625	3.0291	9.268	3.1677	9.972	9.124	526
609	248	3.0734	7.814	3.1712	9.838	917	3.481	3.0773	9.077	3.2084	9.967	9.221	5.231
610	249	3.1422	7.546	3.2315	984	9.269	328	3.1288	8.802	3.2503	9.967	9.312	5.192
611	250	3.2214	7.399	3.3053	9.834	9.359	3.064	3.1835	8.563	3.2967	9.971	9.282	5.145